THE
PHYSICAL REVIEW

A journal of experimental and theoretical physics established by E. L. Nichols in 1893

SECOND SERIES, VOL. 66, NOS. 5 AND 6 SEPTEMBER 1 AND 15, 1944

The Apparent Breakdown of Meek's Streamer Criterion in Divergent Gaps due to the Failure of Townsend's Ionization Function

LEON H. FISHER* AND GERHARD L. WEISSLER**
Department of Physics, University of California, Berkeley, California

(Received June 20, 1944)

Meek's criterion postulates that a streamer will propagate if the positive ion space charge field close to the anode is equal to K times the impressed field, where K should be a constant independent of gap configuration and pressure. Measurements in confocal paraboloid gaps, designed to substantiate this, revealed that K was not constant, but decreased with decreasing pressures. Morton showed that on a negatively charged smaller electrode Townsend's ionization functions do not represent the ionization produced in divergent fields. Consequently it was believed that the calculations of the space charge field of the positive ions produced in such gaps must be inaccurate in view of this erroneous assumption. A series of measurements on the dark current i in the same gap showed that it was not represented by $i=i_0 \exp[\int \alpha dx]$ at lower pressures. The trend and the apparent quantitative variation of K with pressure is explained if the apparent i_0 *versus* voltage curves are extrapolated to streamer onset for each pressure. Thus for practical purposes under the conditions studied K is sensibly constant in conformity with Meek's theory. *Per contra*, the applications of Meek's theory to gaps with very divergent fields where the currents can be expected to deviate markedly from those computed by the relation $i=i_0 \exp[\int \alpha dx]$ are not justified, thus placing a practical limitation on the use of Meek's theory to streamer studies. Roughly this phenomenon appears when the change of the field exceeds two percent change over an average electron free path.

INTRODUCTION

FOR some time it has been clear that the classical Townsend theory of sparking cannot account for the formation of sparks in air when the product of pressure and plate distance exceeds 200 mm of Hg×cm. Summaries of the inadequacy of the Townsend theory have been given by Meek[1] and by Loeb and Meek.[2]

The discovery of the streamer in the positive point-to-plane corona and its explanation by Loeb, Kip, and Trichel[3] supplied a new mechanism for spark breakdown. Almost simultaneously the same mechanism was proposed by Raether[4] on the basis of cloud-track pictures. The streamer theory of sparking was developed qualitatively by Loeb, but it was not until Meek proposed his criterion for streamer formation that the theory was placed on a quantitative basis.

Meek's criterion states that a streamer will form when the positive ion space charge field close to the anode is equal to K times the impressed external field (providing the photoionization in the gas is adequate). The space charge field is computed on the assumption that most of the positive ions created by the first electron avalanches are contained in a hemi-

* Now at the University of New Mexico.
** Now at the University of California Hospital.
[1] J. M. Meek, Phys. Rev. **57**, 722 (1940).
[2] L. B. Loeb and J. M. Meek, *The Mechanism of the Electric Spark* (Stanford University Press, Stanford, 1941).
[3] A. F. Kip, Phys. Rev. **54**, 139 (1938); G. W. Trichel, *ibid.* **55**, 382 (1939); L. B. Loeb and A. F. Kip, J. App. Phys. **10**, 142 (1939).
[4] H. Raether, Zeits. f. Physik **107**, 91 (1937); **110**, 611 (1938); **112**, 464 (1939); H. Costa, *ibid.* **113**, 531 (1939).

spherical boss which has a radius equal to the radius of electron diffusion at the head of the avalanche. The radius of electron diffusion depends upon the quantity $\lambda_0/\sqrt{f}$, where λ_0 is the electron free path at 760 mm of Hg, and f is the fraction of energy lost by an electron per impact. Both λ_0 and f are functions of the electron energy. Since the electron energy distribution function is not well known, especially at high pressures and in strong electric fields, there is some uncertainty in the value of $\lambda_0/\sqrt{f}$ which should be used. It has been shown, however, that the error introduced by this uncertainty is not serious.[5]

Originally, Meek chose the empirical condition that $K=1.0$, and his calculations gave a fair agreement with published values of sparking potentials, but a more careful scrutiny of the data indicated that a value of $K=0.1$ was more nearly correct.

If the streamer theory is to have physical significance, K should be a constant, independent of pressure and gap configuration. In order to study the behavior of K, one can use values of measured sparking potentials in plane parallel gaps. Analysis of reliable sparking potentials in the literature yields a factor of K which varies by a factor of 60 at atmospheric pressure. More recent measurements[6] of sparking potentials yielded data for which K varies only by a factor of two. At lower pressures, however, there are no adequate sparking potential values and, as recent studies[6] have indicated, there are not likely to be any reliable values of sparking potentials at lower pressures for some time.

Another method can be used to evaluate K. Fitzsimmons[7] determined the onset potentials for streamers in air in confocal paraboloid gaps at atmospheric pressure. By knowing the field distribution over the axis of the gap at the measured potential, it is possible to evaluate the positive ion space charge field, and values of K may be calculated. The results of Fitzsimmons showed that K has the value 0.1 for air, and this conclusion seemed consistent with the value of K selected by Loeb and Meek from sparking potential data. But there was still no information about the behavior of K with pressure. It was therefore decided to extend Fitzsimmons' observations to lower pressures, and for the sake of generality to other gases. The results of these measurements, based on the assumptions given above, revealed that K is not a constant but decreased with decreasing pressure. A careful analysis of the physical processes involved in streamer formation indicated that no *known* factor could be responsible for the results. It was therefore concluded that either some unknown factor was being neglected, or that Meek's criterion was in principle fundamentally wrong. In view of the fact that the criterion, rough as it was, appeared to be reasonable, and was based on physical processes believed to operate in the streamer, it was hoped that a reasonable explanation could be found. At this time, Morton[8] was investigating the validity of applying Townsend's ionization coefficients to ionization produced in divergent fields and discovered that they were not applicable where the field-change per electron mean free path exceeded 2 percent. It occurred to one of the writers (L. H. F.) to inquire whether the space charge field of the positive ions in applying Meek's criterion to divergent gaps was thus not being calculated upon erroneous assumptions. Experimental data bearing out this hypothesis were obtained in the very gap in which the variation of K was observed. The two sets of experiments will be presented separately, while a combined treatment of both will be given in the discussion.

THE DEPENDENCE OF K ON PRESSURE

The experimental arrangements were the same as those used by Fitzsimmons[7] except for the gap itself. A hollow paraboloid electrode of focal length four centimeters was used as a plate in conjunction with a paraboloid point of focal length either 0.02 or 0.005 cm. Both point paraboloids were considerably sharper than those used by Fitzsimmons. The surfaces of the electrodes were nickel. These gaps were enclosed in a large Pyrex bulb and were connected to a mercury diffusion pump and gas purification system. Mercury, however, was carefully excluded from the chamber. Provisions were made

[5] See reference 2, page 52, last paragraph.
[6] L. Fisher, Phys. Rev. **65**, 153 (1944).
[7] K. E. Fitzsimmons, Phys. Rev. **61**, 175 (1942).
[8] P. L. Morton, Thesis, University of California Library, Berkeley, California.

to circulate air through the chamber, but this procedure was found to be unnecessary if the currents passing through the gap were smaller than one microampere. If the currents exceeded this value by increasing the potential above that for streamer onset, oxides of nitrogen were formed which changed the streamer onset potential. The chamber was baked out under vacuum at 400°C for several hours and filled with either air or hydrogen. However, after hydrogen had been admitted to the chamber, baking alone was not adequate to remove the hydrogen. It was found necessary to subject the gap to a prolonged glow discharge with nitrogen at low pressure. Only in this way could the hydrogen dissolved in the nickel be eliminated. The air was dried by passing it over three traps surrounded by a mixture of alcohol and dry ice, while the hydrogen was cleaned over hot copper filings in order to remove oxygen.

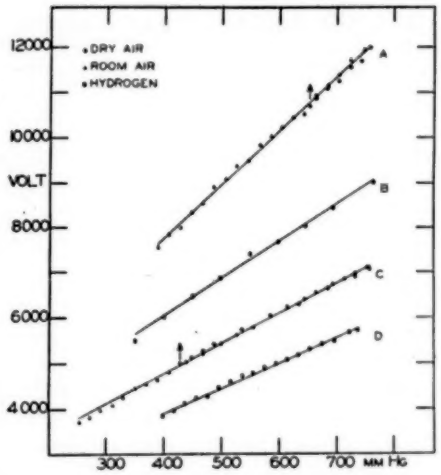

FIG. 1. Streamer onset potentials *versus* pressure. Curves *A* and *B* were obtained with a point paraboloid of 0.02-cm focal length, curves *C* and *D* with a point paraboloid of 0.005-cm focal length. The arrows indicate the lowest pressure where streamers were observed in dry air.

In order to facilitate the pulse formation preceding corona onset, a sample of thorianite was placed about eight inches from the gap, thus increasing the dark current, and making the observations more reproducible.

The chamber was initially filled with the gas to approximately atmospheric pressure and the potential difference across the gap was increased until pre-corona onset streamers appeared. The pressure was then decreased in steps of 20 mm of Hg, and corresponding streamer onset potentials were observed at each pressure, until a pressure was reached at which streamers were no longer formed. The pressure at which streamers no longer appear is in no case clearly defined. On decreasing the pressure of a given gas, and maintaining a suitable potential difference across the gap, fewer and fewer streamers occur, while the number of burst pulses increases. This observation indicates that at lower pressures, the discharge tends to spread laterally over the point forming a burst pulse rather than to grow out of the high field region in the form of a streamer. This preferential formation of burst pulses at low pressures is probably due to a decrease in the *density* of photo-ionization in the gas. The curves for pre-corona streamer onset potentials *versus* pressure showed a linear relationship in all cases (Fig. 1). Within the common pressure range for streamer formation, the curves for dry air coincided with those for room air within one percent. No attempt was made to determine the relative humidity of the room air used. Hydrogen would not show any pre-corona onset streamers if the gas had been purified by negative corona from an auxiliary point in the chamber[9] in addition to the hot copper treatment. However, since all measurements of the first Townsend coefficient α in hydrogen were taken without electrical purification of the gas, this step was omitted in the present experiments. Consequently, streamers were observed in the potential region preceding corona onset.

Since the constant K is the ratio of the field X_1 of the positive ion space charge to the impressed field X at the tip of the point parabola, it was necessary to calculate both X_1 and X. The surface field corresponding to a measured streamer onset potential was calculated from the relation

$$X=\frac{V}{\log_e (f/F)}\frac{1}{x+f}\ \text{volt/cm}. \qquad (1)$$

This expression is the solution of Laplace's equation for the field on the axis between two confocal paraboloids with focal lengths, f for the point parabola, and F for the plate parabola,

[9] G. L. Weissler, Phys. Rev. **63**, 96 (1943).

TABLE I. Values of K and associated factors.

Gas	Pressure mm Hg	Streamer onset Point potential	Streamer onset Surface field X v/cm	Focal length (cm)	x_s	$(x_s/p)^{\frac{1}{2}}$	Space charge field X_1 v/cm	$K=X_1/X$	α_s	$\int_0^{x_s}\alpha dx$	$\alpha_{st}\int_0^{x_s}\alpha dx$	$\int_0^{x_{st}}\alpha dx$
Dry air	748	11950v	1.13×10^5	0.02	0.034	6.73×10^{-3}	7.5×10^4	0.67	1210	7.9×10^5	9.6×10^8	13.6
Dry air	654	10600	1.00×10^5	0.02	0.034	7.2×10^{-3}	3.2×10^4	0.32	1100	4.0×10^5	4.4×10^8	12.9
Room air	469	8575	8.10×10^4	0.02	0.034	8.5×10^{-3}	1.50×10^4	0.18	990	2.4×10^5	2.4×10^8	12.4
Room air	370	7260	6.85×10^4	0.02	0.034	9.6×10^{-3}	3.53×10^3	0.05	880	7.3×10^4	6.4×10^7	11.2
H_2	766	9000	8.5×10^4	0.02	0.09	10.8×10^{-3}	3.9×10^4	0.45	613	1.2×10^6	7.35×10^8	14.05
H_2	550	7400	7.0×10^4	0.02	0.09	12.8×10^{-3}	7.4×10^3	0.11	533	3.2×10^5	1.7×10^8	12.7
H_2	450	6470	6.11×10^4	0.02	0.09	14.1×10^{-3}	2.1×10^3	0.04	481	1.1×10^5	5.3×10^7	11.6
H_2	350	5500	5.2×10^4	0.02	0.09	16.1×10^{-3}	6.8×10^2	0.013	427	4.6×10^4	2.0×10^7	10.7
Dry air	746	7070	2.12×10^5	0.005	0.017	4.85×10^{-3}	2.33×10^5	1.1	3000	7.16×10^5	2.15×10^9	13.5
Dry air	547	5810	1.74×10^5	0.005	0.018	5.74×10^{-3}	1.2×10^5	0.69	2460	5.3×10^5	1.31×10^9	13.2
Dry air	429	5040	1.50×10^5	0.005	0.018	6.47×10^{-3}	7.2×10^4	0.48	2250	3.9×10^5	8.8×10^8	12.9
Room air	399	4780	1.43×10^5	0.005	0.018	6.7×10^{-3}	3.8×10^4	0.27	2120	2.24×10^5	4.75×10^8	12.3
Room air	252	3700	1.11×10^5	0.005	0.019	8.7×10^{-3}	7.2×10^3	0.07	1620	7.3×10^4	1.18×10^8	11.2
H_2	738	5700	1.71×10^5	0.005	0.0475	8×10^{-3}	2.2×10^4	0.13	1796	1.78×10^5	3.2×10^8	12.1
H_2	478	4370	1.31×10^5	0.005	0.044	9.6×10^{-3}	4.0×10^3	0.03	1400	4.9×10^4	6.86×10^7	10.8
H_2	399	3850	1.16×10^5	0.005	0.040	10×10^{-3}	8.33×10^2	0.007	1250	1.2×10^4	1.5×10^7	9.4

respectively. The quantity x is the distance from the point parabola to the point in question.

For the calculation of the field X_1 the equation developed by Loeb and Meek[10] was employed.

$$X_1=5.27\times10^{-7}\frac{\alpha_s\exp\left[\int_0^{x_s}\alpha dx\right]}{(x_s/p)^{\frac{1}{2}}}\text{ volt/cm}, \quad (2)$$

where the factor 5.27×10^{-7} contains the numerical value of $\lambda_0/\sqrt{f}$, α_s is that value of the first Townsend coefficient which contributes the largest number of positive ions to the formation of the space charge boss (and is consequently found at or near the surface of the point), p is the gas pressure in mmm of Hg, and x_s is that distance from the point surface in cm where, on the average, one ion pair is formed by an electron advancing toward the point, that is, $\int_0^{x_s}\alpha dx=1$. Since the field varies rapidly over the gap, the calculation of X_1 involves the graphical integration of αdx over the axis of the gap. For this purpose, α must be known as a function of distance from the point. Such values are obtained from the measurements of α/p as a function of X/p *in uniform fields* from the measurements of Sanders[11] for air and from those of Hale[12] for hydrogen. Since the integral occurs as an exponent in Eq. (2), its value will be the dominant factor. Even if the value of α_s is replaced by the value of α corresponding to a distance of one ionizing free path away from the surface, and even if one allows x_s to take on different values, the final value of X_1 will be changed only slightly.

The numerical constant in (2) refers to air only. In order to calculate the constant for hydrogen, it is assumed that the electrons have an average energy of about two volts. For this case Ramien[13] gives $f=0.03$, and Brose and Saayman[14] give $\lambda_0=3\times10^{-5}$ cm, and thus $\lambda_0/\sqrt{f}=1.74\times10^{-4}$ cm. (If we assume an average electron energy of seven ev we find $\lambda_0/\sqrt{f}=4.8\times10^{-4}$ cm.) Thus for hydrogen, Eq. (2) becomes

$$X_1=\frac{5.55\times10^{-7}\,\alpha_s\exp\left[\int_0^{x_s}\alpha dx\right]}{(x_s/p)^{\frac{1}{2}}}\text{ volt/cm}. \quad (2')$$

The calculated results of the pre-onset streamer studies at lower pressures are compiled in Table I. In the case of room air, K varies by a factor of 12 in either gap, while for hydrogen the factor is 20 for the more divergent gap and even larger for the other gap. In dry air, and in both gaps, K varies only by a factor of two. Not too much

[10] See reference 2, page 45, Eq. (25).
[11] F. H. Sanders, Phys. Rev. **41**, 667 (1932); **44**, 1020 (1933).
[12] D. H. Hale, Phys. Rev. **54**, 241 (1938); **56**, 815 (1939).
[13] H. Ramien, Zeits. f. Physik **70**, 351 (1931).
[14] H. L. Brose and Saayman, Ann. d. Physik **5**, 797 (1930).

weight can be attributed to the absolute value of K since both x_s and α_s are not uniquely defined. Nevertheless, the decrease in K with decreasing pressure appears to be real.

The range of pressure in which onset streamers occur is much larger in room air than in dry air. It has been pointed out[9] that the efficiency of photo-ionization is very sensitive to extremely slight changes in the composition of a gas. This dependency of photo-ionization on purity, together with the knowledge that photo-ionization in the *gas* is the primary mechanism involved in streamer formation, provides a probable explanation for the difference in pressure ranges for streamer formation in dry and in room air.

ION CURRENTS IN DIVERGENCE GAPS

In order to determine K from the onset potentials of streamers, it has been seen that the space charge field of the positive ions must be calculated, and that this field is proportional to $\exp[\int \alpha dx]$. It has been recently pointed out by Morton[8] that in the glow discharge, the ionization does not take place where the values of the field strength are high, and that one cannot use the Townsend ionization functions when the field strength varies appreciably over a mean free path. Such considerations induced Morton to study Townsend currents in concentric cylinders in hydrogen and have led to the most interesting results. In much less divergent fields than were used in the present study, and at pressures of the order of a millimeter, he finds that the ionization is not given properly by integrating the ionization functions for uniform fields.

The question arose as to whether the calculations of the space charge field X_1 given in the earlier part of the paper could be in error due to the same phenomenon, thus explaining the variations in K. True, the pressures employed in the streamer studies were 300 to 700 times as large as the pressures used by Morton, but then the fields of the confocal paraboloids were very much more divergent than the fields of Morton's cylinders.

In order to decide whether the space charge calculations in the confocal paraboloid gap were falsified, the more divergent gap was provided with an external source of radiation, and the currents *well below* streamer onset were measured as a function of potential and pressure. From these measurements it is possible to determine the importance of the divergent field in calculating the space charge field X_1.

The sharpest point parabola (focal length 0.005 cm) was used and the gap length was again four centimeters. Ultraviolet light from a quartz mercury arc was focused by means of a quartz lens through a graded quartz seal on the center of the plate paraboloid. The radius of the circular image was estimated as two millimeters. The chamber was thoroughly baked out and was filled with hydrogen purified over hot copper. The current below onset was measured by means of a Dolezalek quadrant electrometer (sensitivity 1000 mm/volt) which was used to determine the potential drop across a high ohmage resistor. By keeping the ultraviolet arc on continuously during the run, the intensity of illumination was kept constant. The entire set of readings was taken during one continuous run, and the current through the arc changed by less than one percent.

Table II gives the different pressures and

TABLE II. Dark currents and related quantities as a function of voltage and pressure.

$P_{22°}$	Voltage	$\int \alpha dx$	$e\int \alpha dx$	Current (ampere)	i_0 (apparent) $\times 10^{13}$ (ampere)
676	3200	4.74	114	1.68×10^{-11}	1.47
676	3550	5.67	290	4.32×10^{-11}	1.49
676	3770	6.31	550	9.16×10^{-11}	1.67
676	3850	6.75	854	1.32×10^{-10}	1.55
676	3910	6.95	1043	1.82×10^{-10}	1.74
676	4150	7.63	2059	4.96×10^{-10}	2.41
676	4200	7.81	2463	6.68×10^{-10}	2.71
676	4270	8.10	3294	9.60×10^{-10}	2.91
676	4390	8.67	5825	1.71×10^{-9}	2.93
616	3350	5.58	265	4.32×10^{-11}	1.63
616	3560	6.25	493	1.02×10^{-10}	2.07
616	3660	6.33	561	1.68×10^{-10}	3.00
616	3950	7.24	1394	6.20×10^{-10}	4.43
616	4060	7.87	2617	1.13×10^{-9}	4.33
616	4150	8.22	3714	1.70×10^{-9}	4.57
548	3110	5.47	237	4.12×10^{-11}	1.74
548	3310	5.88	358	1.01×10^{-10}	2.83
548	3410	6.36	578	1.64×10^{-10}	2.84
548	3750	7.48	1772	6.96×10^{-10}	3.93
548	3840	7.74	2298	1.25×10^{-9}	5.43
477	2910	4.89	133	5.24×10^{-11}	3.94
477	3070	5.38	217	1.03×10^{-10}	4.74
477	3200	5.90	365	2.07×10^{-10}	5.67
477	3480	6.65	773	7.48×10^{-10}	9.68
408	2660	5.09	162	5.52×10^{-11}	3.41
408	2860	5.75	314	1.30×10^{-10}	4.14
408	2970	6.17	478	2.20×10^{-10}	4.60
408	3200	6.95	1043	7.80×10^{-10}	7.48
408	3350	7.56	1920	1.92×10^{-9}	10.0

potentials at which currents were measured. Also given are values of $\int \alpha dx$ and of $\exp[\int \alpha dx]$ calculated from the field distribution by graphical integration over the axis of the gap. The current *versus* potential curves are given by Fig. 2 for various pressures.

If the current is correctly determined by the use of Townsend's coefficient alpha, the measured current i is given by $i_0 \exp[\int \alpha dx]$, where i_0 is the initial photoelectric current. By dividing the measured current by $\exp[\int \alpha dx]$, one obtains an *apparent* i_0 which should be constant. The departure of i_0 from constancy is a direct measure of the discrepancy of the true ionization from the Townsend value predicted from $i_0 \exp[\int \alpha dx]$. A plot of the apparent i_0 against potential is given in Fig. 3 for the various pressures.

Experiments of the nature of those reported above were also performed in air, but the currents below streamer onset were too small to be measured conveniently. The currents in air were certainly less than one-hundredth of the currents measured in hydrogen. Comparison of values of Townsend's alpha for air and hydrogen leads one to expect currents of the same order of mag-

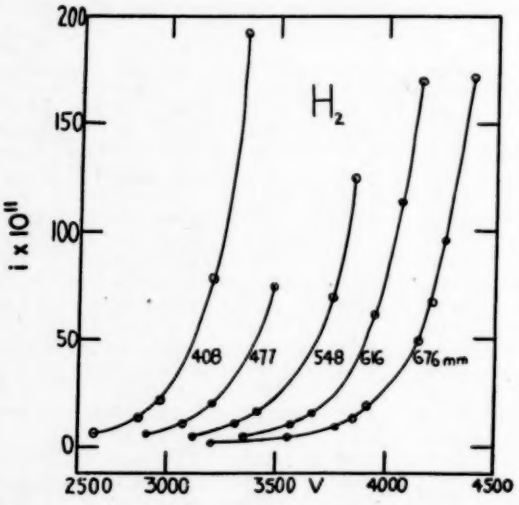

FIG. 2. Dark current *versus* potential curves for various pressures.

nitude in the two gases. The large currents in hydrogen must be ascribed to the great transparency of the gas to electrons and photons, and to the small energy losses of electrons in hydrogen as shown by the smaller threshold potentials for streamers in hydrogen as compared to air. Kip[15] has reported measurable currents in air with positive points below streamer onset only under strong radioactive irradiation.

CONCLUSIONS CONCERNING THE TWO EXPERIMENTS

It is clear from Fig. 3 that the ionization predicted from Townsend's function is far from correct, and that the apparent value of i_0 is not constant even at a constant pressure at varying potentials. At the highest pressure the value of the apparent i_0 is sensibly constant for a considerable voltage range and Townsend's equation is not far from correct. This pressure region corresponds to the pressure studied by Fitzsimmons. But as the pressure decreases, the deviation of the apparent i_0 from constancy becomes more and more marked. At high pressures the mean free path of the electrons are short; at low voltages all of the apparent i_0 *versus* voltage curves seem to be approaching roughly the same limiting value of i_0. From these considerations it seems reasonable to assume that the ionization at high pressure and low voltage may be taken as being accuractely represented by $i = i_0 \exp[\int \alpha dx]$, but that there is more ionization at lower pressures than is accounted for by Townsend's coefficient as applied to this equation. Such increased ionization at low pressures effectively introduces an *apparent* decrease in the value of K, not because of the failure of Meek's criterion, but because the theoretical calculation of the space charge field X_1 with Townsend's alpha does not correspond to reality.

The experiments on the onset of streamers actually determined the factor by which the actual space charge field in the gap differed from the space charge field calculated by means of $\exp[\int \alpha dx]$. Therefore the apparent variation of K is not due to a failure of Meek's criterion. The current measurements below onset are not only in the right direction to explain the trend in K, but the quantiative variation of K with pressure is explained in order of magnitude if the apparent i_0 *versus* voltage curves are extrapolated to streamer onset for each pressure. Thus the apparent failure of a constant value of K is to

[15] A. F. Kip, Phys. Rev. **54**, 139 (1938).

be ascribed to the use of the first Townsend coefficient in calculations which Morton showed cannot be applied when the change of field strength per electron free path is approximately two percent or larger, which applies to these investigations.

AN ATTEMPT TO EVALUATE THE FAILURE OF TOWNSEND'S IONIZATION FUNCTIONS

Between impacts, an electron in a gas in an electric field acquires the full energy of the work done by the field over the length of the component of the mean free path directed in the field direction. Suppose electrons exist in a gas in a divergent field such that the field strength varies appreciably over the distance of an electron free path, and such that the electrons travel from strong to weak fields. In such cases, where the field changes very rapidly over a few mean free paths, as they do about sharp points, the electrons gain a large share of the energy of the total potential drop (hundreds of electron volts) in a very few free paths. Under these conditions, the excitation functions and free paths are such that energy loss due to excitation and inelastic impacts is very small. The electrons gain a terminal energy nearly equal to the potential drop and thereafter can ionize more efficiently than they excite. Such ionization is not materially different from cathode-ray or slow β-ray ionization, where ionization reaches the order of an ion pair for 20 to 30 ev of energy expended.

In a uniform field of the same length as the gap, the energy gain of an electron free path near sparking is of the order of one electron volt. The electrons gain their terminal energy slowly, passing through regions in which excitation and energy losing impacts are quite frequent before and after gaining the ionizing energy. The electrons rarely gain much more than twice or three times the ionizing energy, with the result that the average energy expenditure per ion pair is much more than the 20 to 30 ev where electrons obtain an initial high energy at once and then proceed to ionize in relatively weak field regions.

Thus, under nearly uniform field conditions, where Townsend's equation holds, the ion production is small compared to the case where, as in glow discharges or about negative points, the energy gain is very rapid and is succeeded by a low field region where the energy is expended in ionization.

In the present experiments, however, the point is positive, and it would appear as if the ionization should not be greater than for the equi-

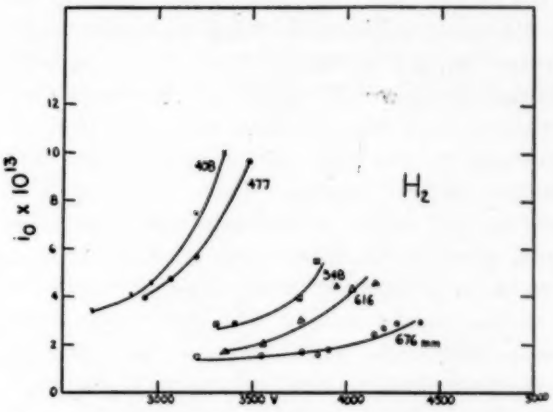

FIG. 3. The variation of the apparent i_0 with different potentials for various pressures.

librium case where Townsend's equation applies. In fact, it might even be expected to be *less*. In the equilibrium Townsend case the value of $\int \alpha dx$ is constant, irrespective of whether the electrons travel from high to low fields, or vice versa; that is, the function $\int \alpha dx$ is independent of the sign of the field. However, where the free paths are longer and the field changes appreciably over a free path it was seen that as in Morton's case, where the high field was negative, the ionization could be expected to be, and was, in fact, found to be greater than for the uniform Townsend case.

If now we consider the case where the high field region is positive with large gradients over the free paths near the anode, the situation is different. In the cathode region, electrons gain energy and may fritter away even more energy in excitation and in elastic impacts than in the higher Townsend gradients. However, near the anode, the sharp gradients over a mean free path will again rapidly raise the electron energy to possibly hundreds of electron volts over the last free paths with very little energy loss to excitation and elastic impacts. Now if pressures are so low that the electrons make very few collisions before they strike the anode, then in fact their whole energy will be lost and the ionization will be *less* than in Townsend's case. If, on the other

hand, the pressure is not too low, the high energy of the electrons and their random motions, despite the high anode field, will cause again a greater ionization than in the Townsend case. It is not inconceivable that owing to the attraction of the anode, these high energy electrons will not have as many collisions with gas molecules before capture by the anode as they did in moving through the low field region in Morton's case. However, both the electrons and their progeny generated in the high field region can be most effective before capture. This is indicated in Bradbury's[16] study of photoelectric currents in gases, where back diffusion of electrons is large even in the presence of fields, especially when the electronic energy is large. The magnitude of the excess ionization will obviously be critically pressure dependent, and will depend on Ramsauer free paths, excitation, and ionization functions. The effect will vary in different gases. Thus the excess ionization observed in the present experiment will be expected, as indicated above, provided the electrons, before being drawn in, spend more time than anticipated in the neighborhood of the point. Actually, high energy electrons of 100 ev near the anode will do just this at higher pressures, as has been recognized in Bradbury's study of photoelectric currents in gases. Thus it is not surprising that, under the conditions of the present experiments, the currents were found to be in excess of the value of $i_0 \exp[\int \alpha dx]$ calculated from Townsend's alpha, though one would expect the currents to be relatively less in excess than would be the case with the high field region at the cathode as in Morton's experiments.

In the present experiment, the field strength changes by 50 percent over a distance of 2.5×10^{-3} cm from the point, and the electrons just capable of ionization have approximately a mean free path of 10^{-4} cm at the lowest pressure studied. Hence, in the most extreme case, the field strength varies by approximately two percent over a mean free path. This is the amount of variation in the field strength over mean free path at which Morton finds abnormalities to begin in his currents.

The effect is undoubtedly a very complicated one, and its explanation must lie in the behavior of the energy distribution functions of the electrons as a function of voltage and pressure in a divergent field, as well as in the spatial distribution of collisions of higher energy electrons with atoms.

The present results in air may be explained by the attachment of electrons to oxygen molecules in the weak portion of the field. Loeb[17] has shown that such ions do not shed their electrons until they are in a field of $X/p = 90$ volts/cm/mm. In these extremely divergent fields, perhaps, the electron is released even closer to the point than corresponds to $X/p = 90$. If this explanation is correct, the calculation of Townsend currents in a divergent gap in air should be approached with even more caution than a similar calculation in hydrogen.

The authors wish to express their sincere thanks to Professor L. B. Loeb for his many helpful suggestions and for his valuable assistance in the interpretation of this work.

[16] N. E. Bradbury, Phys. Rev. **40**, 980 (1932); L. B. Loeb, *Fundamental Processes of Electrical Discharges in Gases* (John Wiley & Sons, Inc., New York, 1939), Chapter 7.

[17] L. B. Loeb, Phys. Rev. **48**, 684 (1935).

On the Binding Energy of Deuteron and the Neutron-Proton Scattering by a New Potential

MU-HSIEN WANG
Department of Physics, National University of Chekiang, Meitan, Kweichow, China
(Received June 2, 1944)

The binding energy of deuteron and scattering cross section of proton by fast neutron are calculated by using new forms of nuclear potential suggested by Wang. The results obtained are found to be in good agreement with the experimental values, when "zero cut-off" of the potential is employed.

IT is pointed out by Wang[1] that the force between two nuclear particles may be related to the gravitational force. He takes two alternative forms of the nuclear potential,

$$V=-Ae^{K/r}, \tag{1a}$$

and

$$V=-(B/r)e^{K/r}, \tag{1b}$$

with

$$K=\hbar/mc=3.84\times10^{-11}\text{ cm},$$

where the constants A and B, as determined by the gravitational constant, are 4.78×10^{-45} and 1.84×10^{-55}, respectively.

The purpose of the present work is to determine whether the potential (1a) and (1b) can give correct results about the binding energy of a deuteron and the scattering cross section of the neutron by the proton. The calculations follow closely those of Bethe and Bacher.[2]

I. THE BINDING ENERGY OF THE DEUTERON

The wave equation for the relative motion of the two nuclear particles is

$$\Delta\psi+(M/\hbar^2)(E-V)\psi=0. \tag{2}$$

The potential is spherically symmetric; (2) can thus be separated in polar coordinates r, θ, ϕ, by putting

$$\psi(r,\theta,\phi)=(1/r)u_lP_{lm}(\theta)e^{im\phi},$$

where P_{lm} is a spherical harmonic. The wave equation for u_l is then

$$\frac{\hbar^2}{M}\left(\frac{d^2u_l}{dr^2}-\frac{l(l+1)}{r^2}u_l\right)+(E-V)u_l=0.$$

For the ground state $l=0$, we have

$$\frac{d^2u_0}{dr^2}+\frac{M}{\hbar^2}(E-V)u_0=0. \tag{3}$$

To solve Eq. (3), two ways of cut-off of the potential given by (1a) and (1b) are employed; *viz.*,

(a) zero cut-off:

$V=0$, for $r<a$; $V=V(r)$, for $r>a$.

(b) straight cut-off:

$V=V(a)$, for $r<a$; $V=V(r)$, for $r>a$.

(a) Zero Cut-Off

For $r<a$, $V=0$; Eq. (3) takes the form,

$$\frac{d^2u_0}{dr^2}-\frac{M\epsilon}{\hbar^2}u_0=0,$$

where $\epsilon=-E$, the binding energy of the deuteron. Its solution is

$$u_0=D(e^{\beta r}-e^{-\beta r}),$$

where

$$\beta=(M\epsilon/\hbar^2)^{\frac{1}{2}},$$

and

$$du_0/dr=D\beta(e^{\beta r}+e^{-\beta r}).$$

Therefore

$$\left(\frac{1}{u_0}\frac{du_0}{dr}\right)_{r=a}=\beta\coth\beta a. \tag{4}$$

For $r>a$, $V=V(r)$; the asymptotic solution of (3) is

$$u_0=ce^{-\beta r}.$$

Now we treat c as a slowly varying quantity whose second derivative with respect to r may be set equal to zero. In so doing, we have

$$du_0/dr=c'e^{-\beta r}-\beta ce^{-\beta r},$$

$$d^2u_0/dr^2=-2\beta c'e^{-\beta r}+\beta^2ce^{-\beta r}.$$

[1] K. C. Wang and H. L. Tsao, Phys. Rev. **66**, 155 (1944).
[2] H. A. Bethe and R. E. Bacher, Rev. Mod. Phys. **8**, 82 (1936).

TABLE I. Numerical values for Eq. (7) when $V=-Ae^{K/r}$ for $r>a$ and $V=0$ for $r<a$.

ϵ, in 10^{-6} erg	coth $[1.24\times10^{15}a(V_0-\epsilon)^{\frac{1}{2}}]$	$\frac{V_0}{2\epsilon}-1$
3.50	1.33	1.38
3.60	1.32	1.32
3.70	1.31	1.26

TABLE II. Numerical values for Eq. (7) when $V=-(B/r)e^{K/r}$ for $r>a$ and $V=0$ for $r<a$.

ϵ, in 10^{-6} erg	coth $[1.24\times10^{15}a(V_0-\epsilon)^{\frac{1}{2}}]$	$\frac{V_0}{2\epsilon}-1$
3.50	1.29	1.38
3.60	1.29^-	1.32
3.70	1.27	1.26
3.80	1.26^+	1.19

Substituting this last expression in (3), we get the differential equation for c,

$$dc/dr=c'=-MVc/2\beta\hbar^2,$$

the solution of which is

$$c=F\exp\left(-\int\frac{MV}{2\beta\hbar^2}dr\right).$$

Thus

$$u_0=F\exp\left(-\beta r-\int\frac{MV}{2\beta\hbar^2}dr\right),$$

and

$$\left(\frac{1}{u_0}\frac{du_0}{dr}\right)_{r=a}=\frac{M|V(a)|}{2\beta\hbar^2}-\beta. \qquad (5)$$

In order that the wave function u_0 could be joined at $r=a$ smoothly, the expressions (4) and (5) must be equal; i.e.,

$$\frac{M|V(a)|}{2\beta\hbar^2}-\beta=\beta\coth\beta a. \qquad (6)$$

(b) Straight Cut-Off

For $r<a$, $V=V(a)$; Eq. (3) takes the form

$$\frac{d^2u_0}{dr^2}+\frac{M}{\hbar^2}(|V(a)|-\epsilon)u_0=0.$$

Its solution is

$$u_0=G\sin\gamma r,$$

with

$$\gamma=\left[\frac{M}{\hbar^2}(|V(a)|-\epsilon)\right]^{\frac{1}{2}}.$$

Thus

$$\left(\frac{1}{u_0}\frac{du_0}{dr}\right)_{r=a}=\gamma\cot\gamma a.$$

For $r>a$, $(1/u_0)(du_0/dr)$ is same as given by (5). Therefore, instead of (6), we have

$$\frac{M|V(a)|}{2\beta\hbar^2}-\beta=\gamma\cot\gamma a. \qquad (6a)$$

Equations (6) and (6a) serve to determine the binding energy of the deuteron ϵ if we use the experimental value of $-V(a)=V_0$, the depth of the potential well, and calculate a, the range of the nuclear force, from (1a) or (1b). Conversely, if we use the experimental value of ϵ, we can calculate the value of V_0, and a by the aid of Eq. (1a) or (1b).

(c) Numerical Calculations

(1) $V=0$, for $r<a$; $V=-Ae^{K/r}$, for $r>a$. We take the recent experimental value $V_0=10.5$ Mev; then a calculated from (1a) is equal to 4.21×10^{-13} cm. Equation (6) becomes numerically,

$$\coth[1.24\times10^{15}a(V_0-\epsilon)^{\frac{1}{2}}]=V_0/2\epsilon-1. \qquad (7)$$

From Table I we see that the root of (7), the binding energy of deuteron, is 3.60×10^{-6} erg or 2.26 Mev.

(2) $V=0$, for $r<a$; $V=-(B/r)e^{K/r}$, for $r>a$. Also take $V_0=10.5$ Mev; then a is equal to 4.42×10^{-13} cm from (1b).

TABLE III. Numerical values for Eq. (7) when $V=V(a)$ for $r<a$ and $V=-Ae^{K/r}$ for $r>a$.

ϵ, in 10^{-6} erg	cot $[1.24\times10^{15}a(V_0-\epsilon)^{\frac{1}{2}}]$	$\frac{V_0/2\sqrt{\epsilon}-\sqrt{\epsilon}}{(V_0-\epsilon)^{\frac{1}{2}}}$
7.80	0.018	0.067
8.00	0.038	0.037
8.20	0.061	0.027

TABLE IV. Numerical values for Eq. (7) when $V=V(a)$ for $r<a$ and $V=-(B/r)e^{K/r}$ for $r>a$.

ϵ, in 10^{-6} erg	cot $[1.24\times10^{15}a(V_0-\epsilon)^{\frac{1}{2}}]$	$\frac{V_0/2\sqrt{\epsilon}-\sqrt{\epsilon}}{(V_0-\epsilon)^{\frac{1}{2}}}$
8.20	−0.020	0.206
8.30	−0.013	0.005
8.40	−0.004	−0.083

The binding energy of deuteron from Table II is 3.66×10^{-6} erg or 2.30 Mev. The results given by (1) and (2) are in good agreement with the experimental value 2.17 Mev.

(3) $V=V(a)$, for $r<a$; $V=-Ae^{K/r}$, for $r>a$. Also take $V_0=10.5$ Mev, then a is 4.21×10^{-13} cm from (1a). Equation (6a) turns out numerically to be

$$\cot\,[1.24\times10^{15}a(V_0-\epsilon)^{\frac{1}{2}}]$$
$$=[(V_0/2\sqrt{\epsilon})-\sqrt{\epsilon}]/(V_0-\epsilon)^{\frac{1}{2}}.$$

(4) $V=V(a)$, for $r<a$; $V=-(B/r)e^{K/r}$, for $r>a$.

From Tables III and IV, the binding energy of the deuteron is 8.0×10^{-6} and 8.3×10^{-6} erg, respectively. These values are too large in comparison with the experimental value. The correct value will be obtained if we take $V_0=5.93$ Mev.

II. THE SCATTERING OF NEUTRON BY PROTON

Let us denote E the kinetic energy of a proton and a neutron in a coordinate system in which the center of gravity of the two particles is at rest, which is equal to one-half of the kinetic energy of the incident neutron in a system at rest. The wave function u_l will satisfy the equation,

$$\frac{\hbar^2}{M}\left(\frac{d^2u_l}{dr^2}-\frac{l(l+1)}{r^2}u_l\right)+(E-V)u_l=0. \quad (8)$$

Asymptotically for large r, the solution of (8) is

$$u_l=c\,\sin\,(Kr-\tfrac{1}{2}l\pi+\delta_l), \quad (9)$$

with

$$K=(ME/\hbar^2)^{\frac{1}{2}}.$$

Then the cross section $d\sigma$, the number of the neutrons scattered per unit time through an angle θ and $\theta+d\theta$, if there is one neutron crossing unit area per unit time in the incident beam, is given by the well-known formula,

$$d\sigma=(\pi/2K^2)$$
$$\times|\textstyle\sum_l(2l+1)P_l(\theta)[\exp\,(2i\delta_l)-1]|^2\sin\theta d\theta. \quad (10)$$

It has been shown[3] that if $1/K\gg a$, a being the range of the force, all phases δ_l will be small except δ_0. Then

$$d\sigma=2\pi K^{-2}\sin^2\delta_0\sin\theta d\theta,$$

[3] Cf. reference 2, p. 115.

TABLE V. Comparison of values of $\sigma\times10^{24}$.

E, Mev	σ_0	σ	$\sigma_0(B)$	$\sigma(B)$	σ(obs.)
2.15	0.85	1.43	1.2	1.8	(0.5–0.8)
1.05	1.03	1.86	1.6	2.4	(1.1–1.5)

and

$$\sigma=\int d\sigma=4\pi K^{-2}\sin^2\delta_0. \quad (11)$$

For the ground state of deuteron, we have already shown that

$$\left(\frac{1}{u_0^-}\frac{du_0^-}{dr}\right)_{r=a}=\left(\frac{MV_0}{2\beta\hbar^2}-\beta\right)\equiv\alpha. \quad (12)$$

Now, in the present case E is positive; we should have[3]

$$\left(\frac{1}{u_0^+}\frac{du_0^+}{dr}\right)_{r=a}=\alpha-\frac{M(E+\epsilon)}{\hbar^2u_0^+(a)u_0^-(a)}\int_0^a u_0^+u_0^-dr$$
$$=\alpha-\frac{\eta aM(E+\epsilon)}{\hbar^2}\equiv A, \quad (13)$$

where u_0^+ and u_0^- are the u_0 functions for $r<a$ corresponding to the positive and negative values of E, respectively; i.e.,

$$u_0^+=B\sin Kr,\quad u_0^-=D(e^{\beta r}-e^{-\beta r});$$

therefore

$$\eta a=\frac{1}{u_0^+(a)u_0^-(a)}\int_0^a u_0^+u_0^-dr$$
$$=\frac{\beta\coth\beta a-K\cot Ka}{\beta^2+K^2}. \quad (14)$$

For large r,

$$\left(\frac{1}{u_0^+}\frac{du_0^+}{dr}\right)_{r=a}=K\cot\,(Ka+\delta_0). \quad (15)$$

In order to join the wave function at $r=a$ smoothly, the expressions given by (13) and (15) must be equal, thus

$$K\cot\,(Ka+\delta_0)=A. \quad (16)$$

Under the assumption that Ka is small, we have

$$\cot\,\delta_0=A/K, \quad (17)$$

and by (11),

$$\sigma=4\pi/K^2+A^2. \quad (18)$$

If η is small $A\approx\alpha$, and we have

$$\sigma_0=4\pi/K^2+\alpha^2. \quad (19)$$

The numerical results are given in Table V in taking $V=-Ae^{K/r}$, and the values of α are obtained from Table I at the point $r=a$. Corresponding to (18) and (19), Bethe and Bacher have derived[3] the formulae: $\sigma_0(B)=4\pi\hbar^2/\epsilon+E$, $\sigma(B)=3\sigma_0/2$, and the values calculated from these are given for comparison in the fourth and fifth columns of Table V.

It is seen that the present results are in better agreement with the experimental results than those given by Bethe and Bacher. If we take $V=-(B/r)e^{K/r}$, the results do not differ appreciably from that given above.

In conclusion, the author wishes to express his thanks to Dr. K. C. Wang for suggesting the calculation and for helpful discussions.

PHYSICAL REVIEW VOLUME 66, NUMBERS 5 AND 6 SEPTEMBER 1 AND 15, 1944

Momentum and Energy of Photon and Electron in the Čerenkov Radiation

R. T. Cox
Johns Hopkins University, Baltimore, Maryland

(Received June 22, 1944)

The conservation of momentum and energy between an emitted photon and an electron in the Čerenkov radiation gives an equation for the direction of emission. This equation differs from the one which Frank and Tamm derived from electromagnetic theory only by a negligible term involving the ratio of the wave-length of the electron to that of the photon.

IT has been observed by Čerenkov[1] that fast electrons traversing a transparent medium emit a radiation, continuous through the visible spectrum and beyond, which differs in respect to its polarization and angular distribution from radiation previously found with similar sources. Frank and Tamm[2] have given an electrodynamic theory of this radiation similar to the dynamic theory of the bow wave of a ship or the conical wave around the path of a bullet moving through the air at a speed greater than the speed of sound. According to this theory the emitted radiation has a component of every wave-length of which the speed in the medium is less than the speed of the electron. The energy per unit length of path radiated by the electron in the frequency range $d\nu$ is $(2\pi e/c)^2(1-1/\beta^2n^2)\nu d\nu$, where e is the electronic charge, c the speed of light in vacuum, β the ratio to this speed of the speed of the electron, and n the index of refraction of the medium for light of frequency ν. The emitted rays make an angle θ with the electron velocity given by $\cos\theta=1/n\beta$, and they are polarized with the electric vector in the plane of this angle. The theory accords with the observations of Čerenkov, and it has been confirmed by observations under more favorable experimental conditions made by Collins and Reiling[3] and, over a considerable range of electron speeds, by Wyckoff and Henderson.[4]

Although the phenomenon has thus an adequate classical explanation, it is interesting also to treat it by considering the conservation of momentum and energy between the electron and an emitted photon of the radiation. Let it be supposed that the electron, traversing the medium with a speed u, emits a photon of energy $h\nu$ in a direction making an angle θ with the initial velocity of the electron. After the emission, let the speed of the electron be v and let the angle between its final and initial velocities be ϕ. By the conservation of momentum, the angles θ and ϕ will be coplanar and on opposite sides of the initial direction of the velocity of the electron.

Also, by the conservation of momentum,

$$mv(1-v^2/c^2)^{-\frac{1}{2}}\cos\phi+(h/\lambda)\cos\theta = mu(1-u^2/c^2)^{-\frac{1}{2}},$$

$$mv(1-v^2/c^2)^{-\frac{1}{2}}\sin\phi-(h/\lambda)\sin\theta=0.$$

[1] P. A. Čerenkov, Comptes rendus Acad. Sci. U.S.S.R. **8**, 451 (1934); **12**, 413 (1936); **14**, 102 (1937); **14**, 105 (1937); Phys. Rev. **52**, 378 (1937).

[2] I. Frank and Ig. Tamm, Comptes rendus Acad. Sci. U.S.S.R. **14**, 109 (1937). The subject has also been treated by Fermi, Phys. Rev. **57**, 485 (1940), in the development of a classical theory of the retardation of charged particles in gaseous and condensed media.

[3] G. B. Collins and V. G. Reiling, Phys. Rev. **54**, 499 (1938).

[4] H. O. Wyckoff and J. E. Henderson, Phys. Rev. **64**, 1 (1943).

And by the conservation of energy

$$mc^2(1-v^2/c^2)^{-\frac{1}{2}}+h\nu=mc^2(1-u^2/c^2)^{-\frac{1}{2}},$$

where m is the rest-mass of the electron and λ the wave-length of the photon in the medium. That the wave-length in the medium, rather than in vacuum, is the divisor of h in the momentum is required by the fact that in quantum mechanics it is the momentum which determines any interference pattern in the medium which might be used for the measurement of the wave-length. It has also been pointed out elsewhere[5-7] that this value for the momentum is needed for consistency with the laws of refraction and radiation pressure.

In the paper just cited, Michels and Patterson, considering relativity in a non-dispersive medium, have also proposed that c/n, the speed of light in the medium, should replace c in the expressions for the momentum and energy of a particle. If there were a non-dispersive medium, the calculation of Frank and Tamm indicates that in it a charged particle would have as its limiting speed c/n, rather than c as in empty space. For the expression $(2\pi e/c)^2(1-1/\beta^2n^2)\nu$ would have to be integrated, with n constant, over all values of the frequency ν to give the energy radiated per unit length of path. This integral being infinite, an infinite force would be required to maintain the particle at any speed above c/n. Thus the calculation of Frank and Tamm provides some support, at least of a formal kind, to the conclusion of Michels and Patterson. At the same time, however, it shows that the assumption of a non-dispersive medium is inappropriate for the treatment of the Čerenkov radiation, since in this phenomenon the electrons actually traverse appreciable distances at speeds greater than the speed of the radiation in the medium.

In the present treatment the use of c/n rather than c in the relativistic expressions for the momentum and energy of the electron would make them and hence also the momentum and energy of the photon imaginary at electron speeds at which radiation is actually emitted.

Justification for considering the modification which the medium makes, through its modification of the wave-length, upon the momentum of the photon, while ascribing to it no modification of the momentum of the electron, may probably be based on a comparison of the wave-lengths of photon and electron with the interatomic distances in the medium. The wave-lengths of light for which the index of refraction is appreciably greater than unity are so much greater than the interatomic distances that it appears reasonable to treat the medium as continuous in considering the motion of the photons. On the other hand, the wave-lengths of fast electrons are so much smaller than the interatomic distances that in considering their motion it would seem necessary to regard the medium from the Lorentzian point of view as simply space with a distribution of charged particles. Thus the ordinary relativistic expression for the momentum of a particle in space would be required.

The elimination of ϕ and v among the three equations above, together with the substitution $\nu=c/n\lambda$, gives the result

$$\cos\theta=c/nu+h(1-u^2/c^2)^{\frac{1}{2}}(n^2-1)/(2mun^2\lambda).$$

This may be written

$$\cos\theta=1/n\beta+(\Lambda/\lambda)(n^2-1)/2n^2,$$

where $\beta=u/c$ and Λ is the de Broglie wave-length of the electron before the emission of the photon. The first term on the right is the expression for $\cos\theta$ derived classically by Frank and Tamm. The second, in which h is a factor, illustrates the rule that a quantum equation becomes identical with the corresponding classical one when h is replaced by zero. Or, to say much the same thing in another way, this term is a natural one to find as the difference between a quantum calculation and a classical one, since the classical calculation of course ignores any effect associated with the wave-length of the electron.

This term will be very small since, as was mentioned earlier, the wave-length of the electron is very much smaller than that of the photon. Hence the classical approximation is a very good one, and the direction of emission of the light does not appreciably depend upon its wave-length except as the wave-length determines the refractive index.

[5] L. Brillouin, Comptes rendus **178**, 1696 (1924).
[6] R. T. Cox and J. C. Hubbard, Proc. Nat. Acad. Sci. 11, 498 (1925).
[7] W. C. Michels and A. L. Patterson, Phys. Rev. **60**, 589 (1941).

Free Vibrations of Anisotropic Bodies

H. EKSTEIN
Research Laboratory, Commercial Equipment Company, Kansas City, Missouri
(Received April 17, 1944)

Approximate solutions for free vibrations of a finite anisotropic body are derived by a perturbation method. As an example, some extensional modes of thin crystal plates are calculated. Calculated frequencies and deformation patterns are compared with observations.

1. SKETCH OF THE METHOD

ONLY very few problems of elastic vibration are susceptible of rigorous solution by the methods of the general theory of elasticity. During the last years stationary vibrations of crystalline bodies have become of practical importance because of the discovery of piezoelectric excitation of vibrations. Rigorous solutions for free vibrations of a crystalline body are known only for an infinitely extended plane parallel plate and an infinitely thin rod. It has become desirable to obtain even rough approximations, as rigorous solutions for most problems are inaccessible. Some attempts in this direction have been made by Mason[1] and Bechmann.[2]

It is attempted here to give a more systematic method of approach. The perturbation method has been used for a long time especially in quantum mechanics. To our knowledge, adaptation of this powerful method to the theory of elasticity has not been made.

We first make a resume of well-known equations of elastic vibrations. If U, V, W are the Cartesian components of the displacement and if we have stationary vibrations of angular frequency $\Omega=2\pi\nu$, they take the form[3]

$$\begin{aligned}\rho\Omega^2U&=\partial X_x/\partial x+\partial X_y/\partial y+\partial X_z/\partial z,\\ \rho\Omega^2V&=\partial X_y/\partial x+\partial Y_y/\partial y+\partial Y_z/\partial z,\\ \rho\Omega^2W&=\partial X_z/\partial x+\partial Y_z/\partial y+\partial Z_z/\partial z.\end{aligned}\tag{1}$$

The strain components are defined by

$$\begin{aligned}x_x&=\partial U/\partial x, & x_y&=\partial U/\partial y+\partial V/\partial x,\\ y_y&=\partial V/\partial y, & y_z&=\partial V/\partial z+\partial W/\partial y,\\ z_z&=\partial W/\partial z, & x_z&=\partial U/\partial z+\partial W/\partial x.\end{aligned}\tag{2}$$

The general linear relation between stress components and strain components is

$$\begin{aligned}-X_x&=c_{11}x_x+c_{12}y_y+c_{13}z_z+c_{14}y_z+c_{15}x_z+c_{16}x_y,\\ &\cdots\cdots\cdots\cdots\cdots\\ -X_y&=c_{61}x_x+c_{62}y_y+c_{63}z_z+c_{64}y_z+c_{65}x_z+c_{66}x_y,\end{aligned}\tag{3}$$

with

$$c_{ik}=c_{ki};$$

and the inversion of (3) is

$$\begin{aligned}-x_x&=s_{11}X_x+s_{12}Y_y+\cdots+s_{16}X_y,\\ &\cdots\cdots\cdots\cdots\cdots\\ -x_y&=s_{61}X_x+s_{62}Y_y+\cdots+s_{66}X_y.\end{aligned}\tag{4}$$

If we eliminate the strain and stress components from these equations, we obtain three equations of the form

$$\begin{aligned}\rho\Omega^2U+K(U,V,W)&=0,\\ \rho\Omega^2V+L(U,V,W)&=0,\\ \rho\Omega^2W+M(U,V,W)&=0,\end{aligned}$$

with

$$K(U,V,W)=-\left(\frac{\partial X_x}{\partial x}+\cdots\right),\tag{5}$$

$$\cdots\cdots\cdots\cdots$$

where K, L, M are linear operators of second order which act on three components U, V, W.

The boundary conditions for the free body take the form:

$$\begin{aligned}X_x\cos(n,x)+X_y\cos(n,y)+X_z\cos(n,z)&=0,\\ X_y\cos(n,x)+Y_y\cos(n,y)+Y_z\cos(n,z)&=0,\\ X_z\cos(n,x)+Y_z\cos(n,y)+Z_z\cos(n,z)&=0,\end{aligned}\tag{6}$$

where n signifies the normal to the surface, directed inwardly to the body.

The fact is remembered that any two rigorous solutions of (5) and (6) are orthogonal to each other:[4]

$$\int(U_1U_2+V_1V_2+W_1W_2)dv=0,\tag{7}$$

where the integration is extended over the body.

[1] W. P. Mason, Bell Sys. Tech. J. **13**, 405 (1934).
[2] R. Bechmann, Zeits. f. Physik **117**, 180 (1941); **118**, 515 (1941); **120**, 107 (1942).
[3] W. Voigt, *Lehrbuch der Kristallphysik* (B. G. Teubner, Leipzig, 1910).
[4] A. E. H. Love, *The Mathematical Theory of Elasticity* (Cambridge University Press, 1934).

We shall try to represent the solution (U, V, W) approximately as a sum of zero-order functions (u_i, v_i, w_i) which are chosen so that they are rough approximations of the actual solution. We write:

$$U=\sum A_i u_i, \quad V=\sum A_i v_i, \quad W=\sum A_i w_i. \tag{8}$$

However, this expansion is possible only if the functions (u_i, v_i, w_i) satisfy the boundary conditions (6). In the following, we shall not suppose this to be true, so that (8) does not hold in general. We will construct a set of auxiliary functions (u_i', v_i', w_i') so that they are equal to the functions (u_i, v_i, w_i) everywhere but in a small domain close to the boundary. In this domain, (u_i', v_i', w_i') will behave so as to satisfy the conditions (6). We will write:

$$U=\sum A_i u_i', \quad V=\sum A_i v_i', \quad W=\sum A_i w_i'. \tag{9}$$

We now define strain and stress functions:

$$x_{xi}=\partial u_i/\partial x \cdots x_{yi}=\partial u_i/\partial y+\partial v_i/\partial x, \tag{10}$$

and

$$-X_{xi}=c_{11}x_{xi}+\cdots+c_{16}x_{yi}. \tag{11}$$

. . . . . .

The functions (u_i, v_i, w_i) will not satisfy Eq. (5), but will satisfy equations of the form:

$$\begin{aligned}
-K(u_i, v_i, w_i)&=\partial X_{xi}/\partial x+\partial X_{yi}/\partial y\\
&\quad+\partial X_{zi}/\partial z=-f_i,\\
-L(u_i, v_i, w_i)&=\partial X_{yi}/\partial x+\partial Y_{yi}/\partial y\\
&\quad+\partial Y_{zi}/\partial z=-g_i,\\
-M(u_i, v_i, w_i)&=\partial X_{zi}/\partial x+\partial Y_{zi}/\partial y\\
&\quad+\partial Z_{zi}/\partial z=-h_i.
\end{aligned} \tag{12}$$

Instead of the boundary conditions (6), the functions (u_i, v_i, w_i) will satisfy equations of the form:

$$\begin{aligned}
X_{xi}\cos(n, x)+\cdots&=\varphi_i(s),\\
X_{yi}\cos(n, x)+\cdots&=\psi_i(s),\\
X_{zi}\cos(n, x)+\cdots&=\chi_i(s).
\end{aligned} \tag{13}$$

Similarly, the corresponding functions derived from the auxiliary functions (u_i', v_i', w_i') will be denoted by

$$f_i', g_i', h_i' \quad \text{and} \quad \varphi_i', \psi_i', \chi_i'.$$

It will be noticed that $u_i \cdots$ can be considered as solution of the following problem: Given a volume force of components $-f_i/\rho$, $-g_i/\rho$, and $-h_i/\rho$, respectively, and surface tractions of components φ_i, ψ_i, χ_i, respectively, the equilibrium deformations of the body are to be determined. From Eqs. (12) and (13) it can be seen that the requirements for the solution of this problem are met by u_i, v_i, and w_i.

Let S' be a surface internal to the surface S of the body and parallel to S, having a small distance ϵ from S so that to each point s on S there corresponds a point s' on S'. The corresponding points are joined by the normal n which is directed toward the interior. Let the domain included between S and S' be called D, while the rest of the body volume is V. The tractions across S' which have the form of the first members of (13) will be found by integrating the functions $-f_i$, $-g_i$, $-h_i$ along the normal n:

$$\begin{aligned}
&\int\left(\frac{\partial X_{xi}}{\partial x}+\frac{\partial X_{yi}}{\partial y}+\frac{\partial X_{zi}}{\partial z}\right)dn\\
&\quad=|X_{xi}\cos(n, x)+X_{yi}\cos(n, y)\\
&\qquad+X_{zi}\cos(n, z)|_{n=0}^{n=\epsilon},
\end{aligned} \tag{14}$$

$$\int\left(\frac{\partial X_{yi}}{\partial x}+\cdots\right)dn=|X_{yi}\cos(n, x)+\cdots|_{n=0}^{n=\epsilon},$$

$$\int\left(\frac{\partial X_{zi}}{\partial x}+\cdots\right)dn=|X_{zi}\cos(n, x)+\cdots|_{n=0}^{n=\epsilon}.$$

If we use (12) and (13) we obtain

$$\begin{aligned}
&\{X_{xi}\cos(n, x)+X_{yi}\cos(n, y)\\
&\qquad+X_{zi}\cos(n, z)\}_{n=\epsilon}=\varphi_i(s)-\int_0^\epsilon f_i\,dn,
\end{aligned} \tag{15}$$

. . . . . .,

where the dots stand for the two analogous equations.

The same calculation for the functions $u_i' \cdots$ yields similarly:

$$\begin{aligned}
&\{X_{xi}'\cos(n, x)+X_{yi}'\cos(n, y)\\
&\qquad+X_{zi}'\cos(n, z)\}_{n=\epsilon}=\varphi_i'(s)-\int_0^\epsilon f_i'\,dn,
\end{aligned} \tag{16}$$

. . . . . .

Returning to the definition of the auxiliary functions $u_i' \cdots$, we remember that they should be equal to $u_i \cdots$ within V. Therefore, they must be solutions of a problem involving the

same forces $-f_i/\rho\cdots$ within V and the tractions across S' given by (15). Thus, the first members of (15) and (16) are equal:

$$\varphi_i(s)-\int_0^s f_i dn=\varphi_i'(s)-\int_0^s f_i' dn. \quad (17)$$

By definition of the $u_i'\cdots$, the tractions $\varphi_i'\cdots$ must vanish:

$$\begin{aligned}\int_0^s f_i' dn&=\int_0^s f_i dn-\varphi_i,\\ \int_0^s g_i' dn&=\int_0^s g_i dn-\psi_i, \quad (18)\\ \int_0^s h_i' dn&=\int_0^s h_i dn-\chi_i.\end{aligned}$$

We substitute (9) into (5):

$$\begin{aligned}\rho\Omega^2\textstyle\sum A_i u_i'+\sum A_i K(u_i', v_i', w_i')&=0,\\ \rho\Omega^2\textstyle\sum A_i v_i'+\sum A_i L(u_i', v_i', w_i')&=0, \quad (19)\\ \rho\Omega^2\textstyle\sum A_i w_i'+\sum A_i M(u_i', v_i', w_i')&=0.\end{aligned}$$

We multiply these equations by u_k', v_k', w_k', respectively, add them, and integrate over the crystal:

$$\begin{aligned}\sum_i A_i\Big[\rho\Omega^2\int(u_i'u_k'+v_i'v_k'+w_i'w_k')dv&\\ +\int\{u_k'K(u_i', \cdots)+v_k'L(u_i', \cdots)&\\ +w_k'M(u_i', \cdots)\}dv\Big]&=0. \quad (20)\end{aligned}$$

As $u_i'\cdots$ tends toward $u_i\cdots$, the first integral in (20) becomes:

$$\int(u_iu_k+v_iv_k+w_iw_k)dv=N_{ik}. \quad (21)$$

In view of (7) the non-orthogonality integrals N_{ik} would vanish for $i\neq k$ if the functions $(u_i\cdots)$ were exact solutions of the problem.

The integrals N_{ii} will be determined arbitrarily by normalization:

$$\int(u_i^2+v_i^2+w_i^2)dv=1=N_{ii}. \quad (22)$$

The volume V inside of S' contributes to the second integral of (20) the term:

$$\int[u_kK(u_i, \cdots)+v_kL(u_i, \cdots)+w_kM(u_i, \cdots)]dv.$$

The contribution of D to this integral is

$$\begin{aligned}\int_D[u_k'K(u_i', \cdots)+\cdots]dv&=\int_D(u_k'f_i'+\cdots)dv\\ &=\int_S ds\Big[u_k\int_0^s f_i' dn+\cdots\Big], \quad (23)\end{aligned}$$

where u_k' is put equal to u_k and considered as a constant along the normal n. Substituting (18) into (23) we find

$$\begin{aligned}\int_D[u_k'K(u_i', \cdots)+]dv=\int_S ds\Big[u_k\Big\{\int_0^s f_i dn-\varphi_i\Big\}&\\ +v_k\Big\{\int_0^s g_i dn-\psi_i\Big\}+w_k\Big\{\int_0^s h_i dn-\chi_i\Big\}\Big].&\end{aligned}$$

When ϵ tends toward zero, the integrals $\int_0^s f_i dn\cdots$ vanish and we have

$$\begin{aligned}\int_D[u_k'K(u_i', \cdots)+\cdots]dv&\\ =-\int_S ds(u_k\varphi_i+v_k\psi_i+w_k\chi_i).&\end{aligned}$$

Equation (20) now takes the form:

$$\begin{aligned}\sum_i A_i\Big[\rho\Omega^2N_{ik}+\int\{u_kK(u_i, \cdots)+v_kL(v_i, \cdots)&\\ +w_kM(u_i, \cdots)\}dv&\\ -\int(\varphi_iu_k+\psi_iv_k+\chi_iw_k)ds\Big]&=0,\end{aligned}$$

or

$$\textstyle\sum_i A_i(\rho\Omega^2N_{ik}-H_{ik})=0, \quad (24)$$

where

$$\begin{aligned}H_{ik}=-\int(f_iu_k+g_iv_k+h_iw_k)dv&\\ +\int(\varphi_iu_k+\psi_iv_k+\chi_iw_k)ds.& \quad (25)\end{aligned}$$

If we consider, as above, two sets of functions u_i, v_i, w_i and u_k, v_k, w_k as solutions of two different equilibrium problems involving the given volume forces and surface tractions,

$$\begin{aligned}&-f_i/\rho, -g_i/\rho, -h_i/\rho;\quad \varphi_i, \psi_i, \chi_i\\ \text{and}\quad&-f_k/\rho, -g_k/\rho, -h_k/\rho;\quad \varphi_k, \psi_k, \chi_k,\end{aligned}$$

respectively, then a theorem due to Betti[3] states that:

$$-\int(f_i u_k+g_i v_k+h_i w_k)dv + \int(\varphi_i u_k+\psi_i v_k+\chi_i w_k)ds = -\int(f_k u_i+g_k v_i+h_k w_i)dv + \int(\varphi_k u_i+\psi_k u_i+\chi_k w_i)ds, \quad (26)$$

or, according to Eq. (25):

$$H_{ik}=H_{ki}. \quad (27)$$

In other words, the matrix H_{ik} is symmetric.

If the Eqs. (24) are to be compatible, the determinant

$$\begin{vmatrix} \rho\Omega^2-H_{11} & \rho\Omega^2 N_{12}-H_{12} & \cdots \\ \rho\Omega^2 N_{12}-H_{12} & \rho\Omega^2-H_{22} & \cdots \\ \vdots & \vdots & \end{vmatrix}=0 \quad (28)$$

must vanish. This will be possible only when Ω^2 assumes certain characteristic values which correspond to the approximate characteristic frequencies of the free vibrations. With a particular value Ω_i^2 we can solve Eqs. (24) for the coefficients A_i and by substitution into (9) we can obtain the approximate solutions U, V, W. For all practical purposes, the functions $u_i \cdots$ can then be substituted for the u_i'; in other words, Eq. (8) can be used instead of (9).

2. APPLICATION: EXTENSIONAL VIBRATIONS OF THIN CRYSTAL PLATES

Let a crystal plate have its two parallel larger surfaces normal to the Z axis of the reference system. The origin is situated in a plane midway between the layer surfaces. On the boundaries, for a free crystal

$$X_z=Y_z=Z_z=0. \quad (29)$$

For a thin crystal, we may assume that the variation of the stress is linear, in a first approximation. As (29) is true for both surfaces, it must then hold everywhere. Substituting (29) into (4), we obtain

$$\begin{aligned} -x_x &= s_{11}X_x+s_{12}Y_y+s_{16}X_y, \\ -y_y &= s_{12}X_x+s_{22}Y_y+s_{26}X_y, \\ -x_y &= s_{16}X_x+s_{26}Y_y+s_{66}X_y. \end{aligned} \quad (30)$$

And if we solve (30) for the stresses:

$$\begin{aligned} -X_x &= \gamma_{11}x_x+\gamma_{12}y_y+\gamma_{16}x_y, \\ -Y_y &= \gamma_{12}x_x+\gamma_{22}y_y+\gamma_{26}x_y, \\ -X_y &= \gamma_{16}x_x+\gamma_{26}y_y+\gamma_{66}x_y. \end{aligned} \quad (31)$$

In this equation, X_x, Y_y, X_y mean the average value of the stresses taken over the thickness of the plate. Equation (31) is the equation given by W. Voigt.[3] Explicit formulas for the γ_{ik} are given in the same book.

As explained by Voigt, Eq. (31) applies really only to points of the plane $z=0$. For these points, $W=0$ in the case of extensional vibrations, and the strains (more exactly, the average values of the strains) are given similarly to Eq. (2):

$$x_x=\frac{\partial U}{\partial x}, \quad y_y=\frac{\partial V}{\partial y}, \quad x_y=\frac{\partial U}{\partial y}+\frac{\partial V}{\partial x}. \quad (32)$$

The dynamical equation (1) reduces to:

$$\rho\Omega^2 U=\frac{\partial X_x}{\partial x}+\frac{\partial X_y}{\partial y}, \quad \rho\Omega^2 V=\frac{\partial X_y}{\partial x}+\frac{\partial Y_y}{\partial y}. \quad (33)$$

This problem has been solved for the special case of a circular isotropic plate by Love.[4] For a rectangular plate, no general solution is known. V. Petrzilka[5] has given an exact solution for a mode of an isotropic rectangular plate, but the solution exists only for certain dimensions of the rectangle.

For this two-dimensional case, Eqs. (10)–(13), (21), (22), and (25) are simplified:

$$x_{xi}=\frac{\partial u_i}{\partial x}, \quad y_{yi}=\frac{\partial v_i}{\partial y}, \quad x_{yi}=\frac{\partial u_i}{\partial y}+\frac{\partial v_i}{\partial x}, \quad (10a)$$

$$\begin{aligned} -X_{xi} &= \gamma_{11}x_{xi}+\gamma_{12}y_{yi}+\gamma_{16}x_{yi}, \\ -Y_{yi} &= \gamma_{12}x_{xi}+\gamma_{22}y_{yi}+\gamma_{26}x_{yi}, \\ -X_{yi} &= \gamma_{16}x_{xi}+\gamma_{26}y_{yi}+\gamma_{66}x_{yi}, \end{aligned} \quad (11a)$$

$$\frac{\partial X_{xi}}{\partial x}+\frac{\partial X_{yi}}{\partial y}=-f_i, \quad \frac{\partial X_{yi}}{\partial x}+\frac{\partial Y_{yi}}{\partial y}=-g_i, \quad (12a)$$

$$\begin{aligned} X_{xi}\cos(n,x)+X_{yi}\cos(n,y) &= \varphi_i(s), \\ X_{yi}\cos(n,x)+Y_{yi}\cos(n,y) &= \psi_i(s), \end{aligned} \quad (13a)$$

[5] V. Petrzilka, Zeits. f. Physik 97, 436 (1935).

$$\int (u_i u_k + v_i v_k)\,dxdy = N_{ik}, \tag{21a}$$

$$\int (u_i^2 + v_i^2)\,dxdy = 1, \tag{22a}$$

$$H_{ik} = -\int (f_i u_k + g_i v_k)\,dxdy + \int (\varphi_i u_k + \psi_i v_k)\,ds. \tag{25a}$$

(a) Low Frequency Longitudinal Modes

A group of extensional modes has been called longitudinal because the strain components x_x and y_y are large in comparison to the shear x_y.

These vibrations have been studied experimentally and theoretically by several authors.[1,2,6,7] Their analysis is, however, unsatisfactory in several respects, mainly because it fails to account for the fact that *three* low frequency longitudinal modes are observed, usually with nearby frequencies.

We shall obtain the zero-order solutions from consideration of a simplified problem. In (31), we put

$$\gamma_{11} = \gamma_{22}, \quad \gamma_{66} = \tfrac{1}{2}\gamma_{11}, \quad \gamma_{12} = \gamma_{16} = \gamma_{26} = 0. \tag{34}$$

These are the equations for an isotropic plate with vanishing Poisson's ratio. Furthermore, we suppose that the plate is square, the edge having the length a. The directions X and Y shall be parallel to the edges, and the origin is in one corner of the plate. One exact solution is the one given by Petrzilka:

$$u_1 = C_1 \cos kx \sin ky, \quad v_1 = -C_1 \sin kx \cos ky, \quad \text{where } k = \pi/a. \tag{35}$$

The constant C_1 is arbitrary, but will later be defined by the normalization (22a).

Two other solutions are the longitudinal plane waves in the directions X and Y, respectively:

$$u_2 = C_2 \cos kx, \quad v_2 = 0, \tag{36}$$

and

$$u_3 = 0, \quad v_3 = C_3 \cos ky. \tag{37}$$

These three modes are degenerate, i.e., they have the same frequency:

$$\rho\omega^2 = k^2\gamma_{11}. \tag{38}$$

We now abandon the simplifying assumptions (34). We then will find the familiar phenomenon of splitting of a degenerate eigenvalue by a perturbation.

For the more general case, we let two unequal edges of lengths a and b be parallel to X and Y, respectively. The zero-order functions can be written:

$$u_1 = C_1 \cos k_1 x \sin k_2 y, \quad v_1 = -C_1 \sin k_1 x \cos k_2 y, \tag{39}$$

$$u_2 = C_2 \cos k_1 x, \quad v_2 = 0, \tag{40}$$

$$u_3 = 0, \quad v_3 = C_3 \cos k_2 y, \tag{41}$$

where

$$k_1 = \pi/a, \quad k_2 = \pi/b.$$

The normalization (22a) requires that:

$$C_1^2 = C_2^2 = C_3 = 2/ab. \tag{42}$$

The non-orthogonality integrals N_{ik} are, according to (21a):

$$N_{12} = 2/\pi, \quad N_{13} = -2/\pi, \quad N_{23} = 0. \tag{43}$$

The equations (10a), (11a), (12a), (13a), and (25a) yield after some elementary calculations:

$$H_{11} = \tfrac{1}{2}[k_1^2\gamma_{11} + k^2{}_2\gamma_{22} - 2k_1k_2\gamma_{12} + (k_2 - k_1)^2\gamma_{66}],$$
$$H_{12} = H_{21} = (2/\pi)[k_1^2\gamma_{11} - k_1k_2\gamma_{12}],$$
$$H_{22} = k_1^2\gamma_{11}$$
$$H_{13} = H_{31} = (2/\pi)[k_1k_2\gamma_{12} - k_2^2\gamma_{22}], \tag{44}$$
$$H_{33} = k_2^2\gamma_{22},$$
$$H_{23} = H_{32} = (8/\pi^2)k_1k_2\gamma_{12}.$$

These are the elements of the secular determinant (28).

We first discuss the case where the major face is normal to a crystallographic threefold axis. In this case, according to Voigt, the plate behaves as if it were isotropic, i.e.,

$$\gamma_{11} = \gamma_{22}; \quad \gamma_{16} = \gamma_{26} = 0; \quad \gamma_{66} = \tfrac{1}{2}(\gamma_{11} - \gamma_{12}). \tag{45}$$

If the plate is also square ($k_1 = k_2 = k$) the expressions (44) reduce to:

$$H_{11} = k^2(\gamma_{11} - \gamma_{12}), \quad H_{12} = (2/\pi)k^2(\gamma_{11} - \gamma_{12}),$$
$$H_{22} = k^2\gamma_{11}, \quad H_{13} = -(2/\pi)k^2(\gamma_{11} - \gamma_{12}), \tag{46}$$
$$H_{33} = k^2\gamma_{11}, \quad H_{23} = k^2(8/\pi^2)\gamma_{12}.$$

[6] A. Lissütin, Zeits. f. Physik **59**, 265 (1930).
[7] V. Petrzilka, reference 5, and Hoch: tech. u. Elek: akus. **50**, 1 (1937).

The secular determinant (28) has the form:

$$\begin{vmatrix} \rho\Omega^2-k^2(\gamma_{11}-\gamma_{12}) & \frac{2}{\pi}\rho\Omega^2-\frac{2}{\pi}k^2(\gamma_{11}-\gamma_{12}) & -\frac{2}{\pi}\rho\Omega^2+\frac{2}{\pi}k^2(\gamma_{11}-\gamma_{12}) \\ \frac{2}{\pi}\rho\Omega^2-\frac{2}{\pi}k^2(\gamma_{11}-\gamma_{12}) & \rho\Omega^2-k^2\gamma_{11} & -k^2\frac{8}{\pi^2}\gamma_{12} \\ -\frac{2}{\pi}\rho\Omega^2+\frac{2}{\pi}k^2(\gamma_{11}-\gamma_{12}) & -k^2\frac{8}{\pi^2}\gamma_{12} & \rho\Omega^2-k^2\gamma_{11} \end{vmatrix} = 0. \tag{47}$$

One root of (47) is obvious from inspection:

$$\rho\Omega_1^2 = k^2(\gamma_{11}-\gamma_{12}). \tag{48}$$

With this value, the ratio of the coefficients A_i in (24) is:

$$A_1^{(1)}:A_2^{(1)}:A_3^{(1)} = 1:0:0. \tag{49}$$

The first solution is, according to (8) and (39):

$$\begin{aligned} U_1 &= C_1 \cos kx \sin ky, \\ V_1 &= -C_1 \sin kx \cos ky; \end{aligned} \tag{39}$$

i.e., the result is the unchanged function (39). This was to be expected, for (39) is known to be a rigorous solution for the isotropic case with $a=b$.

To find the two other roots of (48), only a quadratic equation has to be solved. The result is:

$$\rho\Omega_2^2 = k^2\gamma_{11}, \quad \rho\Omega_3^2 = k^2(\gamma_{11}+(8/\pi^2)\gamma_{12}), \tag{50}$$

and with these values

$$\begin{aligned} &A_1^{(2)}:A_2^{(2)}:A_3^{(2)} = 1:-\frac{\pi}{4}:+\frac{\pi}{4}, \\ &A_1^{(3)}:A_2^{(3)}:A_3^{(3)} = 0:1:1. \end{aligned} \tag{51}$$

TABLE I. Frequencies of square Z-cut quartz plates with edge $a=1$ mm (in kilocycles).

Mode	$N_{calc.}$	$N_{obs.}$
1	2.537×10^3	
	2.564×10^3	2.551×10^3
2	2.721×10^3	
	2.734×10^3	2.724×10^3
3	2.861×10^3	
	2.863×10^3	2.8962×10^3

TABLE II. Frequencies of a square Z-cut tourmaline plate with edge $a=1.836$ cm (in kilocycles).

Mode	Calc.	Obs.
1	218	215.1
2	253	247.6
3	278	291.0

The two equations (51) refer to the roots Ω_2^2 and Ω_3^2, respectively. The solutions U_2, V_2 and U_3, V_3 are then:

$$\begin{aligned} U_2 &= C(\sin ky-(\pi/4))\cos kx, \\ V_2 &= C(-\sin kx+(\pi/4))\cos ky \end{aligned} \tag{52}$$

and

$$U_3 = C\cos kx, \quad V_3 = C\cos ky.$$

R. Bechmann[8] has observed some resonant frequencies of square quartz plates of the Z-cut type. He finds three frequencies for longitudinal modes and expresses them in terms of the frequency constant N, i.e., the frequency (in kilocycles) of a plate with $a=1$ mm so that $N=10^{-3}\nu a$. Table I gives a comparison between these measurements and the constants N as computed by Eqs. (48) and (50).

In this case, the parameters γ_{ik} are given by:

$$\gamma_{11} = \frac{s_{11}}{s_{11}^2-s_{12}^2}, \quad \gamma_{12} = -\frac{s_{12}}{s_{11}^2-s_{12}^2}.$$

For s_{11} and s_{12} the values

	s_{11}	s_{12}
	12.948×10^{-13}	-1.690×10^{-13}
and	12.79×10^{-13}	-1.535×10^{-13}

are given by Bechmann[8] (according to Voigt's measurements) and W. P. Mason,[9] respectively.

The calculated values have been obtained with these two sets of elastic constants of Voigt (upper figure) and by W. P. Mason (lower figure), respectively. Two of the observed frequencies agree numerically with the formulas given by Bechmann although the expression in terms of the s_{ik} is quite different.

V. Petrzilka[7] has measured the frequencies of a square tourmaline plate of edge $a=1.836$ cm.

[8] R. Bechmann, Zeits. f. Physik **118**, 515 (1941).
[9] W. P. Mason, Bell Sys. Tech. J. **22**, 178 (1943).

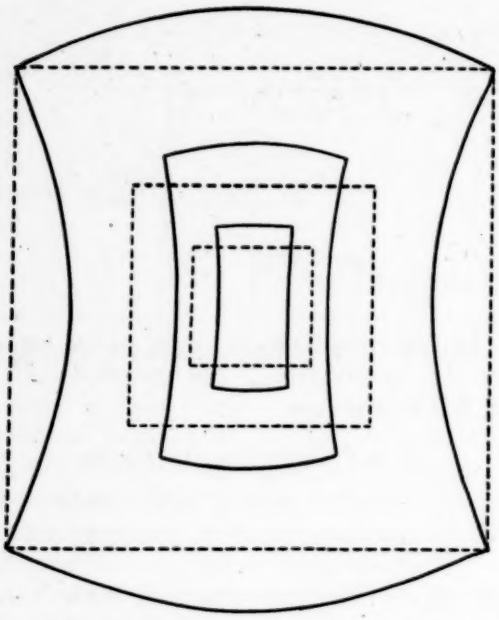

FIG. 1. Longitudinal vibration of a thin square plate. Mode 1: $U_1 = C\cos(\pi/a)x \sin(\pi/a)y$, $V_1 = C\sin(\pi/a)x\cos(\pi/a)y$. Dotted lines—crystal at rest. Full lines—crystal vibrating.

The frequencies calculated by Eqs. (48) and (50) with Voigt's values for the elastic moduli of tourmaline are shown in Table II.

Two of these calculated frequencies are equal to those given by Petrzilka. The first frequency is the rigorous value and is, of course, in agreement with our value.

The vibrational modes calculated by Eqs. (39) and (52) are represented by Figs. 1–3. It can be seen that none of them has nodal lines, but only nodal points. Petrzilka attributed to the frequency (2) a mode equal to our zero-approximation modes (40) or (41), but did not find the expected nodal line by lycopodium powder observations.

The calculated mode (3), Fig. 3, involves a nearly radial motion. It can clearly be identified with the picture of the lycopodium powder pattern published by Petrzilka. In this mode, according to the author, the powder is displaced radially and stays at rest only at the center. This is also what the theoretical picture predicts.

We now apply Eqs. (44) to a square Y-cut quartz plate, i.e., a plate whose large face is normal to the crystallographic Y axis, while the edges are parallel to the optic and electric axis, respectively. Using Voigt's values for the elastic moduli, we obtain:

$$\begin{aligned} \gamma_{11} &= 78.67\times10^{10}, \\ \gamma_{22} &= 103.08\times10^{10}, \quad \gamma_{16}=\gamma_{26}=0. \\ \gamma_{12} &= 12.180\times10^{10}. \end{aligned} \tag{53}$$

The secular equation takes the form:

$$\begin{vmatrix} \rho\Omega^2-\frac{1}{2}k^2[\gamma_{11}+\gamma_{22}-2\gamma_{12}] & \frac{2}{\pi}\rho\Omega^2-\frac{2}{\pi}k^2[\gamma_{11}-\gamma_{12}] & -\frac{2}{\pi}\rho\Omega^2+\frac{2}{\pi}k^2[\gamma_{22}-\gamma_{12}] \\ \frac{2}{\pi}\rho\Omega^2-\frac{2}{\pi}k^2[\gamma_{11}-\gamma_{12}] & \rho\Omega^2-k^2\gamma_{11} & -k^2\frac{8}{\pi^2}\gamma_{12} \\ -\frac{2}{\pi}\rho\Omega^2+\frac{2}{\pi}k^2[\gamma_{22}-\gamma_{12}] & -k^2\frac{8}{\pi^2}\gamma_{12} & \rho\Omega^2-k^2\gamma_{22} \end{vmatrix} = 0. \tag{54}$$

The three eigenvalues of (55) are: $\rho\Omega^2 = k^2\times73.9\times10^{10}$; $k^2\times89.6\times10^{10}$; $k^2\times106.8\times10^{10}$.

The corresponding frequencies expressed in terms of the frequency constant $N=10^{-2}\nu a$ are shown in Table III. As a comparison the values observed by Bechmann[8] and Wright and Stuart[10] are given. The second calculated frequency was not observed by these authors.

Wright and Stuart studied the mode No. 1 ($N=2.67\times10^3$) by means of powder patterns. While the experiments with powder on the crystal surface are difficult to interpret, the pattern created by the air currents from the periph-

TABLE III. Frequencies of square Y-cut quartz plates edge = 1 mm, in kilocycles.

Mode	$N_{calc.}$	Bechmann	Wright and Stuart
1	2.64×10^3	2.68×10^3	2.675×10^3
2	2.90×10^3		
3	3.17×10^3	3.19×10^3	

[10] R. B. Wright and D. M. Stuart, Bur. Stand. J. Research 7, 519 (1931).

ery of the crystal should give a simple idea of the motion of the boundary.

In attempting to calculate the ratio $A_1:A_2:A_3$ corresponding to the mode No. 1, one meets a difficulty. While the discrepancy between the observed and calculated values of the frequency (2.64 and 2.68) is as small as can be expected from the uncertainty of the elastic moduli, the ratio $A_1:A_2:A_3$ is very sensitive to small variations of the root, so that the mode cannot be described definitely. As a first approximation, we can expect it to be similar to the mode No. 2 described for the Z-cut plate (Fig. 2). In this mode, the corners of the plate move in a tangential direction and create thereby a wind such as is shown in Wright and Stuart's Fig. 13a. The agreement between this picture and the air currents to be expected from the theoretical figure is quite satisfactory.

(b) Shear Modes

A type of modes where the shearing strain x_y predominates is usually called "shear mode."

The zero-order modes will be found by considering two extreme cases: If the plate is infinitely extended along the x direction ($a\to\infty$) standing shear waves are exact solutions:

$$\begin{aligned} u_{py} &= C\cos pk_2 y, \\ v_{py} &= 0, \end{aligned} \qquad p=1, 2, 3\cdots. \tag{55}$$

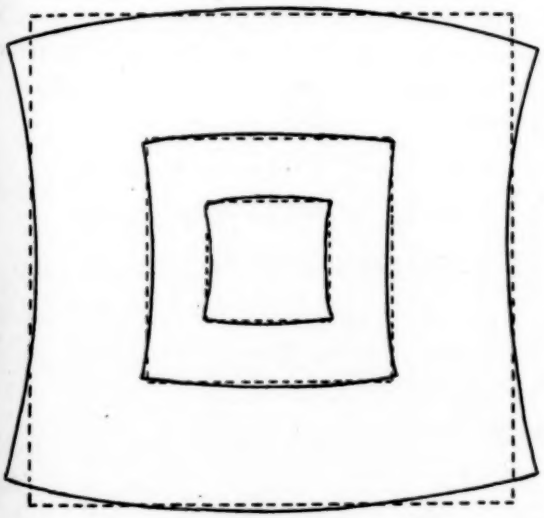

FIG. 2. Longitudinal vibration of a thin square plate. Mode 2: $U_2=C[\sin(\pi/a)y-(\pi/4)]\cos(\pi/a)x$, $V_2=C[-\sin(\pi/a)x+(\pi/4)]\cos(\pi/a)y$. Dotted lines—crystal at rest. Full lines—crystal vibrating.

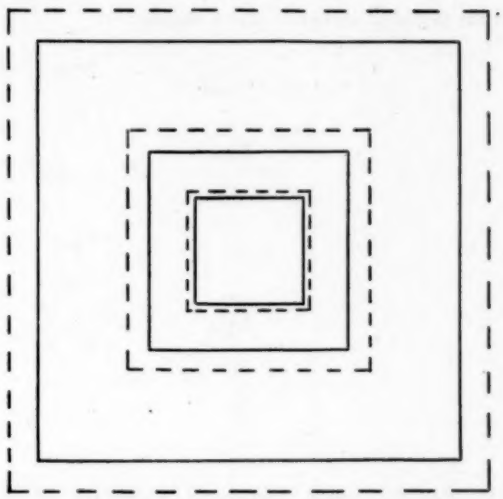

FIG. 3. Longitudinal vibration of a thin square plate. Mode 3: $U_3=C\cos kx$, $V_3=C\cos ky$. Dotted lines—crystal at rest. Full lines—crystal vibrating.

If the dimension b is very long, standing shear waves along the y direction are solutions:

$$\begin{aligned} u_{pz} &= 0, \\ v_{pz} &= C\cos pk_1 x, \end{aligned} \qquad p=1, 2, 3\cdots, \tag{56}$$

where again

$$k_1=\pi/a, \quad k_2=\pi/b.$$

The modes (55) and (56) will be taken as zero-order modes for the study of almost square plates.

The normalization (22a) requires that

$$C^2=2/ab \tag{57}$$

for all these modes.

The definition (25a) yields, after elementary calculations, the elements of the matrix H:

$$\begin{aligned} &H_{py,\,qy}=H_{pz,\,qz}=0, \quad (p\neq q) \\ &H_{py,\,py}=\gamma_{66}p^2k_2^2, \\ &H_{pz,\,pz}=\gamma_{66}p^2k_1^2, \\ &H_{pz,\,qy}=\begin{cases} 0 \text{ if } p \text{ or } q \text{ is even} \\ (8/ab)\gamma_{66} \text{ if } p \text{ and } q \text{ are odd,} \end{cases} \\ &N_{ik}=0 \text{ for any two different modes.} \end{aligned} \tag{58}$$

There is no interaction between the modes with p or q even and the odd modes. Therefore, the even modes can be dropped, and in the following, p and q will be only odd integers.

The secular determinant reads:

$$\begin{vmatrix} \rho\Omega^2-\gamma_{66}k_1^2 & -\frac{8\gamma_{66}}{ab} & 0 & -\frac{8\gamma_{66}}{ab} & \cdots \\ -\frac{8\gamma_{66}}{ab} & \rho\Omega^2-\gamma_{66}k_2^2 & -\frac{8\gamma_{66}}{ab} & 0 & \cdots \\ 0 & -\frac{8\gamma_{66}}{ab} & \rho\Omega^2-9\gamma_{66}k_1^2 & -\frac{8\gamma_{66}}{ab} & \cdots \\ -\frac{8\gamma_{66}}{ab} & 0 & -\frac{8\gamma_{66}}{ab} & \rho\Omega^2-9\gamma_{66}k_2^2 & \cdots \\ \vdots & \vdots & \vdots & \vdots & \end{vmatrix} = 0. \tag{59}$$

As $k_1 \geqq k_2$, each diagonal element of H is quasi-degenerate with one neighboring diagonal element. The first step in the solution of (59) is to find new linear combinations of the zero-order functions so that this degeneracy is removed. Considering the case of the square plate ($k_1=k_2$) and disregarding the coupling between non-degenerate functions, we find Eq. (24) to be:

$$\begin{aligned} A_{px}(\rho\Omega^2-\gamma_{66}p^2k^2)-A_{py}(8\gamma_{66}/a^2)=0, \\ -A_{px}(8\gamma_{66}/a^2)+A_{py}(\rho\Omega^2-\gamma_{66}p^2k^2)=0. \end{aligned} \tag{60}$$

These two equations are compatible if

$$A_{px}=A_{py} \quad \text{or} \quad A_{px}=-A_{py}. \tag{61}$$

Consequently, the sought linear combinations are:

$$\begin{aligned} &u_{p+}=C\cos pk_2y, \quad u_{p-}=-C\cos pk_2y, \\ &\qquad\qquad \text{where } p=1, 3, 5\cdots \\ &v_{p+}=C\cos pk_1x, \quad v_{p-}=C\cos pk_1x. \end{aligned} \tag{62}$$

With these new zero-order functions the matrix elements of H and N are found to be:

$N_{ik}=0$ for any two functions (62),

$$\begin{aligned} H_{p+,\,p+}&=\gamma_{66}\left(p^2\frac{k_1^2+k_2^2}{2}-\frac{8}{ab}\right), \\ H_{p+,\,q+}&=\frac{8}{ab}\gamma_{66}, \quad (p\neq q) \\ H_{p+,\,q-}&=\begin{cases} 0 & (p\neq q) \\ \gamma_{66}p^2\dfrac{k_1^2-k_2^2}{2} & (p=q). \end{cases} \end{aligned} \tag{63}$$

The interaction between the modes $p+$ and $p-$ is so small for our case that it can be neglected.

Putting

$$b=a(1-\epsilon), \tag{64}$$

where ϵ is a small number, we find that the matrix elements referring to the modes $p+$ become

$$\begin{aligned} H_{p+,\,p+}&=(1/a^2)(1+\epsilon)(p^2\pi^2+8)\gamma_{66}, \\ H_{p+,\,q+}&=(1/a^2)(1+\epsilon)8\gamma_{66} \quad (p\neq q). \end{aligned} \tag{65}$$

Now, the secular determinant has the form:

$$\begin{vmatrix} \rho\Omega^2-\frac{\gamma_{66}}{a^2}(1+\epsilon)(\pi^2+8) & -\frac{8}{a^2}\gamma_{66}(1+\epsilon) & -\frac{8}{a^2}\gamma_{66}(1+\epsilon) & \cdots \\ -\frac{8}{a^2}\gamma_{66}(1+\epsilon) & \rho\Omega^2-\frac{\gamma_{66}}{a^2}(1+\epsilon)(9\pi^2+8) & -\frac{8}{a^2}\gamma_{66}(1+\epsilon) & \cdots \\ -\frac{8}{a^2}\gamma_{66}(1+\epsilon) & -\frac{8}{a^2}\gamma_{66}(1+\epsilon) & \rho\Omega^2-\frac{\gamma_{66}}{a^2}(1+\epsilon)(25\pi^2+8) & \cdots \\ \vdots & \vdots & \vdots & \end{vmatrix}. \tag{66}$$

If we put

$$r=\rho\Omega^2a^2/8\gamma_{66}(1+\epsilon) \tag{67}$$

and divide each row of (66) by $8\gamma_{66}(1+\epsilon)/a^2$, the determinant is simplified:

$$\begin{vmatrix} r-\left(1+\frac{\pi^2}{8}\right) & -1 & -1 & \cdots \\ -1 & r-\left(1+\frac{9\pi^2}{8}\right) & -1 & \cdots \\ -1 & -1 & r-\left(1+\frac{25\pi^2}{8}\right) & \cdots \\ \vdots & \vdots & \vdots & \end{vmatrix}=0. \tag{68}$$

The roots of (68) are approximated by the Schrödinger perturbation formula:

$$r_p=1+\frac{p^2\pi^2}{8}-\frac{8}{\pi^2}\sum_{q=1}^{\infty}{}'\frac{1}{q^2-p^2}. \tag{69}$$

The sum in this expression can be readily calculated. As p and q are odd numbers, the substitutions $p=2n+1$ and $q=2m+1$ give:

$$\sum_{m=0}^{\infty}{}'\frac{1}{(2m+1)^2-(2n+1)^2}=\frac{1}{4(2n+1)}\sum{}'\left(\frac{1}{m-n}-\frac{1}{m+n+1}\right),$$

where m takes all integer values except $m=n$. Inspection of this expression shows that the sum has the value

$$\frac{1}{4(2n+1)}\times\frac{1}{2n+1}.$$

Thus, (69) yields:

$$r_p=1+\frac{p^2\pi^2}{8}-\frac{2}{\pi^2p^2}. \tag{70}$$

In view of (67), the frequencies are:

$$\nu_p=\frac{(1+\epsilon)^{\frac{1}{2}}}{2a}\left(\frac{\gamma_{66}}{\rho}\right)^{\frac{1}{2}}\left(\frac{8}{\pi^2}r_p\right)^{\frac{1}{2}},$$

or, in view of (64):

$$\nu_p=\frac{1}{a+b}\left(\frac{\gamma_{66}}{\rho}\right)^{\frac{1}{2}}\left(p^2+\frac{8}{\pi^2}-\frac{16}{\pi^4p^2}\right)^{\frac{1}{2}}. \tag{71}$$

Systematic observations were made on the lowest shear mode of nearly square quartz plates by Hight and Willard.[11] They studied quartz plates whose edge was parallel to the crystallographic X axis. In this case

$$s_{16}=s_{26}=\gamma_{16}=\gamma_{26}=0;\quad \gamma_{66}=1/s_{66}.$$

Equation (71) gives, for $p=1$,

$$\nu_1=\frac{1}{a+b}\left(\frac{1}{s_{66}\rho}\right)^{\frac{1}{2}}\times 1.28,$$

while Hight and Willard's observations give

$$\nu_1=\frac{1}{a+b}\left(\frac{1}{s_{66}\rho}\right)^{\frac{1}{2}}\times 1.25,$$

so that the difference between theory and experiment is 2.5 percent. Later observations of Bechmann[8] agree within 1 percent with those of Hight and Willard.

For the resultant modes, the Rayleigh-Schrödinger perturbation formula yields from Eq. (68):

$$\begin{aligned} U_p&=u_p+\frac{8}{\pi^2}\sum_{q\neq p}\frac{u_{q+}}{q^2-p^2}, \\ V_p&=v_p+\frac{8}{\pi_2}\sum_{q\neq p}\frac{v_{p+}}{q^2-p^2}. \end{aligned} \tag{72}$$

The lowest mode is

$$\begin{aligned} U_1&=\cos k_2y+\frac{8}{\pi^2}\sum_{q\neq 1}^{\infty}\frac{\cos qk_2y}{q^2-1}, \\ V_1&=\cos k_1x+\frac{8}{\pi^2}\sum_{q\neq 1}\frac{\cos qk_1x}{q^2-1}. \end{aligned} \tag{73}$$

[11] S. C. Hight and G. W. Willard, Proc. I.R.E. 25, 549 (1937).

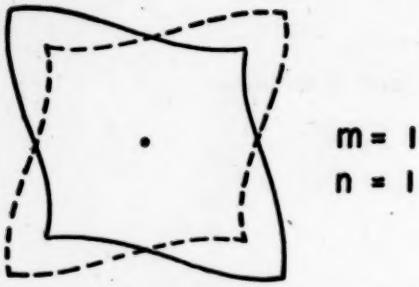

FIG. 4. Shear vibration of a thin square plate. Observations by R. A. Sykes. Full and dotted lines represent the contour deformation in two opposite phases.

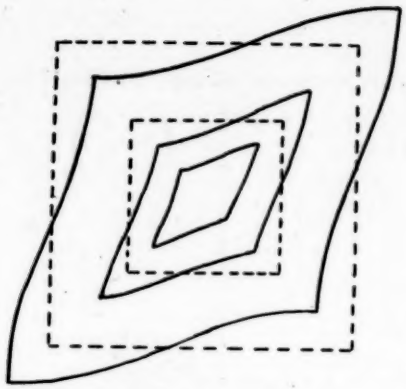

FIG. 5. Shear vibration of a thin square plate (calculated). $U=\cos(\pi/a)y$, $V=\cos(\pi/a)x$. Dotted line—crystal at rest. Full line—crystal vibrating.

This result can be compared with observations on the mode of a square quartz plate vibrating in the lowest shear mode. Figure 4 shows the distorted edges in opposite phases, one a solid curve and the other a dotted curve, according to microscopic observations by Sykes.[12] Figure 5 shows one phase (full line) of the motion calculated by (73). Only the first terms of (73) have been used for the drawing because the supplementary terms are small. The agreement between observation and theory is satisfactory.

Theoretical considerations of the shear mode by Mason[1] and Bechmann[13] led to a mode in which the corners of the plate should be at rest. Their solution apparently bears no resemblance to the experimental picture.

All comparisons with experiment for the longitudinal as well as shear modes were made in cases where the parameters γ_{16} and γ_{26} vanish. Where these parameters are not negligibly small, the longitudinal and shear modes would be coupled and could not be treated separately as is done here.

The author is indebted to Dr. F. Beer for advice and help. He wishes to thank Mr. A. H. Schlesinger for his help in numerical calculation.

[12] R. A. Sykes, Bell Sys. Tech. J. **23**, 52 (1944).
[13] R. Bechmann, Zeits. f. Physik **117** and **118** (1941).

PHYSICAL REVIEW VOLUME 66, NUMBERS 5 AND 6 SEPTEMBER 1 AND 15, 1944

Electromagnetic Waves in Metal Tubes Filled Longitudinally with Two Dielectrics

L. PINCHERLE
King's College, London, England
(Received January 10, 1944)

The propagation of e-m waves is investigated: (1) in a rectangular metal tube half-filled longitudinally with a dielectric; (2) in a cylindrical dielectric guide of radius a, surrounded by a coaxial metal tube of radius b. In (1) the waves are of the longitudinal-section type; for high frequencies they are confined to the medium of higher dielectric constant. The problem is discussed also with the model of the criss-cross component waves. In (2) the waves are linear combinations of E and H waves. The case of axial symmetry is considered, in which there are simple E and H waves. For E_0 a critical wave-length exists, depending only on the dimensions of the inner dielectric, and on the dielectric constants, below which the system behaves more or less as a dielectric guide in free space, and above which as an ordinary hollow tube. For H_0 this critical wave-length depends also on the ratio b/a. The case in which the external medium has a higher dielectric constant is also briefly investigated.

1

THE purpose of this note is to investigate from a purely theoretical point of view the propagation of electromagnetic waves in hollow metal tubes, the interior of which is filled with two different dielectrics, the distribution in all

cross sections being constant. If one of the media is air, the problem may be called that of a dielectric guide contained in a metal tube. The features of the phenomenon are similar in all problems of this kind. Two examples will be treated: (a) a rectangular tube with two dielectrics, each half filling it longitudinally; (b) a cylindrical dielectric guide of radius a, enclosed by a coaxial cylindrical metal tube of radius $b>a$.[1]

2

We consider a hollow metal tube with infinitely conducting walls, of rectangular cross section, with axis parallel to the Z axis. The dimensions of the tube are a in the X direction and b in the Y direction. The whole length of the tube is filled, from $X=0$ to $X=\frac{1}{2}a$, with a non-absorbing dielectric of constant ϵ_1, and from $X=\frac{1}{2}a$ to $X=a$ with a non-absorbing dielectric of constant ϵ_2 (Fig. 1), the magnetic permeability of both media being taken equal to that of empty space. We shall take $\epsilon_2>\epsilon_1$.

The differential equation satisfied by the longitudinal component of the electric field for E waves (or by the longitudinal component of the magnetic field for H waves) is:

$$\frac{\partial^2 E_Z}{\partial X^2}+\frac{\partial^2 E_Z}{\partial Y^2}+(h^2+\epsilon\mu\omega^2)E_Z=0. \tag{1}$$

Here m.k.s. rationalized units are used; $\omega=2\pi\cdot$frequency, and it is supposed that the dependence of each field component on Z and t is given by a factor $e^{-hZ+i\omega t}$. ϵ has the value ϵ_1 in the first medium and ϵ_2 in the second medium. We may further assume that the dependence on Y is the same as for ordinary tubes, namely, that we can write:

$$E_Z=f(X)\sin\left(\frac{l\pi}{b}Y\right)e^{-hZ+i\omega t},\quad l=0,1,2\cdots. \tag{2}$$

$f(X)$ satisfies then the equation

$$\frac{d^2 f}{dX^2}+\left(h^2+\epsilon\mu\omega^2-\frac{l^2\pi^2}{b^2}\right)f=0. \tag{3}$$

[1] For the bibliography on the propagation of e-m waves in metal tubes, see: H. R. L. Lamont, *Wave Guides* (Methuen & Company, 1942); articles by E. U. Condon in Rev. Mod. Phys. (1943).

Writing

$$m=\frac{l\pi}{b},\qquad k_1^2=h^2+\epsilon_1\mu\omega^2-m^2,\qquad k_2^2=h^2+\epsilon_2\mu\omega^2-m^2, \tag{4}$$

we obtain the solution

$f(X)=A_1\sin k_1X+B_1\cos k_1X$ in the first medium,

$f(X)=A_2\sin k_2X+B_2\cos k_2X$ in the second medium.

The boundary conditions at the walls give

$$B_1=0;\quad B_2=-A_2\tan k_2a, \tag{5}$$

so that

$$f(X)=A_1\sin k_1X \qquad (0<X<\tfrac{1}{2}a),$$
$$f(X)=-(A_2/\cos k_2a)\sin k_2(a-X) \qquad (\tfrac{1}{2}a<X<a). \tag{6}$$

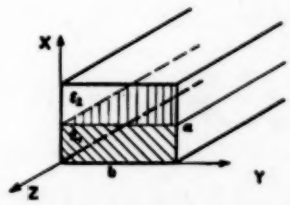

FIG. 1. System of coordinates and dimensions of the tube studied in the first problem.

The expressions of the field components are: $(f'(X)=df/dX)$

$$E_X=-\frac{h}{h^2+\epsilon\mu\omega^2}\frac{\partial E_Z}{\partial X}=-\frac{hf'(X)}{k^2+m^2}\sin mY e^{-hZ+i\omega t},$$

$$E_Y=-\frac{h}{h^2+\epsilon\mu\omega^2}\frac{\partial E_Z}{\partial Y}=-\frac{hf(X)}{k^2+m^2}m\cos mY e^{-hZ+i\omega t},$$

$$E_Z=f(X)\sin mY e^{-hZ+i\omega t},$$

$$H_X=\frac{i\omega\epsilon}{h^2+\epsilon\mu\omega^2}\frac{\partial E_Z}{\partial Y}=\frac{i\omega\epsilon}{k^2+m^2}f(X)m\cos mY e^{-hZ+i\omega t},$$

$$H_Y=-\frac{i\omega\epsilon}{h^2+\epsilon\mu\omega^2}\frac{\partial E_Z}{\partial X}=-\frac{i\omega\epsilon}{k^2+m^2}f'(X)\sin mY e^{-hZ+i\omega t},$$

$$H_Z=0,$$

where we must insert for each medium the corresponding values of ϵ, k, and $f(X)$.

Similarly for H waves, writing

$$H_Z = \varphi(X) \cos mY,$$

we find:

$$\varphi(X) = C_1 \cos k_1 X \qquad \text{in the first medium,}$$

$$\varphi(X) = \frac{C_2}{\cos k_2 a} \cos k_2(a-X) \qquad (6')$$

in the second medium;

and the expressions for the field components are:

$$\begin{aligned}
E_X &= \frac{i\omega\mu}{k^2+m^2}\varphi(X) m \sin mY e^{-hZ+i\omega t},\\
E_Y &= \frac{i\omega\mu}{k^2+m^2}\varphi'(X) \cos mY e^{-hZ+i\omega t},\\
E_Z &= 0,\\
H_X &= -\frac{h}{k^2+m^2}\varphi'(X) \cos mY e^{-hZ+i\omega t},\\
H_Y &= \frac{h}{k^2+m^2}\varphi(X) m \sin mY e^{-hZ+i\omega t},\\
H_Z &= \varphi(X) \cos mY e^{-hZ+i\omega t}.
\end{aligned} \qquad (7)$$

We have now to determine the constants A_1, A_2, C_1, C_2, in order to satisfy the boundary conditions at the separation of the two dielectrics. This, however, is found to be impossible with a simple E or H wave (with the exception of the H wave for $m=0$). The waves in our tube must then be a linear combination of E and H waves. Including the coefficients of this linear combination in the constants A_1, A_2, C_1, C_2, and introducing the (dimensionless) quantities

$$x = \tfrac{1}{2}k_1 a, \quad y = \tfrac{1}{2}k_2 a, \qquad (8)$$

the continuity of the tangential components of E and H at the boundary gives the following system of homogeneous equations:

$$\begin{aligned}
A_1 \sin x &= -A_2 \frac{\sin y}{\cos 2y},\\
-\frac{(A_1 hm + C_1 i\omega\mu k_1)\sin x}{k_1^2+m^2} &= \frac{(A_2 hm + C_2 i\omega\mu k_2)\sin y}{(k_2^2+m^2)\cos 2y},\\
C_1 \cos x &= C_2 \frac{\cos y}{\cos 2y},\\
\frac{(-A_1 i\omega\epsilon_1 k_1 + C_1 hm)\cos x}{k_1^2+m^2} &= \frac{(-A_2 i\omega\epsilon_2 k_2 + C_2 hm)\cos y}{(k_2^2+m^2)\cos 2y}.
\end{aligned} \qquad (9)$$

In order to obtain a solution different from 0 for A_1, A_2, C_1, C_2, the determinant of the coefficients must vanish.

Expansion of this determinant leads, if we discard trivial solutions, to the two transcendental equations

$$\tan y/y = -\tan x/x, \qquad (10)$$

$$y \tan y = -(\epsilon_2/\epsilon_1)x \tan x. \qquad (11)$$

As we shall see, different waves correspond to these two equations. Equations (10) and (11) are easily solved numerically or graphically, and curves can be plotted of y against x. In the case of Eq. (11) different curves are obtained for different values of the ratio ϵ_2/ϵ_1. If we had considered media with magnetic permeability different from that of empty space, Eq. (10) would have contained the ratio μ_2/μ_1.

x and y are further connected by the equation, deduced from (4):

$$y^2 - x^2 = \frac{\epsilon_2-\epsilon_1}{\epsilon_0}\frac{\omega^2 a^2}{4c^2} = \frac{\epsilon_2-\epsilon_1}{\epsilon_0} f^2 = f'^2 \qquad (12)$$

(ϵ_0 = dielectric constant of vacuum),

$$f = \frac{\omega a}{2c} = \frac{\pi a}{\lambda_0}, \qquad (13)$$

(λ_0 being the wave-length in vacuum), which, together with either (10) or (11), completely determines them for a given frequency. When x and y are known, the wave-length λ in the guide is found from (4):

$$h^2 = -\beta^2 = k_1^2 + m^2 - \epsilon_1\mu\omega^2 = k_2^2 + m^2 - \epsilon_2\mu\omega^2;$$

or writing

$$g=\tfrac{1}{2}a\beta=\pi a/\lambda \tag{14}$$

and

$$p=\tfrac{1}{2}am=\tfrac{1}{2}\pi al/b \quad l=0, 1, 2\cdots, \tag{15}$$

we have

$$g^2=\frac{\epsilon_1}{\epsilon_0}f^2-p^2-x^2=\frac{\epsilon_2}{\epsilon_0}f^2-p^2-y^2$$

$$=\frac{y^2-\frac{\epsilon_2}{\epsilon_1}x^2}{\frac{\epsilon_2}{\epsilon_1}-1}-p^2, \tag{16}$$

showing that a cut-off frequency exists as in ordinary tubes. This, and the ratio λ/a, depend on the shape of the tube, which affects the parameter p.

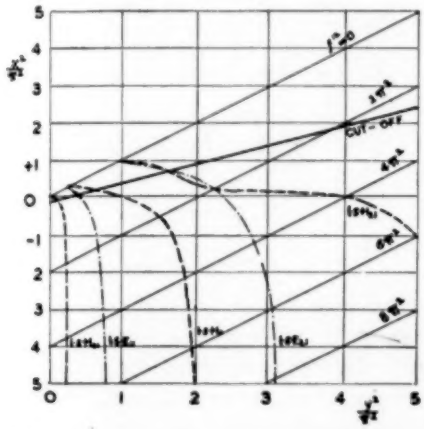

FIG. 2. Values of x^2 and y^2 at different frequencies for the first two l-s $E_{n,1}$, and the first three l-s $H_{n,1}$ waves with $\epsilon_2/\epsilon_1=2$. Cut-off line refers to tube of square cross section.

The phase velocity of the waves is $v=\omega/\beta=fc/g$, and the group velocity $u=d\omega/d\beta=gc/f$. We see that in this problem x and y are not constant for a certain wave, as is the case for the single quantity which appears in their place in a one-dielectric tube, but are functions of the frequency and of the dielectric constants. In the case of Eq. (10), however, they depend on the single variable

$$f'=\left(\frac{\epsilon_2-\epsilon_1}{\epsilon_0}\right)^{\frac{1}{2}}\frac{\pi a}{\lambda_0}.$$

With fixed λ_0, infinite pairs of values $y_n(\lambda_0)$, $x_n(\lambda_0)$ are found satisfying (12) and either (10) or (11). To each pair of values corresponds a particular wave that can be labeled with the order of the corresponding root. When $\epsilon_2\to\epsilon_1$ (or $\lambda_0\to\infty$), both x_n and y_n approach $n\pi/2$, the smallest value of n being 1 for Eq. (10) and 0 for Eq. (11), so that we shall label "one" the first wave corresponding to (10) and "zero" the first wave corresponding to (11).

An examination of the fundamental equations shows that when ω increases, y_n increases, while x_n decreases, until, for a certain ω, $x_n=0$. When this happens, y in the case of Eq. (10) has a value which is a root of $y\cot y=-1$, namely,

$$y=0.645,\quad 1.564,\quad 2.54,\quad \cdots,\quad (n-\tfrac{1}{2})\pi,$$

and in the case of (11) has a value which is a root of the equation $\tan y=0$, or $y=n\pi$. If the frequency is further increased, x_n becomes purely imaginary. Equations (10) and (11) become:

$$\frac{\tan y}{y}=-\frac{\tanh|x|}{|x|}, \tag{10'}$$

$$y\tan y=+\frac{\epsilon_2}{\epsilon_1}|x|\tanh|x|, \tag{11'}$$

where the modulus of x is indicated by $|X|$. Then $|x|$ increases steadily for increasing ω, and, for $\lambda_0\to 0$, becomes proportional to ω:

$$|x|\to\left(\frac{\epsilon_2-\epsilon_1}{\epsilon_0}\right)^{\frac{1}{2}}f=\left(\frac{\epsilon_2-\epsilon_1}{\epsilon_0}\right)^{\frac{1}{2}}\frac{a\omega}{2c},\ \text{for all } n,$$

while y_n approaches the value $n\pi$ in the case of (10') and the value $(n+\frac{1}{2})\pi$ in the case of (11').

These results are shown in Fig. 2. y^2/π^2 is plotted as abscissa and x^2/π^2 as ordinate. The diagonal lines give

$$f'^2=\frac{\epsilon_2-\epsilon_1}{\epsilon_0}\frac{a^2\omega^2}{4c^2}.$$

The chain curves give the first and second solution of (10), (10') and are independent of the values of the dielectric constants. The broken line curves give the first, second, and third solution of (11), (11'), for a ratio $\epsilon_2/\epsilon_1=2$. The curves for other values of this ratio are easily deduced from them.

The other line drawn on this graph is the cut-off line for a particular value of p, namely,

$p=\pi/2$, corresponding to $l=1$ for a tube of square cross section. Along this line, if equation $g=0$, or

$$y^2-\frac{\epsilon_2}{\epsilon_1}x^2=\left(\frac{\epsilon_2}{\epsilon_1}-1\right)p^2, \tag{17}$$

the wave-length in the guide becomes infinite. In the region above it no waves are propagated. Lines parallel to the cut-off line, represented by (16) for arbitrary values of g, would give the values of f, x, y, corresponding to a given wave-length in the guide.

In the region of propagation we have generally from (16):

$$\left(\frac{\pi a}{\lambda}\right)^2=\frac{\epsilon_1}{\epsilon_0}\left(\frac{\pi a}{\lambda_0}\right)^2-p^2-x^2. \tag{16'}$$

For small λ_0 we have seen that

$$x\rightarrow\left(\frac{\epsilon_2-\epsilon_1}{\epsilon_0}\right)^{\frac{1}{2}}\frac{\pi a}{\lambda_0}i,$$

and we can neglect p^2, so that, at high frequencies, $\lambda=\lambda_0(\epsilon_0/\epsilon_2)^{\frac{1}{2}}$, the value corresponding to propagation in the dielectric of higher constant, for both kinds of waves.

To see what happens when the frequency decreases, let us consider the case $\epsilon_1=\epsilon_0$; then

$$\left(\frac{\pi a}{\lambda}\right)^2-\left(\frac{\pi a}{\lambda_0}\right)^2=-p^2-x^2.$$

λ remains $<\lambda_0$ when x is imaginary and $|x|>p$; otherwise λ is $>\lambda_0$, and becomes infinite for a value of λ_0 which is higher the higher the dielectric constant of the other medium. As usual the wave-length and the cut-off frequency increase for increasing order of the root.

The general case is analogous.

It is evident from Fig. 2 that for x imaginary the second kind of waves has, at the same frequency, a smaller value of $|x|$ than the first kind of waves of the same order, so that, for x imaginary, the first kind of waves has a smaller wave-length than the second. For x real we see from the figure that the two curves cross several times generally, so that the wave-length in the first case may be larger than, equal to, or smaller than the wave-length in the second.

4

We indicate now by x and y a pair of values of these quantities satisfying either (10) and (12), or (11) and (12). Inserting them in the relations (9), we find that the ratios of the constants A_2, C_1, C_2, to A_1 are:

$$\frac{A_2}{A_1}=-\frac{\sin x}{\sin y}\cos 2y \tag{18}$$

$$\frac{C_1}{A_1}=Gk_1\left(\frac{\epsilon_1}{\mu}\right)^{\frac{1}{2}} \text{ for Eq. (10)};$$

$$\frac{C_1}{A_1}=-\frac{1}{Gk_1}\left(\frac{\epsilon_1}{\mu}\right)^{\frac{1}{2}} \text{ for Eq (11)}; \tag{19}$$

$$\frac{C_2}{A_2}=Gk_2\left(\frac{\epsilon_2}{\mu}\right)^{\frac{1}{2}} \text{ for Eq. (10)};$$

$$\frac{C_2}{A_2}=-\frac{1}{Gk_2}\left(\frac{\epsilon_2}{\mu}\right)^{\frac{1}{2}} \text{ for Eq. (11)}; \tag{20}$$

with

$$G=\frac{ch}{m\omega i}=\frac{1}{m}\frac{\lambda_0}{\lambda}.$$

Indicating now by A in the case of the first equation, and by B in the case of the second equation the only constant which is left, and which depends on the experimental conditions in which the tube is excited, we obtain the following expressions for the field components:

In the case of Eqs. (10), (10') we have in the first medium:

$$\begin{aligned}
&E_X=0,\\
&E_Y=-A\frac{h}{m}\sin k_1X\cos mY e^{-hZ+i\omega t},\\
&E_Z=A\sin k_1X\sin mY e^{-hZ+i\omega t},\\
&H_X=A\frac{h^2-m^2}{\pi m\mu\omega i}\sin k_1X\cos mY e^{-hZ+i\omega t},\\
&H_Y=A\frac{k_1}{\mu\omega i}\cos k_1X\sin mY e^{-hZ+i\omega t},\\
&H_Z=A\frac{hk_1}{m\mu\omega i}\cos k_1X\cos mY e^{-hZ+i\omega t}.
\end{aligned} \tag{21}$$

In the second medium A is replaced by $A\sin x/\sin y$, k_1 by k_2, and k_1X by $k_2(a-X)$.

TABLE I. Ratio of amplitude in medium of higher ϵ to amplitude in medium of lower ϵ.

	For E_Y; E_Z; H_X	For D_X; H_Y; H_Z
l-s E waves	$\dfrac{\sin x}{\sin y}$	$-\dfrac{y \sin x}{x \sin y}$
l-s H waves	$\dfrac{\sin x}{\sin y}$	$-\dfrac{x \sin x}{y \sin y}$

Moreover, there is a change of sign of H_Y and H_Z. In the case of Eqs. (11), (11′) we have in the first medium:

$$
\begin{aligned}
E_X &= -B\frac{h^2-m^2}{hk_1}\cos k_1X \sin mY e^{-hZ+i\omega t},\\
E_Y &= -B\frac{m}{h}\sin k_1X \cos mY e^{-hZ+i\omega t},\\
E_Z &= B \sin k_1X \sin mY e^{-hZ+i\omega t},\\
H_X &= 0,\\
H_Y &= -B\frac{\epsilon_1\omega i}{k_1}\cos k_1X \sin mY e^{-hZ+i\omega t},\\
H_Z &= -B\frac{m\epsilon_1\omega i}{hk_1}\cos k_1X \cos mY e^{-hZ+i\omega t}.
\end{aligned}
\tag{22}
$$

In the second medium B is replaced by $B \sin x/\sin y$, ϵ_1 by ϵ_2, k_1 by k_2, and k_1X by $k_2(a-X)$. There is a change of sign of E_X, H_Y, H_Z. In the region in which x (or k_1) is imaginary, we have $i \sinh |x|$ instead of $\sin x$, and $\cosh |x|$ instead of $\cos x$.

The field described by (21) is characterized by the absence of E_X, and that described by (22) by the absence of H_X. Such waves are called longitudinal-section electric and magnetic waves, respectively, l-s E waves and l-s H-waves),[2] and, when $\epsilon_2=\epsilon_1$, they become those linear combinations of the ordinary E and H waves of the same order, which have a vanishing E_X and H_X, respectively. (For $l=0$ or $n=0$, the wave is simply an H wave.) We label them with the corresponding values of n and l, namely, l-s $E_{n,l}$, l-s $H_{n,l}$. For l-s E waves $l=0$ is possible, and the first wave ($n=1$) reduces, for $\epsilon_2=\epsilon_1$, to $H_{1,0}$; for l-s H waves $l=1$ is the first possible value, and the first wave ($n=0$) reduces, for $\epsilon_1=\epsilon_2$, to $H_{0,1}$. This notation is used to identify the curves of Fig. 2, in which the second index is taken equal to 1, so that the cut-off line applies to a tube of square cross section.

As λ is generally different for the two kinds of waves, we cannot, except in particular cases, form linear combinations of them that will produce ordinary E or H waves. In both media all the field components are sine functions of X, but with different amplitudes, so as to satisfy the boundary conditions. The ratios of the amplitudes in the two media are given in Table I.

When x is real, all these ratios remain finite, as x and y reach together values multiple of π, the limit of $\sin x/\sin y$ being finite. When $x=0$ the ratios are not immediately given by Table I, but it is easily found that the ratio for D_X, D_Y, H_Z remains finite in both case, these components being independent of X in the first medium. For E_Y, E_Z, H_X the ratio is also finite for l-s E waves, but is infinite for l-s H waves, these components being then entirely confined to the second medium.

When x is imaginary, we must write $i \sinh |x|$ instead of $\sin x$ and then when $|x|$ increases, all the ratios approach infinity, namely, for large values of $|x|$ (high frequencies) all components are confined to the medium of higher dielectric constant; we have already seen that the wavelength approaches then the value corresponding to this medium.

Figure 3 shows the dependence on X of the first three components for different values of f' in the case of l-s $E_{1,l}$, Fig. 4 in the case of l-s $H_{1,l}$ for $\epsilon_2/\epsilon_1=2$, and Fig. 5 gives the same for l-s $H_{0,l}$ at a fixed f' ($f'=3.33$) and for different values of $\epsilon_2/\epsilon_1=\epsilon$. All ordinates are in arbitrary scales.

From Eqs. (21), (22) the E and H lines are easily drawn: They present a pattern which is similar to that of i-s waves in one-dielectric tubes, but somewhat distorted. For instance the E lines for l-s $H_{0,1}$ (coinciding with $H_{0,1}$ in a one-dielectric tube) are not straight lines in the X-Y plane.

5

It is interesting to examine the above results by use of the picture of the component criss-cross

[2] H. Buchholz, E.N.T. **16**, 73 (1939).

waves.[3] They are plane transverse waves, crisscrossing along the tube, and moving in each medium with the velocity that they would have in the same medium unrestricted by the tube. The waves in a rectangular tube are generally the

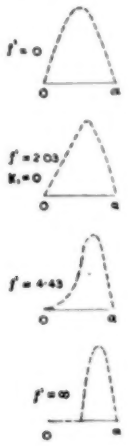

FIG. 3. E_Y, (E_Z, H_X) as function of X at different frequencies for l-s $E_{1,1}$.

resultant of 4 such waves, in some cases only of 2. The angle θ that the propagation vector of the component waves makes with the X axis is (for x real) given by

$$\cos\theta_1=(\epsilon_0/\epsilon_1)^{\frac{1}{2}}(ck_1/\omega)=(\epsilon_0/\epsilon_1)^{\frac{1}{2}}(x/f)$$

in the first medium,

$$\cos\theta_2=(\epsilon_0/\epsilon_2)^{\frac{1}{2}}(ck_2/\omega)=(\epsilon_0/\epsilon_2)^{\frac{1}{2}}(y/f) \tag{23}$$

in the second medium.

θ_1 and θ_2 increase with increasing frequency, always satisfying the law of refraction

$$\frac{\sin\theta_1}{\sin\theta_2}=\left[\frac{1-\dfrac{\epsilon_0x^2}{\epsilon_1f^2}}{1-\dfrac{\epsilon_0y^2}{\epsilon_2f^2}}\right]^{\frac{1}{2}}=\left(\frac{\epsilon_2}{\epsilon_1}\right)^{\frac{1}{2}}, \tag{24}$$

(as $y^2=x^2+(\epsilon_2-\epsilon_1/\epsilon_0)f^2$), until, for $x=0$, θ_1 reaches the value $\pi/2$. $\theta_2(x=0)$ is then the critical angle. This explains why x becomes imaginary when the frequency is further increased: There can be no more ordinary component waves in the first medium, but only waves propagated parallel to the surface of separation, and with an amplitude falling off exponentially (in a region of the order of the wave-length) in a direction normal to this surface. Hence the dependence on X of all the field components involves the hyperbolic functions. Each of the component waves falls off in the first medium according to a factor $e^{-(2/a)|x|X}$. This is in agreement with the well-known expression for the light entering the medium of lower refractive index in total reflection; in fact, this has a factor[4]

$$\exp\left[-(\omega/c)(n^2\sin^2 i-1)^{\frac{1}{2}}X\right]$$

(where i is our θ_2, $n^2=\epsilon_2/\epsilon_0$, and $\epsilon_1=\epsilon_0$); and we have

$$\frac{\omega}{c}\left(\frac{\epsilon_2}{\epsilon_0}\sin^2\theta_2-1\right)^{\frac{1}{2}}=\left[\frac{\omega^2}{c^2}\left(\frac{\epsilon^2}{\epsilon_0}-1\right)-k_2^2\right]^{\frac{1}{2}}$$

$$=|k_1|=\frac{2}{a}|x|.$$

FIG. 4. E_Y, (E_Z), as function of X at different frequencies for l-s $H_{1,1}$ and $\epsilon_2/\epsilon_1=2$.

When the frequency is high and the falling off is rapid, multiple reflections are negligible, and

[3] L. Brillouin, Rev. gén. de l'Elec. **40**, 227 (1936). L. Page and N. I. Adams, Phys. Rev. **52**, 647 (1937). L. Pincherle, Phil. Mag. (in print).

[4] See, for example, the article by W. König in *Handbuch der Physik*, Vol. XX, p. 231.

then also the ratio of the amplitudes of the component waves at the surface of separation coincides with the usual expression. In fact, this ratio in our tube for E_Y and l-s E waves is

$$r=(\sin y e^{|x|})/(\sinh |x|).$$

FIG. 5. E_Y, (E_Z), as function of X for l-s $H_{0,1}$, with $f'=3.33$, and different values of $\epsilon=\epsilon_2/\epsilon_1$.

Now for high frequencies $|x|$ is large, and the ratio is

$$r=2\sin y=\frac{2\tan y}{(1+\tan^2 y)^{\frac{1}{2}}}=\frac{2y}{\left(\frac{y^2}{\tan^2 y}+y^2\right)^{\frac{1}{2}}}.$$

Using (10′) with $\tanh |x|=1$, we have then

$$r=\frac{2y}{(|x|^2+y^2)^{\frac{1}{2}}}=\frac{2y}{f[(\epsilon_2/\epsilon_0)-1]^{\frac{1}{2}}}=\frac{2n\cos i}{(n^2-1)^{\frac{1}{2}}},$$

the well-known expression.

We consider now the propagation of e-m waves in a cylindrical dielectric guide of radius a and constant ϵ_1, surrounded by a medium of dielectric constant ϵ_2, bounded by a coaxial metal tube of radius b (Fig. 6). We use cylindrical coordinates r, φ, z. We assume the conductivity of the two dielectrics to be zero, and that of the metal to be infinite; we take the magnetic permeability of both dielectrics to be that of empty space. This problem reduces to the ordinary hollow tube for $\epsilon_1=\epsilon_2$ (or $a=0$, or $b=a$), and reduces to the problem of the dielectric guide[5] for $b=\infty$. We try to write solutions of Maxwell's equations of the E and H wave type, namely, with either an E_z or an H_z. Writing, as before, $h^2=k_1^2-\epsilon_1\mu\omega^2=k_2^2-\epsilon_2\mu\omega^2$, we consider the solution

$$U=\frac{J_n(kr)}{N_n(kr)}\cos n\varphi e^{-hz+i\omega t} \quad n=0, 1, 2\cdots \tag{25}$$

where J_n and N_n are the Bessel and Neumann functions of order n,[6] and the field components are determined, in the case of E waves, by:

$$E_r=\frac{\partial^2 U}{\partial r\partial z};\quad E_\varphi=-\frac{1}{r}\frac{\partial^2 U}{\partial\varphi\partial z};\quad E_z=\frac{\partial^2 U}{\partial z^2}+\epsilon\mu\omega^2 U;$$
$$H_r=\frac{i\omega\epsilon}{r}\frac{\partial U}{\partial\varphi};\quad H_\varphi=-i\omega\epsilon\frac{\partial U}{\partial r};\quad H_z=0; \tag{26}$$

and in the case of H waves by:

$$E_r=-\frac{i\omega\mu}{r}\frac{\partial U}{\partial\varphi};\quad E_\varphi=i\omega\mu\frac{\partial U}{\partial r};\quad E_z=0;$$
$$H_r=\frac{\partial^2 U}{\partial r\partial z};\quad H_\varphi=\frac{1}{r}\frac{\partial^2 U}{\partial\varphi\partial z};\quad H_z=\frac{\partial^2 U}{\partial z^2}+\epsilon\mu\omega^2 U. \tag{27}$$

We have two different solutions in the two media. In the first (inner) medium we cannot have the Neumann function, as it becomes infinite for $r=0$; the solution in this medium will be:

$$U_1=CJ_n(k_1 r)\cos n\varphi e^{-hz+i\omega t}. \tag{28}$$

In the second (outer) medium the solution is:

$$U_2=[AJ_n(k_2 r)+BN_n(k_2 r)]\cos n\varphi e^{-hz+i\omega t}. \tag{29}$$

At the walls of the tube E_z and E_φ must vanish;

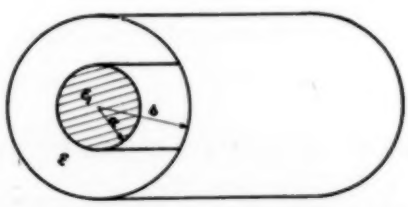

FIG. 6. The tube studied in the second problem.

[5] D. Hondros and P. Debye, Ann. d. Physik **32**, 465 (1910). J. R. Carson, S. P. Mead, and S. A. Schelkunoff, Bell Sys. Tech. J. **15**, 310 (1937).

[6] Definition of Bessel, Neumann, and Hankel functions as in E. Jahnke and F. Emde, *Tables of Functions* (Teubner, Leipzig, 1933), pp. 194–200.

this gives, in the case of E waves,

$$B=-A[J_n(k_2b)/N_n(k_2b)] \tag{30}$$

and in the case of H waves

$$B=-A[J_n'(k_2b)/N_n'(k_2b)], \tag{31}$$

the dash indicating differentiation with respect to the argument. We have further to satisfy the boundary conditions at $r=a$, namely, the continuity of E_φ, E_z, H_φ, H_z. These, as in Section 2, cannot generally be satisfied by a single E or H wave, and a linear combination must be introduced. The calculation can be carried out, the equation for the proper values of k_1 and k_2 deduced, and solutions found in rather a similar way as that used for dielectric guides by Carson, Mead, and Schelkunoff; but, as the solutions for different n's are not fundamentally different, it will be sufficient to discuss the problem for the simpler case $n=0$ (circularly symmetrical waves), in which all the boundary conditions can be satisfied by a simple E or H wave. The fundamental equation is in this case

$$\frac{J_1(x)}{xJ_0(x)}=\frac{\epsilon_2}{\epsilon_1 y}\frac{J_0(my)N_1(y)-J_1(y)N_0(my)}{J_0(my)N_0(y)-J_0(y)N_0(my)} \tag{32}$$

for the E_0 wave, and

$$\frac{J_1(x)}{xJ_0(x)}=\frac{J_1(y)N_1(my)-J_1(my)N_1(y)}{J_0(y)N_1(my)-J_1(my)N_0(y)}\frac{1}{y} \tag{33}$$

for the H_0 wave, where $x=k_1a$, $y=k_2a$, and $m=b/a$. If we write

$$f=\epsilon_0\mu_0\omega a=(2\pi a)/\lambda_0$$

(λ_0 = wave-length in vacuum), (13′)

$$g=(ah)/i=(2\pi a)/\lambda$$

(λ = wave-length in the guide), (14′)

x and y are connected, as in the first problem, by the additional relation

$$y^2=x^2-(\epsilon_1-\epsilon_2/\epsilon_0)f^2=x^2-f'^2, \tag{12′}$$

which, together with either (32) or (33), completely determines them for all frequencies; and the wave-length in the guide is found from the relation

$$g^2=(\epsilon_2/\epsilon_0)f^2-y^2=(\epsilon_1/\epsilon_0)f^2-x^2. \tag{35}$$

Equations (32) and (33) have to be solved numerically. Tables for the left-hand side

$$\varphi(x)=\frac{J_1(x)}{xJ_0(x)}$$

and for the right-hand side (for E waves)

$$\psi(y)=\frac{1}{y}\frac{J_0(my)N_1(y)-J_1(y)N_0(my)}{J_0(my)N_0(y)-J_0(y)N_0(my)}$$

have to be constructed for various values of m. Then the fundamental equation becomes

$$\varphi(x)=\frac{\epsilon_2}{\epsilon_1}\psi(y),$$

and the relation between x and y is immediately found from the tables. We have a series of x-y curves, each of which gives a solution. In the case of H waves the procedure is simpler, as then

$$\varphi(x)=\bar{\psi}(y),$$

and the $x-y$ curves depend only on m and not

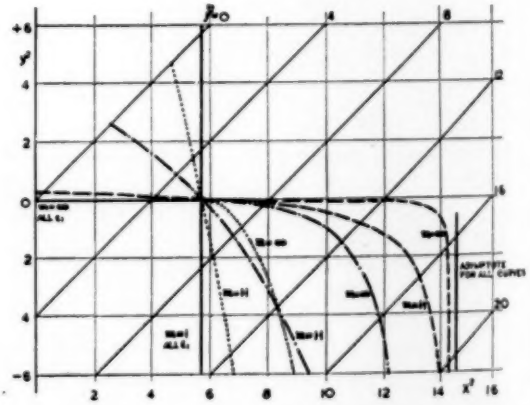

FIG. 7. Values of x^2 and y^2, at different frequencies and for different m, for $E_{0,1}$. Dotted curves $\epsilon_1/\epsilon_2=1.1$; chain curves $\epsilon_1/\epsilon_2=5$; broken line curves $\epsilon_1/\epsilon_2=81$.

on the ratio ϵ_2/ϵ_1. (In media with $\mu\neq\mu_0$, these would depend on μ_2/μ_1).

If the hyperbola given by (12) for the required value of the frequency is also plotted, the intercepts of this hyperbola with the other curves

give the values of x and y at the given frequency and for each solution of the fundamental equation.

7

Each curve corresponds to a different wave in the tube, which can be labeled $E_{0,1}$, $E_{0,2}$, $\cdots$,

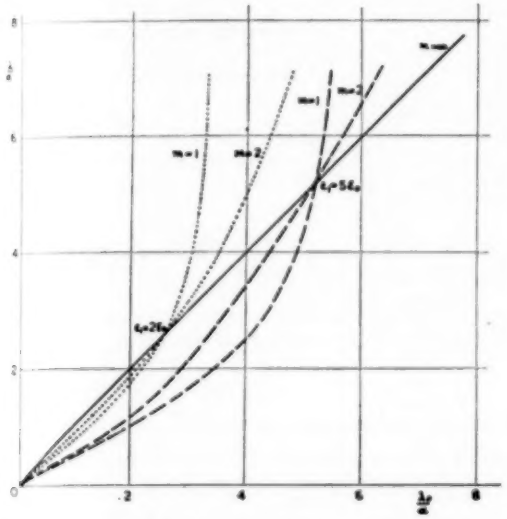

FIG. 8. The relation between the wave-length in the guide λ and the wave-length in vacuum λ_0, for different values of ϵ_1/ϵ_0 and m, in the case of $E_{0,1}$ with $\epsilon_2=\epsilon_0$.

$H_{0,1}$, $H_{0,2}$, $\cdots$, and which reduces to the ordinary $E_{0,l}$, $H_{0,l}$ for $\epsilon_2=\epsilon_1$. When $b=\infty$ the E waves reduce to the waves investigated by Hondros and Debye in a dielectric guide. As in the previous problem the parameter, say y, corresponding to the medium with smaller dielectric constant decreases when the frequency increases, and vanishes for a certain value of it. For higher frequencies the curve $y-x$ is continued for negative values of y^2. When y is imaginary it is convenient to substitute in (29) one of the Hankel functions, say $H_n^{(1)}$, for Neumann's. Equations (32) and (33) remain formally the same with $H_n^{(1)}$ written instead of N_n. When either $m\to\infty$, or the frequency is high, and $|y|$ is large, $H_n^{(1)}(my)$ can be neglected, and we have instead of (32) and (33):

$$\frac{J_1(x)}{xJ_0(x)}=\frac{\epsilon_2}{\epsilon_1 y}\frac{H_1^{(1)}(y)}{H_0^{(1)}(y)} \text{ for } E_0, \tag{36}$$

$$\frac{J_1(x)}{xJ_0(x)}=\frac{1}{y}\frac{H_1^{(1)}(y)}{H_0^{(1)}(y)} \text{ for } H_0. \tag{37}$$

Equation (36) is identical with Hondros and Debye's equation for dielectric guides.

We see that it is then more convenient to plot curves of y^2 against x^2, instead of curves of y against x, so that both cases, y real and y imaginary, may be included in the same diagram. Also in such a diagram the curves representing (12) are straight lines and can be conveniently drawn. Figure 7 gives such a diagram, in which the y^2-x^2 curves are shown for $E_{0,1}$, for the values 1,1 (dotted curves), 5 (chain curves), 81 (broken line curves) of the ratio ϵ_1/ϵ_2, and for $m=1$ (ordinary hollow tube), $m=1,1$, and $m=\infty$ (dielectric guide).

The wave-length in the guide is found from the diagram by means of (35). The equations of the cut-off lines are $y^2=(\epsilon_2/\epsilon_1)x^2$. Figure 8 gives the relation between λ and λ_0 in the case of $E_{0,1}$, for $\epsilon_1/\epsilon_0=2$ and 5, ϵ_2 being equal to ϵ_0, and for $m=1$ and 2. The curves for $m>2$ differ little from the curves for $m=2$ below the critical point. Above this point they remain nearer to the line $\lambda=\lambda_0$, representing propagation in vacuum, than the curves for $m=2$, and they actually coincide with this line for $m=\infty$. We have

$$\lambda \gtrless \lambda_0\left(\frac{\epsilon_0}{\epsilon_2}\right)^{\frac{1}{2}}\left(\lambda \gtrless \lambda_0 \text{ if the second medium is air}\right),$$

according as

$$\frac{\lambda_0}{a} \gtrless 2.613\left[\frac{(\epsilon_1-\epsilon_2)}{\epsilon_0}\right]^{\frac{1}{2}}$$

and independently of the radius of the metal tube. This wave-length

$$\frac{\lambda_c}{a}=2.613\left[\frac{(\epsilon_1-\epsilon_2)}{\epsilon_0}\right]^{\frac{1}{2}} \tag{38}$$

can be called the critical wave-length; it corresponds to $y=0$, and to the component waves (of which there is an infinite number in a circular guide) falling on the surface of separation under the critical angle.

For $\lambda_0<\lambda_c$ our tube behaves more as a dielectric guide than as a hollow tube: The curves $\lambda-\lambda_0$ for all values of m do not differ much from the curve referring to $m=\infty$; λ increases when

TABLE II. Values of x, y, λ at different frequencies for $E_{0,1}$ and $\epsilon_1 > \epsilon_2$.

	x	y	λ
	First root of the equation:*		
Static field	$\dfrac{N_0(mx)}{J_0(mx)} = \dfrac{\epsilon_1 J_1(x) N_0(x) - \epsilon_2 J_0(x) N_1(x)}{(\epsilon_1 - \epsilon_2) J_0(x) J_1(x)}$	$= x$	
$\lambda_0 > \lambda_c$ decreasing	Real and increasing	Real and decreasing	$\lambda > \lambda_0(\epsilon_0/\epsilon_2)^{\frac{1}{2}}$ Decreasing with increasing m
$\lambda_0 = \lambda_c$	2.4048	0	$\lambda/a = (\lambda_0/a)(\epsilon_0/\epsilon_2)^{\frac{1}{2}} = 2.613(\epsilon_1/\epsilon_2 - 1)^{\frac{1}{2}}$
$\lambda_0 < \lambda_c$ decreasing	Real and increasing, approaching the value 3.8317	Imaginary and approaching the value $\left\{14.682 - \dfrac{\epsilon_1 - \epsilon_2}{\epsilon_0}\dfrac{4\pi a^2}{\lambda_0^2}\right\}^{\frac{1}{2}}$	$\lambda < \lambda_0(\epsilon_0/\epsilon_2)^{\frac{1}{2}}$ Approaching the value $\lambda = \lambda_0(\epsilon_0/\epsilon_1)^{\frac{1}{2}}$ increasing with increasing m
Limit case $\epsilon_1 = \epsilon_2$	$2.4048/m$ at all frequencies	$= x$	$\left(\dfrac{a}{\lambda}\right)^2 = \left(\dfrac{a}{\lambda_0}\right)^2 \dfrac{\epsilon_1}{\epsilon_0} - 0.1465$

* This root (for $\epsilon_2 = \epsilon_0$) is 2.4048 when $\epsilon_1 = \epsilon_0$ and $m = 1$; it decreases both for increasing ϵ_1 and increasing m, approaching the value 0, both for $\epsilon_1 \to \infty$, and $m \to \infty$.

the radius of the metal tube increases, in contradiction to the case of one-dielectric tubes.

For $\lambda_0 > \lambda_c$, on the other hand, our tube behaves as an ordinary tube. λ decreases when m increases, and increases rapidly with λ_0 becoming infinite at a value of λ_0 which is the larger, the larger the value of ϵ_1. When $m \to \infty$, λ remains always equal to λ_0 in this region, and the propagation is accompanied by radiation from the sides of the dielectric guide.

For H waves the critical wave-length is not independent of m. For instance, for $H_{0,1}$, λ_c/a is, as before, equal to 2.613 $[(\epsilon_1 - \epsilon_2)/\epsilon_0]^{\frac{1}{2}}$ for $m = \infty$, but decreases with decreasing m, and reaches the value

$$\lambda_c/a = 1.640[(\epsilon_1 - \epsilon_2)/\epsilon_0]^{\frac{1}{2}}$$

for $m = 1$. For H waves λ decreases with increasing m even when $\lambda_0 < \lambda_c$. Table II for $E_{0,1}$, and Table III for $H_{0,1}$, summarize the variations that x, y, λ undergo when the frequency increases from a static field to very high values.

No experimental results are known for the wave-length in such a guide other than the experiments of Schriever[7] and Kašpar[8] on water guides in air, without metal tube ($m = \infty$); they confirm the theory for $\lambda_0 < \lambda_c$ and the fact that $\lambda = \lambda_0$ at the critical frequency. In this case we expect that for $\lambda_0 > \lambda_c$, λ should always be equal to λ_0. Schriever's experiments show instead that $\lambda > \lambda_0$, and his results are consistent with what would be expected, had there been a metal tube with $m \simeq 5$. These results, however, have been criticized by Kašpar, whose investigation does not extend to the region $\lambda_0 > \lambda_c$. The expressions for the field components are: E_0 wave; first medium:

$$E_r = A_1 \frac{hx}{a} J_1\left(x\frac{r}{a}\right) e^{-hz+i\omega t},$$

$$E_z = A_1 \frac{x^2}{a^2} J_0\left(x\frac{r}{a}\right) e^{-hz+i\omega t}, \qquad (39)$$

$$H_\varphi = A_1 i\omega\epsilon_1 \frac{x}{a} J_1\left(x\frac{r}{a}\right) e^{-hz+i\omega t};$$

E_0 wave; second medium:

$$E_r = A_2 \frac{hy}{a}\left[N_0(my) J_1\left(y\frac{r}{a}\right) - J_0(my) N_1\left(y\frac{r}{a}\right)\right] e^{-hz+i\omega t},$$

[7] O. Schriever, Ann. d. Physik **63**, 645 (1920).
[8] E. Kašpar, Ann. d. Physik **32**, 353 (1938).

TABLE III. Values of x, y, λ at different frequencies, for $H_{0,1}$ and $\epsilon_1 > \epsilon_2$.

	x	y	λ
Static field	$3.8317/m$	$3.8317/m$	——
$\lambda_0 > \lambda_c$ decreasing	Real and increasing	Real and decreasing	$\lambda > \lambda_0(\epsilon_0/\epsilon_2)^{\frac{1}{2}}$ increasing with increasing m
$\lambda_0 = \lambda_c$	First root of the equation* $J_1(x)xJ_0(x) = \frac{1}{2}(1-m^2)$	0	$\lambda/a = (\lambda_0/a)(\epsilon_0/\epsilon_2)^{\frac{1}{2}} = (2\pi/x)(\epsilon_1/\epsilon_2 - 1)^{\frac{1}{2}}$
$\lambda_0 < \lambda_c$ decreasing	Real and increasing, approaching the value 3.8317	Imaginary, approaching the value $\left\{14.682 - \frac{\epsilon_1-\epsilon_2}{\epsilon_0}\frac{4\pi^2a^2}{\lambda_0^2}\right\}^{\frac{1}{2}}$	$\lambda < \lambda_0(\epsilon_0/\epsilon_2)^{\frac{1}{2}}$ approaching the value $\lambda = \lambda_0(\epsilon_0/\epsilon_1)^{\frac{1}{2}}$
Limit case $\epsilon_1 = \epsilon_2$	$3.8317/m$ at all frequencies	$= x$	$\left(\frac{a}{\lambda}\right)^2 = \left(\frac{a}{\lambda_0}\right)^2 \frac{\epsilon_1}{\epsilon_0} - 0.3718$

* This root is 3.8317 for $m = 1$, decreases for increasing m, and is 2.4048 for $m = \infty$.

$$E_z = A_2 \frac{y^2}{a^2}\left[N_0(my)J_0\left(y\frac{r}{a}\right) - J_0(my)N_0\left(y\frac{r}{a}\right)\right]e^{-hz+i\omega t},$$

$$H_\varphi = i\omega\epsilon_2 A_2 \frac{y}{a}\left[N_0(my)J_1\left(y\frac{r}{a}\right) - J_0(my)N_1\left(y\frac{r}{a}\right)\right]e^{-hz+i\omega t}; \tag{40}$$

with

$$A_2 = A_1 \frac{x^2}{y^2}\frac{J_0(x)}{J_0(y)N_0(my) - J_0(my)N_0(y)} \tag{41}$$

(A_1 depending on the experimental conditions). The other components vanish. When y is imaginary we have in (40) one of the Hankel functions instead of the Neumann function. H_0 wave; first medium:

$$E_\varphi = -i\omega\mu B_1 \frac{x}{a}J_1\left(x\frac{r}{a}\right)e^{-hz+i\omega t},$$

$$H_r = B_1 \frac{hx}{a}J_1\left(x\frac{r}{a}\right)e^{-hz+i\omega t}, \tag{42}$$

$$H_z = B_1 \frac{x^2}{a^2}J_0\left(x\frac{r}{a}\right)e^{-hz+i\omega t};$$

H_0 wave; second medium:

$$E_\varphi = -i\omega\mu B_2 \frac{y}{a}\left[N_1(my)J_1\left(y\frac{r}{a}\right) - J_1(my)N_1\left(y\frac{r}{a}\right)\right]e^{-hz+i\omega t},$$

$$H_r = B_2 \frac{hy}{a}\left[N_1(my)J_1\left(y\frac{r}{a}\right) - J_1(my)N_1\left(y\frac{r}{a}\right)\right]e^{-hz+i\omega t}, \tag{43}$$

$$H_z = B_2 \frac{y^2}{a^2}\left[N_1(my)J_0\left(y\frac{r}{a}\right) - J_1(my)N_0\left(y\frac{r}{a}\right)\right]e^{-hz+i\omega t};$$

$$B_2 = B_1 \frac{x^2}{y^2}\frac{J_0(x)}{J_0(y)N_1(my) - J_1(my)N_0(y)}. \tag{44}$$

As in the previous problem, when y is imaginary the waves are confined to the inner medium, the more so, the higher the frequency. For E waves, moreover, E_r and E_z are confined to the medium of higher dielectric constant also at the critical point. The way in which the dependence on r of the field components varies with the frequency is similar to that of the other problem.

TABLE IV. Values of x, y, λ at different frequencies for $E_{0,1}$ and $\epsilon_2 > \epsilon_1$.

λ_0	x	y	λ
		First root of the equation:*	
∞	$=y$	$\dfrac{N_0(my)}{J_0(my)} = \dfrac{\epsilon_2 J_0(y)N_1(y) - \epsilon_1 J_1(y)N_0(y)}{(\epsilon_2-\epsilon_1)J_0(y)J_1(y)}$	——
		First root of the equation:**	
λ_c	0	$\dfrac{\epsilon_2}{\epsilon_1 y}\dfrac{J_0(my)N_1(y) - J_1(y)N_0(my)}{J_0(my)N_0(y) - J_0(y)N_0(my)} = \dfrac{1}{2}$	$\dfrac{\lambda}{a} = \left(\dfrac{\epsilon_0}{\epsilon_1}\right)^{\frac{1}{2}} \dfrac{\lambda_0}{a} = \dfrac{2\pi}{y}\left(\dfrac{\epsilon_2}{\epsilon_1}-1\right)^{\frac{1}{2}}$
		First root of the equation:***	
$\to 0$	$\to \infty i$	$\dfrac{N_0(my)}{J_0(my)} = \dfrac{N_0(y)}{J_1(y)}$	$\lambda \to (\epsilon_0/\epsilon_2)^{\frac{1}{2}}\lambda_0$

* This root, for $\epsilon_1 = \epsilon_0$, is 2.4048 when $\epsilon_2 = \epsilon_0$, $m = 1$, and decreases for increasing m approaching the value 0. For a given m it increases with increasing ϵ_2 approaching, for $\epsilon_2 \to \infty$, a finite limit, always < 2.4048.
** This root (for $\epsilon_1 = \epsilon_0$) is infinite for $m = 1$ for all values of ϵ_2, and decreases when m increases to the value 0 for $m = \infty$. For a given m it increases with increasing ϵ_2, approaching a finite limit for $\epsilon_2 \to \infty$. It has a finite limit also for $\epsilon_2 \to \epsilon_1$.
*** The roots of this equation are independent of the dielectric constants. The first root is ∞ for $m = 1$; it is $= 3.4$ for $m = 1.5$; $= 1.80$ for $m = 2$; $= 0.514$ for $m = 5$; $= 2.4048/m$ for $m \to \infty$.

TABLE V. Values of x, y, λ at different frequencies for $H_{0,1}$ and $\epsilon_2 > \epsilon_1$.

λ_0	x	y	λ
∞	$3.8317/m$	$3.8317/m$	——
		First root of the equation:†	
λ_c	0	$\dfrac{1}{y}\dfrac{J_1(y)N_1(my) - J_1(my)N_1(y)}{J_0(y)N_1(my) - J_1(my)N_0(y)} = \dfrac{1}{2}$	$\dfrac{\lambda}{a} = \left(\dfrac{\epsilon_0}{\epsilon_1}\right)^{\frac{1}{2}} \dfrac{\lambda_0}{a} = \dfrac{2\pi}{y}\left(\dfrac{\epsilon_2}{\epsilon_1}-1\right)^{\frac{1}{2}}$
		First root of the equation:††	
$\to 0$	$\to \infty i$	$\dfrac{J_1(my)}{N_1(my)} = \dfrac{J_1(y)}{N_1(y)}$	$\lambda \to (\epsilon_0/\epsilon_2)^{\frac{1}{2}}\lambda_0$

† This root is independent of the dielectric constants. It is infinite for $m = 1$; $= 6.32$ for $m = 1.5$; $= 3.17$ for $m = 2$; $= 0.847$ for $m = 5$; $= 3.8317/m$ for $m \to \infty$.
†† This root, independent of the dielectric constants, is ∞ for $m = 1$; $= 3.95$ for $m = 1.5$; $= 2.275$ for $m = 2$; $= 0.710$ for $m = 5$; $= 0$ for $m = \infty$.

In the frequency region in which hollow tubes are used, almost all dielectrics are absorbing. The problem should then be treated by introducing a complex ϵ_1: $\bar{\epsilon}_1 = \epsilon_1 - i(\sigma_1/\omega)$, σ_1 being the conductivity of the guide. The solution of the fundamental equations would then require the use of Bessel functions of complex argument, a cumbersome procedure, as complete tables of these functions are not available. The introduction of a conductivity does not, however, lead to any important change in the features of the phenomenon, except those already known for ordinary hollow tubes.

9

If the outer medium has the higher dielectric constant, for high frequencies the waves are confined to the space between the two cylinders of radii a and b. This represents a new kind of guide, limited on the outside by the metal of the tube, and on the inside by the medium of smaller dielectric constant.

Tables IV and V, analogous to Tables II and III, give for these waves the values of x, y, λ at different frequencies for $E_{0,1}$ and $H_{0,1}$, respectively.

The relation between λ and λ_0 is similar to the case $\epsilon_1 > \epsilon_2$.

PHYSICAL REVIEW VOLUME 66, NUMBERS 5 AND 6 SEPTEMBER 1 AND 15, 1944

On the Equation of State of Monolayers

GEORGE JAFFÉ
Louisiana State University, Baton Rouge, Louisiana
(Received May 31, 1944)

The equation of state of monolayers is worked out from exactly the same point of view as the statistical theory of liquids previously given by the author. The formulae obtained should be applicable as well to gaseous films as to condensed films, though not to the domain of transition between the two, since a change in the potential must be supposed to occur in the transition. The resulting formulae are compared with two groups of observations of gaseous films. The first group concerns diesters which form insoluble films where the surface pressure has been observed directly. The second group concerns adsorbed films of fatty acids where the surface pressure has been deduced indirectly from measurements on the surface tension. The agreement is satisfactory in both groups. For condensed films the potential can be determined in such a way that the density and the surface vapor pressure (where this is known) come out correctly. The compressibility is then of the right order of magnitude.

I. INTRODUCTION

IT is well known that in some cases surface films, both the insoluble and the adsorbed kind, approach with a reasonable accuracy the behavior of "two-dimensional gases." [1] However, most measurements of surface pressure, direct or indirect, refer to conditions where the actual area of the molecules and their lateral adhesion cannot be disregarded. Therefore, two-dimensional equations of state of the van der Waals type, with two corresponding constants a and b, have been introduced for the study of adsorbed films. "The usefulness of all such equations is limited to moderate pressures and, as in three dimensions, neither a nor b are really constant." [2]

It was pointed out by Fowler[3] that the difficulties in going beyond the existing treatments are of exactly the same nature as those encountered in the establishment of equations of state for compressed gases and liquids. This suggests that any progress made in the method of evaluating the partition sum in the three-dimensional case will, almost automatically, result in applicability to the two-dimensional case of monolayers.

Now the author[4] has developed recently a statistical theory of liquids which derives the essential features of a liquid from the knowledge of the mutual potential energy of the molecules, and which, after the choice of a special form of potential, leads to a reasonable agreement with experimental data for liquids of widely different character. It seemed worth while to the author to attempt an extension of his method to the equation of state of monolayers. This is being done in what follows. Since the calculations involved are so very similar to those of the previous problem, the reader is referred for details to the two papers quoted.

II. THEORY

Here again we are going to assume that the molecules are extensionless points, of mass m, and that the total potential energy of the molecules in the monolayer is the sum of binary contributions. These assumptions appear to be even more objectionable in the present case than in the idealization of liquids. The molecules forming monolayers consist mostly of long chains, and it is known that these chains lie flat on the surface of the carrier liquid in gaseous films whereas they stand up eventually under some angle, and are closely packed in condensed films. Consequently, there must be a domain of transition which cannot possibly be described by the simple model of central forces.

A more complete treatment would have to take into account at least the dependence of the potential upon the orientations of two interacting molecules. This can be done and has been at-

[1] N. K. Adam, *The Physics and Chemistry of Surfaces* (Clarendon Press, Oxford, 1938). Cf. pp. 40 and 116.
[2] N. K. Adam, reference 1, p. 120.
[3] R. H. Fowler, *Statistical Mechanics* (University Press, Cambridge, 1936), second edition, cf. p. 828.
[4] G. Jaffé, Phys. Rev. **62**, 463 (1942); **63**, 313 (1943). We refer to these two papers in the text as I, II, respectively.

tempted by Mitchell,[5] who used a different approach to the problem. However, so as not to make the calculations too involved, it seemed desirable to the author to start from the simplest assumptions and to investigate how far they would lead. Naturally, the results can be expected to hold, with a fair approximation, only for films which are either gaseous or liquid. In the domain of transition, "expanded films," new phenomena must be anticipated.

Furthermore, we are going to restrict the treatment to one-phase systems. The phenomena of "surface vapor pressure" and of "boundary line tension" could be included in exactly the same way as vapor pressure and surface tension are included in the former theory. However, too few empirical data are known to warrant such a generalization.

Let there be N molecules in a total surface of area S so that $n=N/S$ represents the molecular surface density, and $A=S/N$ the area disposable for each molecule. Let, furthermore, $\varphi(r_{ij})$ be the mutual potential energy of two molecules separated by the distance r_{ij}. Then the total potential energy can be written in the form (compare I, Section I)

$$U=\sum_{i=1}^{N} u_i, \quad u_i=\tfrac{1}{2}\sum_{j=1}^{N}{}' \varphi_{ij}. \tag{2.01}$$

The gist of our method consists in transforming the sum in the expression for u_i into an integral which is to be extended over the entire surface S with the exception of a little circle surrounding the molecule i. The radius of this circle σ is the characteristic parameter of our theory and will be determined separately. The surface S may be replaced by a circle of very large radius, provided boundary effects are to be neglected. Thus we obtain, dropping the index i,

$$u=n\pi\chi(\sigma), \tag{2.02}$$

where $\chi(\sigma)$ is defined by

$$\chi(\sigma)=\int_{\sigma}^{\infty}\varphi(r)rdr. \tag{2.03}$$

Next, the partition function has to be determined (I, Section III). The normalized phase integral can be written as

$$Q=\Theta^N Q_r/N!, \tag{2.04}$$

with

$$\Theta=2\pi mkT/h^2, \tag{2.05}$$

and

$$Q_r=\int\int\cdots\int \exp(-U/kT)dx_1dy_1\cdots dx_Ndy_N. \tag{2.06}$$

Since the potential energy, under our assumptions, separates into N terms not depending on any coordinates, Q_r becomes the product of N identical factors:

$$Q_r=q_r{}^N, \tag{2.07}$$

where q_r is defined as

$$q_r=S\exp(-u/kT). \tag{2.08}$$

Now the work function $\mathbf{A}$ becomes (with the usual approximation for $N!$)

$$\mathbf{A}=-kT\ln Q$$

$$=-kTN\{\ln\Theta+\ln q_r-\ln N+1\}, \tag{2.09}$$

or

$$-\mathbf{A}=kTN\{\ln(\Theta S/N)+1\}-U. \tag{2.10}$$

Here we have reintroduced the total energy (I, Section VI)

$$U=Nu=\pi(N^2/S)\int_{\sigma}^{\infty}\varphi(r)rdr. \tag{2.11}$$

Calling F the surface pressure, we obtain from (2.10) the equation of state of the monolayer in the form

$$F=-\frac{\partial\mathbf{A}}{\partial S}=\frac{NkT}{S}-\frac{\partial U}{\partial S}, \tag{2.12}$$

which corresponds exactly to the three-dimensional case [I, form. (6.04)].

The dependence on n and T of σ, the average value for the distance between nearest neighbors, still remains to be determined. By calculations which are entirely analogous to the three-dimensional case (I, Section V and Appendix II), we find the following results. Let the probable number of mass points in a small fractional area s at the distance r from a given mass point be $p_1(r)ns$; then the probability $p_2(r)dr$ that the nearest neighbor to the given mass point is to be found at distances between r and $r+dr$ will become

$$p_2(r)dr=nP'(r)\exp(-nP(r))dr. \tag{2.13}$$

[5] J. S. Mitchell, Trans. Faraday Soc. **31**, 980 (1935).

Here $P(r)$ is given by

$$P(r)=2\pi\int_0^r p_1(\rho)\rho d\rho. \tag{2.14}$$

For $p_1(r)$ we assume the form (I, p. 470)

$$p_1(r)=\exp(-\varphi(r)/kT), \tag{2.15}$$

and replace the average value $\bar{r}$,

$$\bar{r}=\int_0^\infty r p_2(r)dr, \tag{2.16}$$

by the most probable value, i.e., the value which makes the integrand in (2.16) a maximum.

Thus we obtain for the determination of our characteristic parameter σ the equation

$$1-\sigma\varphi'(\sigma)/kT-2\pi n\sigma^2\exp(-\varphi(\sigma)/kT)=0, \tag{2.17}$$

which corresponds to our former equation I, (5.05) in the three-dimensional case.

In the limiting case $\varphi/kT\to 0$, i.e., either for sufficiently small potentials of interaction, or for sufficiently high temperatures, (2.17) reduces to

$$\sigma=(1/2\pi n)^{\frac{1}{2}} \tag{2.18}$$

in agreement with Hertz's geometrical formula (I, p. 469) for the two-dimensional case.

For the calculation of $\partial U/\partial S$ in (2.12) the knowledge of $\partial\sigma/\partial S$ is required. From (2.17) we derive

$$\partial\sigma/\partial S=(\sigma/S)(1-\sigma\varphi'/kT)/D=(\sigma/S)\epsilon, \tag{2.19}$$

with

$$D=2-2\sigma\varphi'/kT+\sigma^2\varphi''/kT+(\sigma\varphi'/kT)^2. \tag{2.20}$$

In order to obtain numerical results we introduce, as in the case of liquids (I, Section VII), the following form of potential

$$\varphi(r)=fr^{-\lambda}-gr^{-\mu}. \tag{2.21}$$

Then the total energy becomes

$$U=\pi(N^2/S)\times\{f\sigma^{-(\lambda-2)}/(\lambda-2)-g\sigma^{-(\mu-2)}/(\mu-2)\}, \tag{2.22}$$

and the surface pressure

$$F=NkT/S+\pi(N/S)^2\{f\sigma^{-(\lambda-2)}[1/(\lambda-2)+\epsilon]-g\sigma^{-(\mu-2)}[1/(\mu-2)+\epsilon]\}. \tag{2.23}$$

The relation between σ and the area per molecule A is given, from (2.17), by

$$A=2\pi\sigma^2/\delta, \tag{2.24}$$

with

$$\delta=(1-\sigma\varphi'/kT)\exp(\varphi/kT). \tag{2.24a}$$

Making use of this relation we can bring (2.23) into the form

$$FA/kT=1+(\delta/2)\{(f/kT)[1/(\lambda-2)+\epsilon]\sigma^{-\lambda}-(g/kT)[1/(\mu-2)+\epsilon]\sigma^{-\mu}\}. \tag{2.25}$$

It should be remembered that in this equation δ and ϵ are still functions of σ and T given by (2.24a) and (2.19). Since the relation between σ and A cannot be solved with regard to σ in an explicit way, it is necessary, for numerical calculations, to start from given values of σ and to determine A and F as functions of σ. Thus (2.24) to (2.25) represent the equation of state in the parameter form.

A considerable simplification of our result can be realized if we define σ by the purely geometrical formula (2.18). This amounts to taking the limit $\varphi/kT\to 0$, which makes $\delta=1$ and $\epsilon=\frac{1}{2}$. Then the equation of state takes the form

$$FA/kT=1+(1/4)\{f/kT)(\lambda/(\lambda-2))\sigma^{-\lambda}-(g/kT)(\mu/(\mu-2))\sigma^{-\mu}\}, \tag{2.26}$$

with

$$\sigma=(A/2\pi)^{\frac{1}{2}}. \tag{2.27}$$

We shall require the expression for the "bulk coefficient B," i.e., the reciprocal of the compressibility $b=-S(\partial F/\partial S)$. It can be derived from (2.23), if (2.19) and (2.20) are taken into account. For the condensed state a suitable approximation can be obtained by treating δ (for isothermal changes) as a constant (I, Section VII, A). Thus we obtain

$$B=F+(\delta/8A)\{f[\lambda^2/(\lambda-2)]\sigma^{-\lambda}-g[\mu^2/(\mu-2)]\sigma^{-\mu}\}. \tag{2.28}$$

In the same approximation (which amounts to setting $\epsilon=\frac{1}{2}$) we obtain for the equation of state

$$F=kT/A+(\delta/4A)\times\{f(\lambda/(\lambda-2))\sigma^{-\lambda}-g(\mu/(\mu-2))\sigma^{-\mu}\}. \tag{2.29}$$

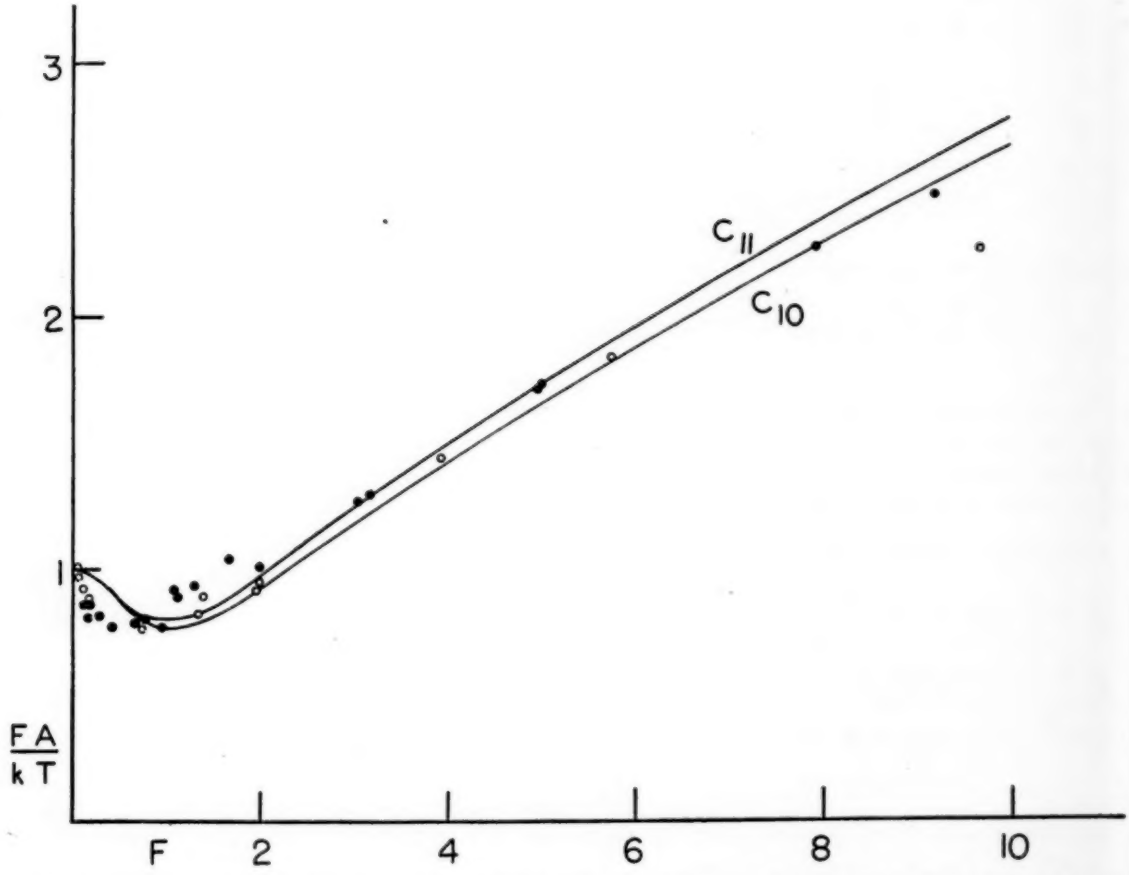

FIG. 1. FA/kT is represented as function of F (in dynes/cm) for insoluble films of the diethyl esters of the two acids $COOH(CH_2)_nCOOH$ with $n=10$ and $n=11$. The curves are theoretical, the points observations by Adam and Jessop.

Finally, the heat of (surface) vaporization per molecule is given by

$$l=-u=-(\delta/2)\{f[1/(\lambda-2)]\sigma^{-\lambda} - g[1/(\mu-2)]\sigma^{-\mu}\}. \quad (2.30)$$

This follows from (2.22) and (2.24).

III. COMPARISON WITH EXPERIMENTAL DATA

A. Gaseous Films

From what has been said above it follows that gaseous and condensed films must be treated separately. For gaseous films we are going to use the formulae (2.26), (2.27). It is true that the condition $\varphi/kT \ll 1$ is not realized except for the highest dilutions.[6] We have, therefore, carried through a considerable number of calculations based on the exact formulae (2.24) to (2.25). These calculations have convinced us that, in the cases tested, the two sets of equations may be made to represent the data about equally well, though with different values of the exponents λ and μ.

It should be pointed out that the two sets of formulae are different only in the calculation of the average distance of nearest neighbors. The simpler geometrical expression (2.18) disregards the influence of the force field about a molecule on that average distance. On the other hand, the expression (2.17) probably exaggerates the influence of this force field as was pointed out on several occasions (I, p. 470, p. 475; II, p. 316). We shall see that the study of condensed films leads to the same conclusion, and it seems that the geometrical formula represents, for iso-

[6] The numerical calculations based on the exact formulae show that, as in the case of liquids, φ/kT comes out of the order 1, and $\sigma\varphi'/kT$ and $\sigma^2\varphi''/kT$ correspondingly larger (I, p. 472).

thermal changes, at least as good an approximation as the dynamical formula.

Under these circumstances we have thought that it was not worth while to carry through the cumbersome calculations based on (2.24) to (2.25), and we have used the simpler expressions (2.26) and (2.27). With these formulae, comparatively low values for the exponents λ and μ have to be chosen. However, the choice is by no means very definite if observations are available only on the equation of state. We have adopted the values $\lambda=5$ and $\lambda=6$, and $\mu=3$. With the exact formulae larger values have to be chosen, namely, $\lambda\sim10$, and $\mu=6$. It follows that not too much significance can be attached to the specific values of λ and μ. However, that is evident from the fact that the simple notion of central forces can, at best, represent a rough approximation to the interaction of molecules in the monolayer.

We have carried through the calculations for two sets of empirical data on gaseous films. The first set deals with insoluble films of dibasic esters having a carboxyl group at each end. The measurements are due to Adam and Jessop[7] and approach, at low pressures, the theoretical value for gaseous films with an accuracy of about 10 percent. The experimental points for the diethyl esters of the two acids $COOH(CH_2)_nCOOH$, with $n=10$ and $n=11$, are represented in Fig. 1 where FA/kT is plotted as function of F.[8] The curves are theoretical curves calculated with the values of the constants λ, μ, f, and g given in the first two rows of Table I. Though there seem to be systematic deviations at low pressures, the general trend of the observations and the almost linear increase of FA/kT with higher values of F is well rendered.[9]

The second set of observations concerns adsorbed films of fatty acids, from 4 to 12 carbons long, on dilute solutions. In this case the surface pressures have not been measured directly but have been calculated by Schofield and Rideal[10] from earlier measurements of the surface tension of solutions,[11] by the aid of Gibbs' adsorption equation. However, it has been pointed out by Adam[12] that the series of curves thus deduced shows a continuous transition without break to the curves obtained by direct measurements for longer chains and that in the case of the 12 carbon acid the two methods yield concordant results. Therefore, this combined set of observations represents a particularly valuable series since it leads from films which are distinctly gaseous through conditions in the neighborhood of the "critical point" to films which are distinctly condensed.

In Fig. 2 the drawn-out curves are calculated from Eqs. (2.26) and (2.27) with the constants tabulated in Table I in lines 3 to 8. The data of Schofield and Rideal are inserted, and it will be seen that the agreement is about as good as might be anticipated from the nature of the data. Schofield and Rideal have pointed out the close resemblance of their curves with the well-known isothermals of CO_2 above and below the critical temperature. It is this very point which is brought out clearly by the theoretical curves.

TABLE I. Constants used in the calculation of Figs. 1 and 2.

	$t=8°C$ Substance	$\lambda=5$ $f\times10^{49}$	$\mu=3$ $g\times10^{36}$
1	Diester C_{10}	4.46	9.21
2	Diester C_{11}	4.85	9.08
	$t=19°C$ Substance	$\lambda=6$ $f\times10^{59}$	$\mu=3$ $g\times10^{37}$
3	Butyric acid	3.17	2.61
4	Valeric acid	3.10	3.64
5	Caproic acid	3.21	5.86
6	Caprylic acid	3.78	11.02
7	Capric acid	3.84	14.35
8	Lauric acid	4.09	18.72

The constants in Table I have been found by trial and error, without any reference to the chemical constitution of the substances studied. It will be noticed that both f and g are almost

[7] N. K. Adam and G. Jessop, Proc. Roy. Soc. London A112, 376 (1926).

[8] We have taken the observed data from N. K. Adam, reference 1, Fig. 12.

[9] Not much importance should be attached to the fact that for $n=10$, the highest point is considerably off the theoretical curve. The authors state (reference 7): ". . . the fact that the curve for 10 appears below that for 11 is probably due to the former being so volatile that the molecules leave the film too rapidly for exact measurements."

[10] R. K. Schofield and E. K. Rideal, Proc. Roy. Soc. London A109, 57 (1925); A110, 167 (1926).

[11] B. von Szyszkowski, Zeits. f. physik. Chemie 64, 385 (1908); A. Frumkin, Zeits. f. physik. Chemie 116, 466 (1925).

[12] N. K. Adam, reference 1, p. 118.

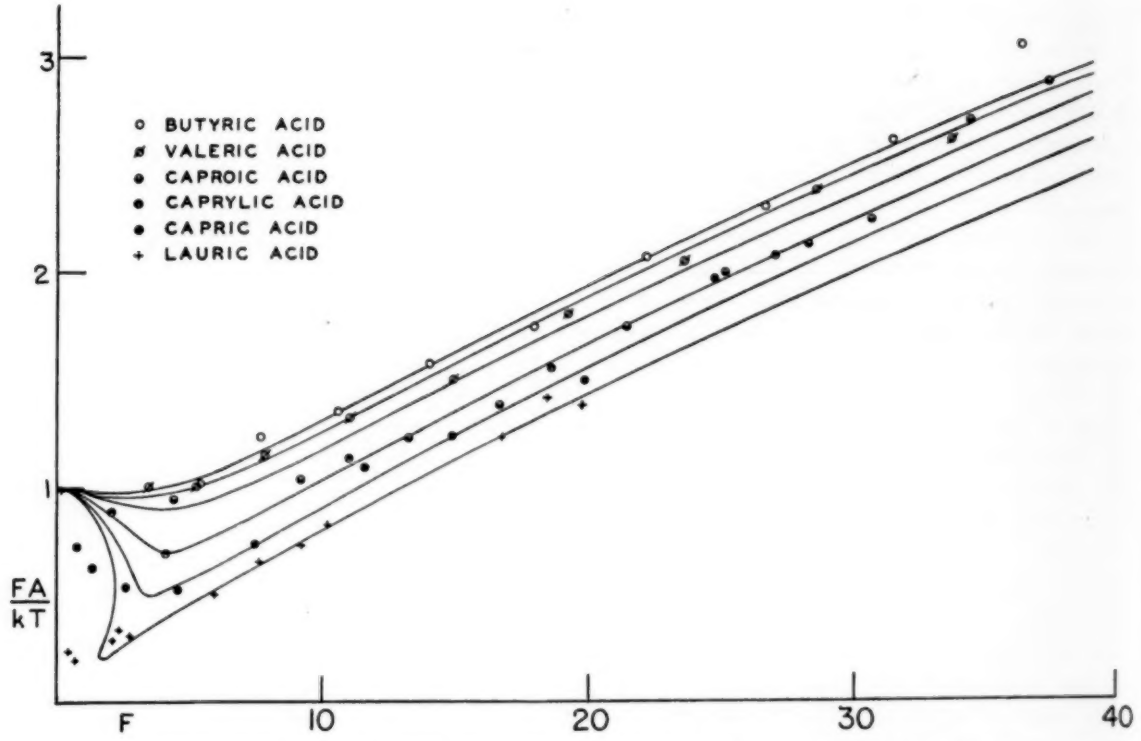

FIG. 2. FA/kT is represented as function of F (in dynes/cm) for adsorbed films of fatty acids with 4 to 12 carbons. The curves are theoretical, the points represent determinations by Schofield and Rideal.

linear functions of the number n of carbons in the chain.

B. Condensed Films

From the last-mentioned fact it is possible to extrapolate the values of f and g to higher values of n. If that is done the resulting isothermals, i.e., F plotted as function of A, begin to descend under the A axis. For $n=13$ the isothermal becomes almost exactly tangent to the A axis (for $A_0=46$ sq.A). For higher values of n there are two intersections. Of these only the intersection on the descending branch can represent a physically possible state since the other intersection would involve a negative compressibility.

The physically possible intersections indicate states in which the condensed film could exist under a surface pressure zero. This fact should not be considered a rigorous consequence of our theory. The consideration of boundary phenomena would introduce a finite surface vapor pressure, exactly as in our theory of liquids the surface tension necessitates a finite vapor pressure (I, Section IV). However, the intersections in question represent the "zero approximation" to the condensed state.

Thus it follows, even from the extrapolated values, that above $n=12$ the films become condensed, as they really do. The values of A_0 thus obtained by extrapolation ($A_0=36, 33, 27$ sq.A for $n=14, 15, 18$, respectively) are of the proper order of magnitude but change with n, whereas it is characteristic of the condensed films in this (and other) series that A_0 is constant, having the value $A_0=20.5$ sq.A for the fatty acids.

This fact, of course, cannot be brought out by potentials obtained from the study of gaseous films. As pointed out in the beginning of Section II the potential must change *in form* when the films pass from the gaseous to the condensed state, and extrapolated values can, at best, give qualitative results. Therefore the liquid films must be studied separately in the present form of our theory.

If sufficient data were available, the four constants involved in our potential (2.21) could be

determined from our equations (2.28), (2.29), and (2.30) to the same extent that this was done for the liquid state previously (I, Section VIII). Unfortunately the available data are very meager.

For the fatty acids from $n=13$ to $n=16$ the surface vapor pressure has been determined directly by Adam and Jessop.[13] This is equivalent to a knowledge of the heat of vaporization. However, the compressibilities are known only roughly and cannot be used for the determination of λ and μ. Under these circumstances the exponents λ and μ have to be assumed from other considerations.

If the surface vapor pressure F_0 is known for any temperature and if it is assumed that the vapor film obeys the gas law

$$F_0=kT/A_0', \tag{3.01}$$

A_0', i.e., the area per molecule in the surface vapor, can be calculated. Then Boltzmann's theorem yields (I, p. 467)

$$A_0/A_0'=\exp(-l/kT), \tag{3.02}$$

where $l=-u$ is the heat of vaporization per molecule. Hence l can be calculated from the knowledge of A_0 and F_0.

Now from (2.29) (with $A=A_0$ and $F=F_0$) and from (2.30) the two combinations of constants

$$x=\delta f\sigma_0^{-\lambda}, \quad y=\delta g\sigma_0^{-\mu} \tag{3.03}$$

can be calculated provided λ and μ are assumed. The value σ_0 corresponds to the condensed state.

Thus our potential, even with λ and μ given within certain limits, is flexible enough to give the correct values for A_0 and F_0. An independent test can then be obtained by calculating the bulk coefficient B from (2.28) and comparing it with experimental data.

We have carried through these calculations for films of tridecylic, myristic, pentadecylic, and palmitic acids, and for two sets of values for λ and μ. The first set is given by $\lambda=6$, $\mu=3$, similar to that used for gaseous films above. The second set, $\lambda=9$ and $\mu=6$, was chosen because it represents the empirical values of density, compressibility, and heat of vaporization for liquid decane without error. Decane data were used because it is the hydrocarbon with the highest n for which the three data in question are available.

The results of our calculations are tabulated in Table II, together with the corresponding constants for decane (as a liquid). It will be seen that the constants (3.03) can be determined, for both sets of exponents, in such a way that A_0 and F_0 come out without error; however, the bulk coefficients are different in the ratio of about 1:3.4.

From indications of Adam[14] it can be derived that the bulk coefficient for condensed films of fatty acids is "usually about" $B=1250$ dynes/cm. "In some instances, on chains of 18 carbon atoms and upward in length" values as high as $B=2500$ dynes/cm are observed. It would follow from this that our theoretical values with $\lambda=9$ and $\mu=6$ are just about correct. If necessary, they could be increased by choosing larger values of λ and μ.

Furthermore it will be seen that the values of the "energy terms" (3.03) are reasonable inasmuch as they are very nearly the same as those obtained for liquid decane in bulk by a similar calculation.

The calculation of the bulk coefficient can be made without an explicit knowledge of δ and σ_0. However, the value of δ is involved implicitly [by its definition (2.24a)] and can be determined in a way similar to that for liquids (I, p. 475).[15] When δ is known, σ_0 can be determined from (2.24).

The values of δ and σ_0 thus determined are added in Table II. It will be seen that they are well in line with the corresponding values obtained for liquid decane. However, the values of σ_0 appear to be too large, even more so for the monolayers than for the liquid. As stated previously, this should be due to the fact that the probability function $p_1(r)$ [see (2.15)] exaggerates the influence of the force field about a molecule.

[13] N. K. Adam and G. Jessop, Proc. Roy. Soc. London A110, 423 (1926).

[14] N. K. Adam, Proc. Roy. Soc. London A101, 452 (1922).

[15] As there is a misprint in the formula I, (8.17) we give here the corrected form

$$\delta=(1-c_2/(2\delta kT))\exp[c_1/(\delta kT)]. \tag{8.17}$$

It should be pointed out that the definition of δ is slightly different in the two-dimensional case from the three-dimensional one.

TABLE II. Constants referring to films of tridecylic, myristic, pentadecylic, palmitic acid, and to liquid decane.

Substance	C_{13}	C_{14}	C_{15}	C_{16}	Decane
Temperat.	14.5°C	14.5°C	14.5°C	12°C	23°C
	$\lambda=6$,			$\mu=3$	
$\delta f\sigma_0^{-6}\times10^{12}$	11.2	12.6	14.2	17.4	
$\delta g\sigma_0^{-3}\times10^{12}$	6.12	6.82	7.67	9.20	
B dynes/cm	279	321	355	447	
δ	17.2	18.6	20.0	23.1	
$\sigma_0\times10^8$	7.5	7.8	8.1	8.7	
	$\lambda=9$,			$\mu=6$	
$\delta f\sigma_0^{-9}\times10^{12}$	42.9	47.7	53.8	64.3	64.1
$\delta g\sigma_0^{-6}\times10^{12}$	37.7	42.0	47.0	56.3	48.7
B dynes/cm	958	1067	1206	1450	
δ	26.5	28.1	30.8	34.1	34.3
$\sigma_0\times10^8$	9.3	9.6	10.0	10.6	12.1

If the geometrical formula for σ is accepted, this amounts to setting $\delta=1$ in Eqs. (2.28) to (2.30). The theoretical values of the bulk coefficient remain the same, but the mean distances between nearest neighbors become, uniformly for all films and with both sets of exponents, $\sigma_0=1.8$A. This appears to be a little too small, and a more correct value of the function $p_1(r)$ would probably lead to a value intermediate between the two values given here.

On the whole it can be said that the agreement between empirical data and our theory is as good as might have been anticipated, given the preliminary nature of the potential of interaction.

PHYSICAL REVIEW VOLUME 66, NUMBERS 5 AND 6 SEPTEMBER 1 AND 15, 1944

On Birkhoff's New Theory of Gravitation

A. BARAJAS, G. D. BIRKHOFF, C. GRAEF, AND M. SANDOVAL VALLARTA
National University of Mexico, Mexico D. F., Mexico, and Harvard University, Cambridge, Massachusetts

(Received May 4, 1944)

It is pointed out in the first place: (1) in Birkhoff's gravitational theory based on "flat" space-time, the "red shift" is accounted for by the energy change of the photon as it travels from the emitting body, whereas the photon plays no especial role in the Einstein theory; (2) the solution of the problem of two or more bodies is feasible in the new theory because of its simpler character. Four comments of H. Weyl concerning the Birkhoff theory are discussed, and it is concluded that these are to be taken with much reserve. In regard to the third of these comments it is pointed out that the "perfect fluid" used by Birkhoff as the ultimate carrier of mass and electric charge is to be characterized as the simplest fluid with disturbance velocity that of light (c). It is affirmed to be a glaring defect of earlier relativistic theories that the disturbance velocity in matter has been taken as arbitrary, although that of gravitation and of the electromagnetic field have been equal to c. The differential equations of the theory are then set up. An additional cosmological term in the gravitational potentials h_{ij} is suggested, namely,

$$h_{ij}^{*}=(K/8)(t^2-x^2-y^2-z^2)g_{ij},$$

where x, y, z, t are Lorentz coordinates and K is the (small) cosmological constant. The explicit formula for the rate of advance of periastron P of two bodies (mass points) of masses m and m_2 is given, as obtained from the solution of the two-body problem in the theory, and its possible application to double stars is referred to. The authors propose to give a detailed development of the theory and its applications in papers to be published shortly elsewhere.

I. PRELIMINARY OBSERVATIONS

IN a recent number of a journal of wide circulation,[1] Hermann Weyl has given expression to several critical remarks on G. D. Birkhoff's theory of gravitation of 1942.[2] In this note we intend first to analyze briefly the substance of Weyl's comments, secondly to consider the structure of the new theory from the physical point of view, and lastly to refer briefly to its physical applications.

Before doing this, however, we would like to make certain general observations.

The explanation of the "red shift" is fundamentally different in the gravitational theories of Einstein and Birkhoff. In the new theory the red shift has turned out to be accounted for by the energy change of the photon as it travels from the emitting body to the Earth; this explanation fully takes account of the role of

[1] H. Weyl, Math. Rev. **4**, 285 (1943).
[2] G. D. Birkhoff, Proc. Nat. Acad. Sci. **29**, 231 (1943).

the light signal (photon). In Einstein's interpretation, on the other hand, the frequency of the light wave emitted by an atom on a distant body is compared with the frequency of the light wave emitted by the same atom on the Earth, and any phenomena taking place while the light signal (photon) travels from the emitting body to the Earth play no part whatsoever.

Again, the difficulties accompanying the two-body problem and other questions in the general theory of relativity are too well known to require mention, while in Birkhoff's theory the solution of the problem of two or more bodies is quite within reach and will soon be available. This is due to the essentially simpler character of the latter theory.

An objection which may be made to Birkhoff's theory is the introduction of an absolute reference system, which runs counter to Einstein's general relativity principle that matter determines space, and analogous philosophical ideas previously developed by Ernst Mach. But, in a sense, this objection to Birkhoff might also be urged against Einstein because in the latter's theory a ***single*** rotating body can still be supposed alone in the universe, which is absurd from Mach's point of view. It would be difficult indeed to set up any physical theory to which objections of this general nature could not be raised.

II. ANALYSIS OF WEYL'S COMMENTS

To begin with, Weyl contends that Birkhoff's theory is much the same as Einstein's theory of 1916, for the case of weak gravitational fields. In a note appearing elsewhere, Barajas[3] has shown that the factual consequences of Einstein's theory in this case differ from Birkhoff's; further, that the choice of the gravitational potentials suggested by Weyl is unsatisfactory; and, lastly, that the trajectories of a test particle in Birkhoff's theory are not geodesics in any four-dimensional space-time.

Weyl further raises four fundamental objections to Birkhoff's theory: (1) "The connection between metric and gravitation is dissolved." (2) The proportionality between inertial and gravitational mass "has again become as mysterious as it was before Einstein." (3) Birkhoff's perfect fluid "appears as a primitive irreducible physical entity." (4) "There seems to be no indication that the mechanical equations spring from a universal law of conservation of energy and momentum." We now propose to take up these points in detail.

(1) With regard to the first, it should be recalled that the connection between matter and geometry, as developed by Einstein, is purchased at the expense of giving up a fundamental reference system. This implies abandoning the description of nature in terms of four fundamental independent variables, essentially unique except for the arbitrariness involved in position and velocity of a single point (Lorentz group). In the abandonment of such coordinates may be discerned a sufficient reason for the early exhaustion of all observational tests of the general theory of relativity, and also for the fundamental difficulty of assigning actual physical meaning to the coordinates introduced in problems of this theory. Indeed, almost thirty years of intensive research have failed to provide another test besides the three classical ones, or to apply the theory to other fields of physics. In spite of a great deal of work, there does not exist any satisfactory solution of the two-body problem, and the n-body problem has not even been formulated. Even in the simple case of Schwarzschild's solution of the one-body problem, no clear-cut physical interpretation of the Schwarzschild coordinates seems to be available. This last difficulty is so serious that it led Milne to give up the use of general coordinates in relativity.

(2) Weyl's second objection seems to be based largely on a misinterpretation. In Birkhoff's theory, just as well as in Einstein's, the equality between inertial and gravitational mass comes out of the fact that in the gravitational equations the energy tensor is linear in the mass density. While nothing similar to Einstein's "equivalence principle" has been explicitly formulated in Birkhoff's theory, it must be stated that the exact significance of the principle has yet to be found. As far as can be seen at the present time it merely asserts that bodies moving freely in empty space near attracting matter behave, relatively to a hypothetical attached reference system, in the same way under all circumstances

[3] A. Barajas, Proc. Nat. Acad. Sci. **30**, 54 (1944).

—insofar as they so behave! From the point of view of differential geometry, it amounts to saying that in the infinitesimal neighborhood of any point in a Riemannian curved space there exists always a tangent flat space, and this is just as true in Einstein's theory as in any other.

According to Einstein, the proper language for the description of nature is that of tensors, together with the underlying group of general transformations; and the equivalence principle expresses the theorem just stated. According to Birkhoff, the proper language for this description is that of four vectors, and the underlying space-time is everywhere flat. In the latter case, the basic group involves only ten arbitrary constants, while in the former it involves four completely arbitrary functions of four completely arbitrary variables. Whichever choice is made, the equality between gravitational and inertial mass follows as a consequence both of Birkhoff's and Einstein's theories.

(3) Birkhoff has chosen the name "perfect fluid" for perhaps the simplest substance in which all disturbances are propagated with the velocity of light, on account of the similarity between the equations governing such a substance and those of a perfect fluid. The particular type of perfect fluid considered by Birkhoff is characterized by only one scalar (the mass density) and vector (the velocity). Fundamental difficulties arise if the disturbance velocity is different from that of light. From our point of view, the fact that in Einstein's theory no attention has been paid to this requirement constitutes a glaring defect, which by itself explains the possibility of Birkhoff's theory. Indeed, the postulation of a primordial substance in which all disturbances are propagated with the velocity of light is fundamentally a consequence of the assumption that the basic space-time is everywhere that of Minkowski. This is actually the only physical assumption made in Birkhoff's theory.

(4) Weyl's fourth objection also seems to spring from a misunderstanding. In Birkhoff's theory the law of conservation of energy and momentum at material velocities small compared with that of light is as much a consequence of the mechanical equations of motion (and conversely) as in Einstein's. It is true that in Birkhoff's case the conservation of energy and momentum is not connected with a fundamental geometrical theorem (Ricci's theorem), as in Einstein's theory. But, although Einstein obtains the formal result that the divergence of the energy-momentum tensor must vanish, this does not imply the conservation of energy and momentum in an exact sense because the four-dimensional integrals of a *covariant* partial derivative in curved space-time cannot be transformed into three-dimensional integrals. Consequently the conservation theorems of Birkhoff's theory are at least much more precise.

These remarks may serve to point out that Weyl's assertions are to be taken with much reserve and that additional research is required before the usefulness of Birkhoff's theory for physics can be adequately assessed.

III. STRUCTURE OF THE BIRKHOFF THEORY

In the light of the preceding remarks, it is possible to recapitulate as follows the considerations which lead to Birkhoff's theory. The fundamental concept of electromagnetic space-time, associated with the names of Fitzgerald, Larmor, Lorentz, Einstein, and Minkowski, has been of the first importance for physics and has played an ever increasing role in the developments of the last fifty years. The revolutionary change which this concept has brought about in physical theory is reflected in the mathematical apparatus employed. Four homogeneous variables of space and time replace the three homogeneous variables of space and the single disparate variable of time; the underlying Lorentz group replaces the Galilean group, and the language of 4 vectors replaces the language of 3 vectors characteristic of classical physics.

The early attempt of Nordström (1912) and others to incorporate gravitation in this framework failed to explain certain delicate gravitational phenomena which alone provide a crucial test. Thus, without an intensive study, electromagnetic space-time was abandoned for a curved or Riemannian space-time, latent in the ideas of Minkowski and realized in Einstein's brilliant gravitational theory of 1916.

It is exceedingly easy to exaggerate the significance of the three so-called critical confirmations of this theory, of which by far the most

certain is afforded by the excessive perihelial advance of the planet Mercury. In fact, the building of theories from the aesthetical-mathematical point of view has shown that dimensional considerations enter which lead always to the same result, aside from simple numerical factors. More definitely, the three formulas for perihelial advance, bending of light, and red shift take always the respective forms

$$qm/a(1-e^2), \quad rm/p, \quad sm(1/r_1-1/r_2)$$

where q, r, s, are simple numerical constants.

Consequently, the basic test of any such theory really reduces to the single requirement that the first constant r has a value not very different from Einstein's value 6π! Thus the theory of Einstein, stripped of all mystical trappings, is seen in its proper perspective. It becomes obvious that the question "What is the simplest theory of gravitation and other physical phenomena, based on electromagnetic space-time, which explains the known facts?" deserves the most careful consideration. This question becomes all the more urgent since the Einstein theory, with its enormous mathematical complication and its lack of proper independent variables, seems to be essentially unworkable.

Table I. Table of disturbance velocities.

	Newton, Maxwell	Nordström, Einstein	Birkhoff
Matter	Arbitrary	Arbitrary	c
Gravitation	∞	c	c
Electromagnetic field	c	c	c

Birkhoff's theory of 1942 provided perhaps the first thoroughgoing attempt to answer this question. Its point of departure arises from the valid criticism of earlier theories that the forms of matter therein employed are inconsistent with the actual requirement that the disturbance velocity be that of light. This situation may be roughly set forth in the comparative Table I, in which the entries indicate disturbance velocity. The physical necessity for a disturbance velocity c of matter appears from the fact that, with any other velocity, the equations of motion break down at the collision of two atomic constituents. Here the matter referred to is not gross matter, but the ultimate carrier of mass and electric charge.

If this requirement is admitted, it appears that the first condition of any new theory based on electromagnetic space-time should be the condition that matter has a disturbance velocity equal to that of light under all circumstances. The theory of Birkhoff is based on one such type, the "perfect fluid," which seems to be the simplest conceivable from a conceptual point of view. But it appears almost certain that any other type of medium obeying this same fundamental requirement will lead to essentially the same gravitational theory. The "perfect fluid" may be approached in the following manner: The state of matter is regarded as characterized by a single scalar density ρ and vector velocity $u^i=dx^i/ds$ in the sense of local causation; the equations of motion are to be linear in the rates of change of these variables; free equilibrium is possible at a certain density ρ_0; the disturbance velocity is to be that of light c, which becomes 1 if the light-second is the unit of distance.

We have established the mathematical theorem that the equations of motion of the perfect fluid may be written in the 4-vector form

$$\text{div } T=\partial T^{ia}/\partial x^a=0, \quad T^{ij}=\rho(u^iu^j-\tfrac{1}{2}g^{ij}),$$

where $g_{ii}=1, -1, -1, -1$ for $i=1, 2, 3, 4$, respectively, and $g_{ij}=0$ for $i\neq j$, with appropriate choice of the scalar density ρ, unique up to a choice of a unit. Furthermore, the perfect fluid so obtained satisfies the conservation principle that the integral $\int\int\int\sqrt{\rho}dv$ is conserved (dv, element of volume referred to a rest system).

The equation of motion under arbitrary force densities f^i may be written correctly

$$\partial T^{ia}/\partial x^a=f^i.$$

There is then the essential further requirement to be imposed on the forces f^i that if the particles of the fluid return to an initial state of position and velocities, the density ρ must also return. For this, it seems necessary and is certainly sufficient that the condition of orthogonality

$$f_au^a=0$$

be identically satisfied. Thus the force vectors are always required to be identically orthogonal to the velocity vectors. A primary force vector of

this type is evidently the acceleration vector itself.

Now all force vectors which have been used in previous relativistic theories are rational and integral in the components of the velocity vector u^i. It is therefore natural to set:

$$f^i = A^i + B^i_\alpha u^\alpha + C^i_{\alpha\beta} u^\alpha u^\beta + \cdots,$$

where the coefficients are functions of position alone, But the electromagnetic force is known to be linear and homogeneous in the velocities and also in the first partial derivatives of the electromagnetic potential φ_i, which itself is of dimension 0 in the unit of length and time. Similarly, in the theory of Einstein, the gravitational forces are homogeneous and quadratic in the velocities, and linear and homogeneous in the first partial derivatives of the gravitational potentials g_{ij} which again are of dimension 0. It is therefore natural to assume that B and C pertain to electromagnetic and gravitational forces, respectively. Birkhoff imposes the analogous requirements upon the vector A and thus arrives at the first (covariant) form for the forces[4]

$$f_i = \rho \frac{\partial \psi}{\partial x^i} + \sigma \left(\frac{\partial \varphi_i}{\partial x^\alpha} - \frac{\partial \varphi_\alpha}{\partial x^i} \right) u^\alpha + \rho \left(\frac{\partial h_{i\alpha}}{\partial x^\beta} - \frac{\partial h_{\alpha\beta}}{\partial x^i} \right) u^\alpha u^\beta,$$

where ψ is his "atomic potential," constant along the world-lines of the fluid, φ_i is the electromagnetic potential satisfying the Maxwell-Lorentz equations (σ, density of electricity)

$$\frac{\partial}{\partial x^\alpha} \left(\frac{\partial \varphi_i}{\partial x^\alpha} - \frac{\partial \varphi_\alpha}{\partial x^i} \right) = -4\pi\sigma u_i,$$

and where h_{ij} is his gravitational potential satisfying

$$\Box h_{ij} = \frac{\partial^2 h_{ij}}{\partial t^2} - \frac{\partial^2 h_{ij}}{\partial x^2} - \frac{d^2 h_{ij}}{\partial y^2} - \frac{\partial^2 h_{ij}}{\partial z^2} = 8\pi T_{ij},$$

which is the generalized form of Poisson's equation of the theory.

Hence the gravitational theory involved may be singled out as follows: If the equations of motion for a small total amount of matter (absence of gravitational force) are written

$$\partial T^{i\alpha} / \partial x^\alpha = f^i;$$

then for the general case, these equations are

$$\frac{\partial T^{i\alpha}}{\partial x^\alpha} = f^i + f^{*i}, \quad f_i^* = \rho \left(\frac{\partial h_{i\alpha}}{\partial x^\beta} - \frac{\partial h_{\alpha\beta}}{\partial x^i} \right) u^\alpha u^\beta,$$

where f^{*i} is the gravitational force and where the gravitational potentials h_{ij} are defined by

$$\Box h_{ij} = 8\pi T_{ij}.$$

Such is the structure of the Birkhoff theory as hitherto formulated. However, to account for the phenomena of nebular recession on this basis, it is necessary to suppose that at some time in the past there was a nuclear distribution of matter, with a wide range of velocities. But from the physical point of view it appears to be more natural to suppose an initial nuclear distribution at low relative velocities. In our recent investigations, we have been led to the following extension of the original theory involving the introduction of a cosmological constant.

From the formal point of view the following more general type of Poisson equation needs to be especially examined:

$$\Box h_{ij} + a T_{ij} + b g_{ij}.$$

With proper choice of a unit of density, it is then possible to specialize further the above equation to the form

$$\Box h_{ij} = 8\pi T_{ij} + K g_{ij},$$

where K is the "cosmological constant," which has the dimensions of a density and is supposed to be very small.

Now, with such an extended Poisson equation, it is no longer possible to demand that the gravitational potentials h_{ij} approach 0 regularly at ∞, nor even that these functions are linearly infinite. However, the condition may be imposed that h_{ij} are regularly infinite to at most the second order, with a boundary distribution at infinity which is spherically symmetric in a spatial sense. Obviously, the most natural possibility from the electromagnetic point of view is to take the cosmological term in the gravitational potentials to be

$$h^*_{ij} = \frac{K}{8}(t^2 - x^2 - y^2 - z^2) g_{ij},$$

where x, y, z, t are any Lorentz coordinates and $x = y = z = t = 0$ is the origin in space-time.

[4] Birkhoff has changed the form of A_i from $\partial\psi/\partial x^i$ to $\rho\partial\psi/\partial x^i$ because of the dimensionality requirement.

It is our purpose to publish shortly detailed studies of the theory outlined above, its cosmological extension, and its applications.

IV. APPLICATIONS AND TESTS OF THE THEORY

It has not yet been possible for us to make an intensive and thoroughgoing study of the Birkhoff theory in relation to known gravitational phenomena; and still less has it been possible for us to consider other possible applications.

However, the basic two-body problem has already been solved by us to the requisite order of approximation. Thus, for instance, the formula for rate of advance of periastron P of two bodies (mass points) of masses m_1 and m_2 has been found to be (in absolute units)

$$P=\frac{3m_1^2+7m_1m_2+3m_2^2}{m_1+m_2}\,\frac{2\pi}{a(1-e^2)}$$

which in case of an infinitesimal mass ($m_1=0$, $m_2=m$) reduces to that made familiar by the Einstein theory, $6\pi m/a(1-e^2)$. Here, of course, the application to the rotation of the line of the apsides for double stars is at once suggested. But such a comparison with observation must await the further analysis of the observations themselves, so that appropriate data may be available in cases where the rotation of the line of the apsides due to tidal forces is relatively small.

We here naturally hoped also that the new theory would account for some of the hitherto unexplained features of lunar motion. However, this does not seem to be a likely outcome although it may turn out that the solution of the three-body problem (Earth, Sun, and Moon) will yield an explanation of the desired type. Instead, at the present writing, we are inclined to think that these supposed features are attributable to the large mass ratio (1/83) of Moon to Earth, which makes the convergency of the mathematical calculations involved slow and uncertain.

It seems not unlikely that the astronomical consequences of this theory for the interpretation of the red shift from extragalactic sources will be of special interest.

As yet no means appear to be available for a decisive experimental test between the gravitational theory of Birkhoff and that of Einstein. This theoretical uncertainty is likely to continue for some time, especially as it appears to be very difficult to carry the Einstein theory to specific conclusions other than those found by him at the outset.

There remains for later consideration the study of atomic phenomena on the basis of the electromagnetic and atomic potentials. It is to be hoped that, by proper assignment of the atomic potential ψ to the constituents of the atom, the explanation of atomic phenomena may be advanced and possibly the fundamental Schroedinger wave equation may be obtained in a conceptual manner.[5] Here the proton and electron constituting the hydrogen atom, for instance, are conceived of as freely interpenetrable and superimposed in case of equilibrium and as oscillating under disturbances.

In conclusion we would like to point out that, for the physicist, all mathematics is fundamentally a form of abstract model building, of more or less general aspects of nature; and that no experiments which the physicist may perform in his laboratory can advance very far without free access to a variety of abstract models which are not to be thought of as final. The new theory of matter, electricity, and gravitation in flat space-time proposed by Birkhoff, would seem to afford a model of unusually fundamental, simple, and complete type.

[5] See G. D. Birkhoff's two notes in the Proc. Nat. Acad. Sci. **13**, 160, 165 (1927).

Density of Potassium Chloride

DWIGHT A. HUTCHISON*
Georgia School of Technology, Atlanta, Georgia
(Received May 29, 1944)

The density of potassium chloride has been determined by the method of "crystal suspension" in a liquid mixture of bromoform, *n*-hexanol, and *n*-pentanol. The density of the liquid mixture at the average suspension temperature of fifty-three different crystals was taken as the density of the potassium chloride. The value determined was:

$$\rho_{25.098°C} = 1.98651 \pm 0.00002 \text{ g/ml}$$

which when corrected to 25°C gave:

$$\rho_{25°C} = 1.98721 \pm 0.00002 \text{ g/ml} = 1.98715 \pm 0.00002 \text{ g/cm}^3.$$

It was found that six precipitations of potassium chloride from aqueous solutions with hydrogen chloride were necessary to effect purification to constant density ($\pm 4 \times 10^{-6}$ g/ml). Exposure of crystals to the atmosphere was found to produce some manner of surface contamination which resulted in a change of density by as much as 7×10^{-4} g/ml within two hours. Storage of crystals over phosphorus pentoxide under vacuum eliminated this effect. An annealing of crystals for four hours at 50° below the melting point with gradual cooling over a period of four hours was found necessary to obtain agreement of suspension temperatures among different crystals. By combination of density and x-ray data, atomic weights have been calculated. The values of the atomic weights of fluorine and calcium were found to be 18.9967 ± 0.0010 and 40.0851 ± 0.0011, respectively. In the crystals of calcite, lithium fluoride, and potassium chloride which were used to obtain the data underlying these calculations, there is no evidence for a secondary structure as proposed by Zwicky.

I. INTRODUCTION

A PRECISION method for the determination of the densities of solid crystalline substances has been developed by C. A. Hutchison and H. L. Johnston.[1]

The method consists of suspending[2] crystals of the substance whose density is to be determined in a liquid of the proper density. The above workers applied this method to the determination of the density of very pure lithium fluoride. Later, H. L. Johnston and the writer[3] were able, with certain refinements of the method, to obtain a value for the density of very pure sodium chloride with reduced probable error over that of the lithium fluoride determination. The present paper deals with the application of the "suspension method" to the determination of the absolute density of very pure potassium chloride.

The purposes of the present determination are: (1) to obtain density data which, in conjunction with x-ray data, can be used in the calculation of various physical constants, e.g., atomic weights,[3,4] and Avogadro's number;[5] (2) to obtain density data which can be used in detecting changes in isotopic abundance ratios of the elements potassium and chlorine due to a given isotopic separation process.[1(b),6]

The most accurate values for the density of potassium chloride, reported to the present time in the literature, appear to be those of Kohler[7] and of Tu.[8]

Kohler determined the density to be 1.9901 ± 0.00015 g/cm³ at 15°C while Tu obtained the value 1.98930 ± 0.00014 g/cm³ at 18°C. When correction is made for the coefficient of thermal expansion of potassium chloride,[9] Kohler's value reduces to

$$\rho_{25°} = 1.9879 \pm 0.00015 \text{ g/cm}^3$$

and Tu's value reduces to

$$\rho_{25°} = 1.98773 \pm 0.00014 \text{ g/cm}^3.$$

* Faculty Associate, Engineering Experiment Station, and Instructor in Chemistry.

[1] (*a*) C. A. Hutchison and H. L. Johnston, J. Am. Chem. Soc. **62**, 3165 (1940); (*b*) H. L. Johnston and C. A. Hutchison, J. Chem. Phys. **8**, 869 (1940).

[2] In previous papers the words "float" and "flotation" are used. These words do not clearly express what is done. Since the temperature is found at which a crystal would be suspended by a given suspension medium, the writer has used the words "suspend" and "suspension" in place of the above words.

[3] H. L. Johnston and D. A. Hutchison, Phys. Rev. **62**, 32 (1942).

[4] (*a*) C. A. Hutchison and H. L. Johnston, J. Am. Chem. Soc. **63**, 1580 (1941); (*b*) C. A. Hutchison, J. Chem. Phys. **10**, 489 (1942).

[5] R. T. Birge, Phys. Rev. **61**, 206A (1942).

[6] H. L. Johnston and D. A. Hutchison, J. Chem. Phys. **10**, 469 (1942).

[7] J. Kohler, Zeits. f. Physik **78**, 375 (1932).

[8] Y. Tu, Phys. Rev. **40**, 662 (1932).

[9] α(cubical) $= 113 \times 10^{-6}$. Klemm, Tilk, and Mullenheim, Zeits. f. anorg. allgem. Chemie **176**, 1 (1928).

Kohler's value exceeds the result of the present determination by 0.038 percent while Tu's value is greater by 0.029 percent. Neither of these workers attempted purification of his potassium chloride, but used the best commercial product available. Their larger values may be due in part to the presence of impurities and to a greater extent to the effect of prolonged exposure to the atmosphere, which, as found in the present work, generally increases the density value (see Table II).

The result of this investigation on very pure potassium chloride when corrected to 25°C gives

$$\rho_{25^\circ} = 1.98721 \pm 0.00002 \text{ g/ml}$$
$$= 1.98715 \pm 0.00002 \text{ g/cm}^3$$

with reduced probable error when compared with other determinations.

II. EXPERIMENTAL DESCRIPTION

A. Preparation of Chemically Pure Potassium Chloride

Chemically pure potassium chloride was prepared by a method similar to that used by H. L. Johnston and the writer[3] in their work on the density of sodium chloride. In essence this is the method employed by Richards and Wells[10] in their determinations of the atomic weights of sodium and chlorine.

Pure hydrochloric acid was prepared by distillation of C. P. Baker's Analyzed reagent hydrochloric acid to which had been added a small quantity of C.P. potassium permanganate. The distillation was carried out in a still composed of a flask and condenser made from pure fused quartz. The middle third of the distillate was saved from each distillate of two successive distillations. The pure hydrochloric acid was stored for future use in clean Pyrex bottles, the inner surface of which had been exposed to concentrated C.P. hydrochloric acid for about four months prior to storing.

Pure sulphuric acid was prepared in a similar manner by double distillation of C. P. Baker's Analyzed reagent sulphuric acid. This acid was also stored in Pyrex which had been exposed to C.P. sulphuric acid for about four months prior to storing.

Pure sodium chloride which was used in the generation of pure hydrogen chloride was fractionally precipitated three times from saturated aqueous solutions of sodium chloride by the addition of hydrogen chloride. The beginning material was Baker's Analyzed C.P. sodium chloride. The hydrogen chloride used in these precipitations was generated by the reaction of pure sulphuric acid (see above) with an aqueous solution of Baker's Analyzed C.P. sodium chloride and pure hydrochloric acid (see above).

Pure water which was used in all reagent preparations was obtained by double distillation from an alkaline permanganate water solution in a pure fused quartz still. Water used in the determination of the volume of the glass bob (see below) was triply distilled and had a specific conductivity of about 10^{-7} ohm^{-1}.

Pure hydrogen chloride which was used in the purification of potassium chloride was generated by the reaction of pure sulphuric acid (see above) with an aqueous solution of pure sodium chloride (see above) and pure hydrochloric acid (see above). The generated gas was passed through two tubes containing ground glass covered with pure sulphuric acid (see above) and finally through a tube containing Baker's Analyzed C.P. phosphorus pentoxide which had been sublimed into this tube.

Purification of the potassium chloride used in the density determination was effected by successively precipitating potassium chloride from a saturated aqueous solution by the addition of pure hydrogen chloride (see above). After each precipitation the potassium chloride was centrifuged to remove the mother liquor. The beginning material was Baker's Analyzed C.P. potassium chloride. Precise density determinations showed that after four precipitations the densities of the potassium chloride from different samples did not agree within the experimental limits of the density determination (see Table III). However, constant density values were obtained from different potassium chloride samples after six precipitations. As a precautionary measure eight precipitations were performed.

After the eight successive precipitations, the hydrochloric acid was expelled from the purified

[10] T. W. Richards and R. C. Wells, "A revision of the atomic weights of sodium and chlorine," Carnegie Institute of Washington, Publication No. 28 (1905).

salt by fusion in a platinum crucible. The salt on cooling was dissolved in pure, triple-distilled water (see above) and given three crystallizations.

B. Preparation and Calibration of the Suspension Liquid

For the crystal suspensions a liquid had to be found which had the proper density, the proper change of density with temperature, and which would not decompose or react with the potassium chloride crystals. A suitable liquid mixture, similar to that used by H. L. Johnston and C. A. Hutchison[1(a)] in their determination of the density of lithium fluoride, was found to have the following composition: bromoform, 40.00 ml; *n*-hexanol, 881 drops; *n*-pentanol, 832 drops (52 drops equal 1 ml). The suspension liquid was prepared as follows: Baker's bromoform (boiling point range, 150°–151°C) U.S.P. IX, was washed with water, dried with calcium chloride, and distilled under vacuum. The middle third of the distillate was collected in a receiver containing a small amount of *n*-hexanol and *n*-pentanol (25 drops of each) which acted as a negative catalyst preventing decomposition. The composition of the bromoform was adjusted to that of the above suspension liquid with Eastman practical grade alcohols. The isothermal density of this suspension liquid was found to remain constant within the experimental limits of error ($\pm 5\times10^{-6}$ g/ml) of the density determination for a period of about seven days. Suspension temperatures after the seven-day period were corrected by means of the standard crystals suspended within the seven-day period.

The density of the suspension liquid at different temperatures was determined by means of hydrostatic weighings. A Pyrex glass bob about 9.4 ml in volume which contained mercury for additional weight was weighed in air, in water, and in the suspension liquid at different temperatures. As in the sodium chloride work,[3] to eliminate surface tension effects[11] at the point of entrance of the 0.01″ platinum suspension wire into the liquid, an auxiliary mercury-weighted Pyrex bob about 1.1 ml in volume was attached to the lower end of the suspension wire. The large bob was detachable from the auxiliary bob. The weighing procedure has been described previously.[3] Two series of weighings were made in the suspension liquid, those of the wire suspension with the auxiliary bob immersed and those of the wire suspension with the auxiliary bob and large bob immersed.

TABLE I. Density of the bromoform mixture as a function of temperature. The bob volume at 25.000°C was taken as 9.41336 ml and corrected to the temperature of each weighing by means of the cubical coefficient of thermal expansion of Pyrex.

Temperature (Centigrade)	Density (g/ml) (at T)	Density (g/ml) (at 28.098°C)
29.320	1.98422	1.98652
29.068	1.98468	1.98651
28.819	1.98515	1.98651
28.547	1.98567	1.98652
28.304	1.98611	1.98650
28.048	1.98661	1.98652
27.806	1.98706	1.98651
27.543	1.98756	1.98651
27.310	1.98799	1.98651
27.060	1.98846	1.98651
26.802	1.98894	1.98650
26.556	1.98940	1.98650
26.301	1.98989	1.98651
26.072	1.99032	1.98651
25.794	1.99084	1.98650
25.553	1.99128	1.98649
25.289	1.99178	1.98649
25.027	1.99229	1.98651

The precise volume of the bob was determined by weighings in triple-distilled water (see above) which had been heated to about 80°C before use to expel dissolved gases. Twenty sets of weighings were made in water at temperatures ranging from 26.174°C to 27.769°C. These twenty independent volume determinations when corrected to 25.000°C by use of the cubical coefficient of thermal expansion of Pyrex glass[12] yielded an average bob volume of 9.41336 ± 0.00002 ml. The densities of the water at the various temperatures were obtained from the *International Critical Tables*.[13] The average deviation from the mean of the twenty determinations was ±0.00001 ml, and the extreme deviation was -0.00009 ml. All weighings were corrected for the buoyant effect of air.

The temperatures at which the weighings were made were determined with a Beckmann ther-

[11] Osborne, McKelvey, and Bearce, Bull. U. S. Bur. Stand., Reprint No. 197 (1912).

[12] R. M. Buffington and W. M. Latimer, J. Am. Chem. Soc. **48**, 2305 (1926). The cubical expansion coefficient was taken as three times the linear coefficient given as 3.6×10^{-6} at 300°K.

[13] *International Critical Tables* (McGraw-Hill Book Company, Inc., New York, 1928), Vol. III, p. 25.

mometer graduated in 0.01° intervals. The scale of this thermometer was shown to be quite uniform by the U. S. Bureau of Standards calibration of the scale. A standard mercury in glass thermometer with a temperature range of 18° to 28°C and with graduations in 0.01° intervals, the scale of which had been calibrated by the U. S. Bureau of Standards, was compared with the Beckmann thermometer at nine different temperatures at 0.5° intervals over a temperature range of 1° to 5° Beckmann. The comparison at the extremes of the temperature range gave

$$1.000° \text{ Beckmann} = 29.320°\text{C}$$

and

$$5.000° \text{ Beckmann} = 25.289°\text{C}.$$

The densities of the bromoform suspension liquid are given in column two of Table I at temperatures covering the range 25.027°C to 29.320°C.

TABLE II. Suspension temperatures of crystals grown from Baker's Analyzed C. P. potassium chloride.*

Crystal designation	Suspension temperatures in ° Beckmann					
	Newly prepared	After 4 days	After 7 days	See footnote[a]		
A2–1	1.998	2.010	2.007			
A2–2	1.991	1.999	2.005			
A2–3	2.009	2.004	2.007			
A2–4	1.986	2.013	2.018			
V2–1	1.999	1.992	1.990			
V2–2	1.995	1.987	1.984			
V2–3	1.887	1.896	1.899			
V2–4	2.006	1.994	1.997			
V4–1	1.984	1.986	1.984	1.985	1.998	1.972
V4–2	1.995	1.995	1.996	1.998	2.017	1.991
V4–3	1.988	1.990	1.989	1.987	2.024	1.999
V4–4	1.976	1.977	1.975	1.975	1.974	1.975

* Explanation: All crystal segments whose suspension temperatures are given in this table were taken from the same melt. The crystal designation A2 denotes crystals which were annealed for two hours at 50° below their melting point and stored exposed to the atmosphere. The designation V2 denotes a two-hour annealing period and storage over phosphorus pentoxide under vacuum. The designation V4 denotes a four-hour annealing period with gradual cooling to room temperature over a period of four hours together with storage over phosphorus pentoxide under vacuum. The Beckmann thermometer graduations are such that increases in numerical values are decreases in temperature.

[a] After the seventh day, crystals V4–1, V4–2, and V4–3 were exposed to the atmosphere for twenty minutes and then resuspended. The suspension temperatures are given in the first column. The second column gives the suspension temperatures after exposure to the atmosphere for two hours. Crystal V4–4 was not exposed. The third column gives the suspension temperatures after a four-hour annealing at 50° below the melting point.

C. Preparation of Suspension Crystals

The suspension crystals were grown from a melt of purified potassium chloride (see Section A) by the method developed by Kyropolous[14] which has been described previously.[1] Similar to the procedure of the density determination for sodium chloride,[3] a four-hour annealing period of about 50° below the melting point was found necessary as shown in Table II. After annealing, the crystals were cooled gradually over a period of four hours. Phosphorus pentoxide was introduced at about 150°C into the furnace around the platinum crucibles containing the crystals. At 60° to 70°C the crystals were removed from the furnace and, with platinum-tipped forceps, were placed in small glass bottles which previously had been heated to about 65°C. The bottles were stored immediately in a desiccator over phosphorus pentoxide under vacuum.

The above procedure was found necessary as evidenced from the observations recorded in Table II. The time required to transfer a crystal from its desiccator to the suspension liquid is short enough that the crystal is not contaminated. The length of time that a crystal may stay in the suspension liquid without change of the suspension temperature is about one week, and then any change is largely due to decomposition of the suspension liquid.

It will be seen from the data of Table II that generally crystals which were exposed to the atmosphere for about two hours or more were suspended at lower temperatures indicating an apparently greater density. This may to a certain degree account for the discrepancy between the value of the density in the present determination and those of Tu[8] and Kohler.[7] The remainder of the discrepancy may be due to the lesser purity of the potassium chloride used by the other workers and to the lesser precision inherent in their methods. (See Tables II and III.)

D. Data for the Absolute Density

Fifty-eight crystal segments were suspended to determine the suspension temperature of the purified potassium chloride. The suspension temperatures are summarized in Table IV.

The average suspension temperature of the fifty-three unstarred crystals in Table IV was 1.989° Beckmann with an average deviation of ±0.000 and an extreme deviation of +0.003 which is equivalent to -5.6×10^{-6} g/ml in the density of potassium chloride. This extreme

[14] S. Kyropolous, Zeits. f. anorg. allgem. Chemie **154**, 308 (1926).

TABLE III. Suspension temperatures of crystals taken at various stages of the purification as outlined in Section A.*

Crystal designation	Suspension temperatures in ° Beckmann
4–1	1.982
4–2	1.999
4–3	1.978
4–4	1.984
6–1	1.987
6–2	1.989
6–3	1.988
6–4	1.987
8–1	1.989
8–2	1.989
8–3	1.987
8–4	1.988

* Explanation: The crystals designated at 4– were grown from potassium chloride that had been precipitated four times with hydrogen chloride from aqueous solutions, followed by fusion in platinum, three crystallizations from triple-distilled water, and a four-hour annealing period at about 50° below their melting point. Those crystals designated as 6– differed in treatment from the 4– in that they were given six precipitations with hydrogen chloride from water. Those designated as 8– were given eight hydrogen chloride precipitations.

TABLE IV. Suspension temperatures of fifty-eight crystals which were prepared and preserved as described above.

Number of crystals suspended at temperatures specified	Suspension temperatures (° Beckmann)
1	1.999*
1	1.998*
1	1.995*
1	1.992
2	1.991
4	1.990
37	1.989
7	1.988
2	1.987
1	1.984*
1	1.980*

* The starred temperatures were not considered in determining the average suspension temperature since they may be excluded on the basis of defects or on the basis that they lie outside a 0.003° range from the mean of the fifty-eight crystals suspended.

deviation is within the experimental limits of the determination.

When the experimental densities of the bromoform mixture (see column 2 of Table I) are plotted against temperature, a straight line is obtained. The slope of this line is $-1.883 \pm 0.004 \times 10^{-3}$ g/ml/degree. Comparison of the Beckmann thermometer with the standard thermometer, calibrated by the U. S. Bureau of Standards, yielded 1.989° Beckmann equal to 28.098°C. By employing the value of the thermal coefficient of density change, the entries in column 2 of Table I have been corrected to the average suspension temperature, 28.098°C. The corrected values are given in column 3 of Table I. The average of these values, 1.98651 g/ml, is taken as the best value for the density of the suspension liquid at 28.098°C. The value for the absolute density of potassium chloride can be stated as

$$\rho_{28.098°C} = 1.98651 \pm 0.00002 \text{ g/ml}.$$

When this value is corrected to 25°C by use of the cubical coefficient of thermal expansion of potassium chloride,[9] the value obtained is

$$\rho_{25°C} = 1.98721 \pm 0.00002 \text{ g/ml}$$
$$= 1.98715 \pm 0.00002 \text{ g/cm}^3.$$

III. MOLECULAR WEIGHT COMPARISONS. THE ATOMIC WEIGHTS OF FLUORINE AND CALCIUM

It has been shown that combination of crystal densities and x-ray data can be used in the comparison of molecular weights.[3,4] With the assumption of certain atomic weights, other atomic weights may be calculated. Combination of the density of potassium chloride obtained in this determination and the density of lithium fluoride obtained by C. A. Hutchison and H. L. Johnston[1(a)] with the x-ray data of Tu[15] and that of Straumanis, Ievins, and Karlsons[16] makes possible the calculation of the atomic weight of fluorine. The resulting atomic weight is found to be 18.9967 ± 0.0010. Combination of the data on potassium chloride with the density of calcite obtained by Bearden[17] and the x-ray data on calcite of Tu[8] and Bearden[17] gives 40.0851 ± 0.0011 as the atomic weight of calcium. A detailed account of the calculations of these and other atomic weights will appear elsewhere.[18]

The results of these atomic weight calculations do not support the hypothesis of Zwicky,[19] who proposed a secondary structure for perfect crystals which requires periodic variations in the grating spaces in a direction normal to the crystal planes.

[15] Y. Tu, Phys. Rev. **40**, 662 (1932).
[16] Straumanis, Ievins, and Karlsons, Zeits. f. physik. Chemie **B42**, 143 (1939).
[17] J. A. Bearden, Phys. Rev. **38**, 2089 (1931).
[18] D. A. Hutchison, to be published elsewhere.
[19] F. Zwicky, Proc. Nat. Acad. Sci. **15**, 816 (1929); **16**, 211 (1930).

Statistical Mechanics at Extremely High Temperatures

G. WATAGHIN
University of São Paulo, São Paulo, Brazil
(Received July 18, 1944)

Equilibrium conditions between elementary particles and nuclei at temperatures $T \gtrsim 10^9$ degrees are studied. Three temperature intervals below the upper limit $\sim 10^{13}$ degrees [$kT \sim 10^8$ ev] are considered. It is found that because of the behavior of some high energy particles, known experimentally from observations on cosmic rays and nuclei, some limitations arise to the validity of the laws of quantum statistics, in accordance with the idea of the existence of a supplementary indeterminacy for high energy particles and a lower limit for measurable lengths. Some astrophysical aspects of the phenomena of pair production and of the gravitational effect of light particles are discussed. The results concerning pair production at temperatures $\sim 10^9$ degrees are summarized in Table I. General formulae for thermal equilibrium between nuclei and light particles are given.

1

IN some previous papers[1] the statistical phenomena taking place at extremely high temperatures were considered. The purpose of the present research is to give a fuller account of some of the results obtained. Although the idea of the supplementary indeterminacy in the high energy regions served as a guiding principle in all this research, we tried to base our conclusions mainly on the known experiments on cosmic rays and nuclei, and on the obvious irreversibility of some of the processes in which particles are created.

We shall distinguish three temperature intervals below the upper limit $T_u \sim k^{-1}\, 137\, mc^2$.

1. Temperatures well below the critical temperature $T_0 = k^{-1}mc^2$, e.g., $T < k^{-1}mc^2/10$, for which the usual quantum statistical laws hold.

2. Temperatures $\frac{1}{3}k^{-1}mc^2 \lesssim T \lesssim T_0$, characterized by the appearance of positrons and electrons produced by thermal photons, at which an approximate treatment of the assembly, by means of elementary statistical formulae, is still possible. In this temperature interval it is possible to neglect, as a first approximation, the production of few high energy particles with $E > 10^8$ ev. However, the increase of density, thermal capacity, and pressure owing to the created electron pairs must be taken into account.

3. Temperatures $T_0 < T < 137\, T_0$ which can be introduced only for assemblages of heavy particles, e.g., for nuclei.

4. Conditions [$kT \gg 10^8$ ev] at which the average amount of energy per particle is so great that the majority of the processes become irreversible and no equilibrium is possible. The lack of the equilibrium is due to the simultaneous or successive creation of many particles (especially of unstable mesotrons) and to the processes involving emission of neutrinos, in which an appreciable fraction of the energy and momentum escapes all observation.

We shall not discuss here the problem of relativistic invariance examined briefly in a preceding paper.[2]

2

Let us consider the equilibrium between photons, electrons, positrons, neutrons, protons, and nuclei at $T \lesssim T_0$. Let N_s, n_{es}, n_{ps}, n_{Ns}, n_{Hs}, n^A_{Zs} be the numbers (per cm^3) of photons, electrons, positrons, neutrons, protons, and nuclei of charge Z_s and atomic weight A, which belong to the momentum-interval $p_s\, p_s + dp_s$. We assume the validity of the laws of conservation of charge:

$$\sum n_{Hs} + \sum Z n^A_{Zs} + \sum n_{ps} - \sum n_{es} = n = \text{const.} \quad (1)$$

conservation of energy:

$$\sum_s [N_s h\nu_s + n_{es}E_{es} + n_{ps}E_{ps} + n_{Hs}E_{Hs} + n^A_{Zs}E^A_{Zs}] + \delta = E = \text{const.} \quad (2)$$

[where δ indicates the interaction energy, $E_{es} = mc^2(1-\beta^2)^{-\frac{1}{2}}$ is the *total* energy of an

[1] G. Wataghin, Phil. Mag. **17**, 910 (1934); Comptes rendus **203**, 909 (1935); Phys. Rev. **63**, 137 (1943); **64**, 248 (1943); **65**, 205 (1944).

[2] G. Wataghin, Phys. Rev. **65**, 205 (1944).

electron, etc.], and of conservation of the total number of neutrons and protons:

$$\sum_s [n_{Ns}+n_{Hs}+A\overset{A}{n}_{Zs}]=N=\text{const.} \quad (3)$$

We assume also that it is possible to specify the states of weakly interacting particles in the usual way, namely, by means of eigenstates having appropriate symmetry. Then, indicating with

$$g_s=8\pi Vh^{-3}p_s^2dp_s=8\pi Vh^{-3}c^{-3}(E_s^2-m^2c^4)^{\frac{1}{2}}E_sdE_s$$

the number of quantum states or eigenvalues of the energy belonging to the sth momentum-interval, we obtain, in the usual way, the following expression for the number of different complexions:

$$W=\Pi\frac{(g_s+N_s-1)!}{(g_s-1)!N_s!}\frac{g_s!}{n_{es}!(g_s-n_{es})!}\cdots. \quad (4)$$

Neglecting the interaction $\mathcal{E}$, and calculating the maximum of

$$\log W-\alpha n-\beta E-\gamma N,$$

we have, in the usual way:

$$\frac{\partial \log W}{\partial n_{es}}=\log\frac{g_s-n_{es}}{n_{es}}+\alpha-\beta E_{es}=0, \text{ etc.},$$

and

$$N_s=\frac{g_s}{\exp(\beta h\nu_s)-1}, \quad n_{es}=\frac{g_s}{\exp(-\alpha+\beta E_{es})+1},$$

$$n_{ps}=\frac{g_s}{\exp(\alpha+\beta E_{ps})+1},$$

$$n_{Hs}=\frac{g_s}{\exp(\alpha+\gamma+\beta E_{Hs})+1}, \quad (5)$$

$$n_{Ns}=\frac{g_s}{\exp(\gamma+\beta E_{Ns})+1},$$

$$\overset{A}{n}_{Zs}=\frac{g_s}{\exp(Z\alpha+A\gamma+\beta E^A_{Zs})\pm 1}.$$

The constant β is $=1/kT$, at least within the limits of applicability of the usual concept of thermodynamical temperature; the other constants α, γ can be determined when we introduce (5) in (1) and (3). In order to take approximately into account the existence of a supplementary indeterminacy in the region of high energy and momenta, the author suggested a more general statistics in which the number g_s of quantum states is: $g_s=8\pi Vh^{-3}G(p_s)p_s^2dp_s$, where $G(p_s)$ is a cut-off factor, which decreases more rapidly than p_s^{-3} for values of $p_s>p_u=137\,mc$ [e.g., $G(p_s)\sim\exp(-p_s^2/p_u^2)$].

For temperatures $T<k^{-1}mc^2$, the following approximation is valid: We can treat the protons, neutrons, and nuclei by the usual statistical methods, neglect the β-ray processes and the concentration of the mesotrons, put $G(p_s)=1$ and $V=1$, and, denoting by n^+, n^- the numbers of positrons and electrons per cm³, assume:

$$\sum n_{es}-\sum n_{ps}=n^--n^+$$

$$=N^+\sim\frac{1}{2}\frac{\rho}{m_H}\sim 3\times 10^{23}\rho_n, \quad (1')$$

where N^+ is the total number of protons per cm³ and ρ_n is the density of the nuclear matter (in g cm^{-3}) calculated with exclusion of the masses of the electron pairs.

Indicating with $x_0=mc^2/kT$, $x=E_s/kT$, where $E_s=c(p_s^2+m^2c^2)^{\frac{1}{2}}$ is the total energy of the electron, and putting in (5)

$$g_s=8\pi h^{-3}c^{-3}(kT)^3(x^2-x_0^2)^{\frac{1}{2}}xdx,$$

we obtain easily the following formulae:

$$n^-=\frac{8\pi}{h^3c^3}(kT)^3\int_{x_0}^{\infty}\frac{(x^2-x_0^2)^{\frac{1}{2}}xdx}{e^{-\alpha+x}+1}, \quad (6)$$

$$n^+=\frac{8\pi}{h^3c^3}(kT)^3\int_{x_0}^{\infty}\frac{(x^2-x_0^2)^{\frac{1}{2}}xdx}{e^{\alpha+x}+1}. \quad (6')$$

Substituting (6), (6'), and (1') and remembering that:

$$(e^{-\alpha+x}+1)^{-1}-(e^{\alpha+x}+1)^{-1}=\frac{\sinh\alpha}{\cosh x+\cosh\alpha},$$

we can calculate α from:

$$n^--n^+=8\pi\left(\frac{mc}{h}\right)^3x_0^{-3}\sinh\alpha$$

$$\int_{x_0}^{\infty}\frac{(x^2-x_0^2)^{\frac{1}{2}}xdx}{\cosh x+\cosh\alpha}, \quad (7)$$

or from:

$$\sinh\alpha\int_{x_0}^{\infty}\frac{(x^2-x_0^2)^{\frac{1}{2}}xdx}{\cosh x+\cosh\alpha}=1.712\times 10^{-7}\rho_nx_0^3. \quad (7')$$

For values of $x_0<1$ and $\alpha\ll 1$, Eq. (7') becomes:

$$3.29\alpha+0.33\alpha^3+\cdots=1.7\times 10^{-7}\rho_nx_0^3 \quad (8)$$

or

$$\alpha\sim 5.2\times 10^{-8}\rho_nx_0^3.$$

TABLE I. Compilation of value calculated for various temperatures.

T	$x_0=(mc^2/kT)$	ρ_n(g/cm³)	α	$\rho_p\sim[n^-+n^+]m$	Thermal capacity of electrons per cm³ $[C_T]$ pair	Thermal capacity of radiation per cm³ $\alpha U/\alpha T=4aT^3$	Radiation density and pressure $U=3p_r$ (erg/cm³)	Density of energy of electrons pairs $E_e^+ + E_e^-$ (erg/cm³)
1.2×10^6	5000	10^{-6}	4983.0					
1.2×10^7	500	10^{-6}	479.8					
1.2×10^7	500	10^2	498.2					
1.2×10^7	500	10^4	506.8*					
1.2×10^8	50	10^{-6}	23.0					
1.2×10^8	50	10^2	44.6					
1.2×10^8	50	10^7	93.0*					
5.9×10^8	10	10^{-6}	4.8×10^{-8}	5.8×10^{-3}	5.0×10^{10}	6.2×10^{12}	9.3×10^{20}	7.2×10^{18}
5.9×10^8	10	10^2	2.3	5.8×10^{-3}	5.0×10^{10}	6.2×10^{12}	9.3×10^{20}	7.2×10^{18}
1.2×10^9	5	10^{-6}	8.7×10^{-11}	3.1	1.3×10^{13}	5.0×10^{13}	1.5×10^{22}	3.7×10^{21}
1.2×10^9	5	1	8.7×10^{-5}	3.1	1.3×10^{13}	5.0×10^{13}	1.5×10^{22}	3.7×10^{21}
1.2×10^9	5	10^2	8.7×10^{-3}	3.1	1.3×10^{13}	5.0×10^{13}	1.5×10^{22}	3.7×10^{21}
3.0×10^9	2	10^{-6}	6.2×10^{-12}	550.0	8.0×10^{14}	8.0×10^{14}	5.8×10^{23}	5.9×10^{23}
3.0×10^9	2	10^2	6.2×10^{-6}	550.0	8.0×10^{14}	8.0×10^{14}	5.8×10^{23}	5.9×10^{23}
3.0×10^9	2	10^5	6.2×10^{-2}	550.0	8.0×10^{14}	8.0×10^{14}	5.8×10^{23}	5.9×10^{23}
1.2×10^{10}	0.5	10^{-6}	6.5×10^{-15}	4.2×10^4	9.0×10^{16}	5.0×10^{16}	1.5×10^{26}	2.5×10^{26}
1.2×10^{10}	0.5	10^2	6.5×10^{-7}	4.2×10^4	9.0×10^{16}	5.0×10^{16}	1.5×10^{26}	2.5×10^{26}
1.2×10^{10}	0.5	10^5	6.5×10^{-4}	4.2×10^4	9.0×10^{16}	5.0×10^{16}	1.5×10^{26}	2.5×10^{26}
1.2×10^{10}	0.5	3×10^7	1.9×10^{-1}	4.2×10^4	9.0×10^{16}	5.0×10^{16}	1.5×10^{26}	2.5×10^{26}
1.2×10^{11}	0.05	10^5	$[6.5\times10^{-7}]$	$[4.2\times10^7]$	$[9.0\times10^{19}]$	$[5.0\times10^{19}]$	$[1.5\times10^{30}]$	$[2.6\times10^{30}]$
1.2×10^{11}	0.05	3×10^7	$[1.9\times10^{-4}]$	$[4.2\times10^7]$	$[9.0\times10^{19}]$	$[5.0\times10^{19}]$	$[1.5\times10^{30}]$	$[2.6\times10^{30}]$
1.2×10^{12}	0.005	3×10^7	$[1.9\times10^{-7}]$	$[4.2\times10^{10}]$	$[9.0\times10^{22}]$	$[5.0\times10^{22}]$	$[1.5\times10^{34}]$	$[2.6\times10^{34}]$

* Degeneracy.

In Table I some values of α, for different temperatures and densities, are given.

The numerical calculations were made on the assumption $N^+=\frac{1}{2}\rho_n/m_H$, that is, by assuming matter contains an equal number of protons and neutrons. In the case when the stellar matter contains a large fraction of hydrogen atoms, one has $N^+\sim\rho_n/m_H$ and one obtains for the coefficient in (7′) a value 3.4×10^{-7}. The corresponding values of α in (8) become nearly twice as great.

From (6) we have:

$$\frac{n^--n^+}{n^-+n^+}=\frac{e^\alpha-e^{-\alpha}}{e^\alpha+e^{-\alpha}}\times\frac{\int_{x_0}^\infty\frac{(x^2-x_0^2)^{\frac{1}{2}}xdx}{e^x+e^{-x}+e^\alpha+e^{-\alpha}}}{\int_{x_0}^\infty\frac{(x^2-x_0^2)^{\frac{1}{2}}xdx}{e^x+e^{-x}+e^\alpha+e^{-\alpha}}\left[1+\frac{e^x}{e^\alpha+e^{-\alpha}}\right]}\sim\frac{e^\alpha-e^{-\alpha}}{e^\alpha+e^{-\alpha}}. \tag{9}$$

Observing that the factor $[1+(e^{-x}/e^\alpha+e^{-\alpha})]$ assumes values between 1 and 2, one has:

$$\frac{n^--n^+}{n^-+n^+}\sim\operatorname{tgh}\alpha \quad\text{or}\quad \frac{n^+}{n^-}\sim e^{-2\alpha}. \tag{10}$$

If $\alpha\ll1$ the total number of pairs is approximately given by

$$1/2(n^-+n^+)\sim1/2\alpha\,N^+.$$

In the case when $\alpha<1$, $x_0<10$ the density of the electron pairs ρ_{pair} can assume values comparable to or greater than ρ_n (see Table I). These values can be calculated from (1′), (8), and (10):

$$\rho_{\text{pair}}=(n^-+n^+)m\sim\alpha^{-1}N^+m\sim6\times10^3x_0^{-3},\qquad n^-\sim n^+\sim3\times10^{30}x_0^{-3}. \tag{11}$$

The question of degeneracy can be treated in a manner similar to that of the Fermi statistics. We note that the graphics of the two characteristic functions $(e^{x\mp\alpha}+1)^{-1}$ can be obtained one from the other by means of a translation of modulus 2α parallel to the x axis (or by changing α in $-\alpha$) and that only values of $x\geqslant x_0>0$ enter into consideration. Then from (6) follows that no degeneracy can occur for the positron gas because the values of $x\geqslant x_0$ correspond always to the quasi-maxwellian region of the distribution curve.

In the low temperature region (large values of x_0) the negatrons are in a degenerated state when $\alpha>x_0$. Introducing into (6′) the critical value of α: $\alpha=x_0\gg1$, we obtain in the non-relativistic approximation:

$$n^-\sim8\pi\left(\frac{mc}{h}\right)^3x_0^{-3}(2x_0)^{\frac{1}{2}}x_0\int_0^\infty\frac{\xi^{\frac{1}{2}}d\xi}{e^\xi+1} \tag{12}$$

or

$$n^-\left(\frac{h}{4\pi mc}\right)^3\sim x_0^{-\frac{1}{2}}. \tag{12′}$$

One can easily verify that this relation coincides with the usual Fermi criterion for degeneracy.

At extremely high temperatures, $x_0 \ll 1$, the values of $\alpha \gtrsim x_0$ correspond to values of

$$\rho_n = 2N^+ m_H \sim 2\alpha(n^- + n^+) m_H \gtrsim x_0^{-2} m_H \Lambda_0^{-3} > \rho_{cr},$$

where $\Lambda_0 = h/2\pi mc$ and $\rho_{cr} = m_H/\Lambda_0^3 \sim 2.9 \times 10^7$ g cm^{-3} is the critical value of the nuclear density. Indeed, the approximate value, for $x_0 \to 0$, of $n^- \sim n^+$, is:

$$n^- \sim n^+ \sim 8\pi \left(\frac{mc}{h}\right)^3 x_0^{-3} \int_0^\infty \frac{x^2 dx}{e^x + 1}$$

$$\sim (\Lambda_0 x_0)^{-3} 1.803/\pi^2 \quad [\Lambda_0^{-3} = 1.736 \times 10^{31}].$$

For such values of ρ_n the average distances between the nuclei (and also between the electrons) become $< \Lambda_0$, and the assumptions of the classical or the quantum electrodynamics, on which the preceding calculations are based, are no longer valid. Thus we exclude such cases from our consideration. At $x_0 < 1$ degeneracy of negatrons does not occur at densities $\rho_n < \rho_{cr}$.

The last columns and lines in Table I are reproduced in order to illustrate some interesting features of pair production and radiation processes in regions where we cannot be sure of the validity of the preceding simple statistical calculations.

3

Obviously we must expect the failure of the preceding simple calculations at temperatures and densities above certain limits for several reasons. Let us examine some of them.

(1) We neglected the nuclear reactions, which can give rise to β-ray processes connected with the emission of neutrinos. In these processes the laws of conservation of energy and momentum are out of our direct experimental control as long as we have no means to measure the energy of the neutrinos or at least to observe them. In some cases, when we can neglect β-ray processes, an approximate treatment of nuclear reactions is possible on the basis of the formulae (5). One can calculate the equilibrium concentration of the protons, neutrons, and nuclei determining the constants α, β, γ from (1), (2), (3). The calculation of γ leads to especially interesting results, which we shall mention briefly later.

(2) At nuclear densities $\rho_n \gtrsim \rho_{cr} \sim 3 \times 10^7$ g cm^{-3} the average distance between the nuclei becomes of the order of the Compton wave-length. At $T \gtrsim 10^{11}$ degrees [$x_0 \lesssim 0.05$] the density of the electron pairs $n^- + n^+$ becomes $\gtrsim 2 \times 10^{31} \sim \Lambda_0^{-3}$. In both cases the linear equations of Maxwell are no longer valid. The field strengths become of the order of or greater than $|\mathbf{E}|_{cr} = e/\rho^2$, where $l \sim e^2/mc^2 \sim h/2\pi mc$ is the universal length. The first non-linear correction terms in the Lagrangian are known to be of the form:

$$\alpha_1(\mathbf{E}^2 - \mathbf{B}^2)^2 + \beta_1(\mathbf{E} \cdot \mathbf{B})^2,$$

where α_1, β_1 are constants calculated by several authors. The representation of a field by means of stationary waves or quantum states of the linear field theories also becomes impossible at least in the region of high frequencies. The writer has suggested[3] that in such conditions our possibilities to distinguish eigenvalues, e.g., measure "observables," is limited in a new way, which depends essentially on a new kind of phenomena appearing at high energy collisions, such as pair production, β-ray processes, and mesotron showers. These phenomena are unavoidable in high energy collisions and thus appear necessarily in the interaction between the measuring devices (which are at rest in the respective reference frames) and the objects of observation. The easiest way to obtain converging results in the usual calculations of collision processes, problems of self-energy, and interaction energy, is to abandon the point source models and to use the so-called cut-off prescriptions. In the foregoing formulae (5) these cut-off factors are introduced by means of the factors $G(p_s)$ appearing in g_s.

(3) Recently the writer pointed out the irreversible character of the collision processes which give rise to the production of several particles, and which are accompanied by β-ray processes. This irreversibility (due to the fact that the inverse processes involve ternary or multiple collisions and emission of neutrinos) is in contrast with the validity of laws of the type (5) at $T \gtrsim 10^{11}$ degrees, but agrees well with the modified formulae obtained from (5) introducing the cut-off factors $G(p_s)$.

For instance, Planck's formula could not be

[3] G. Wataghin, Nature **142**, 393 (1938); Comptes rendus **207**, 358, 421 (1938).

valid at temperatures of the order of 10^{13} degrees [$kT \sim 10^9$ ev]. At these temperatures the number of photons of energy $>10^9$ ev should be 5×10^6 times the number of those having $h\nu<10^6$ ev. From cosmic-ray observations we know that each of the photons or electrons having $E \gtrsim 10^9$ ev gives rise to a multiplication shower in which the initial energy is subdivided among a great number of created particles. The rate of the inverse processes from many low energy particles to a high energy one is negligible. Indeed, the annihilation of an electron pair can occur with the creation of two photons or of one photon. In the first case the number of light particles is not changed (besides, the cross section for annihilation with two-photon production is maximum at $E \sim 10^6$ ev and decreases rapidly with the energy). The probability of a three-particle-collision (two electrons with a nucleus), necessary for a one-photon annihilation, is much smaller than that of a collision of one electron with one nucleus. Only these three-particle collisions give rise to a reduction of the number of particles, and the rate of these processes is necessarily very low. We conclude that the equilibrium is impossible because the processes of multiplication of particles cannot be balanced by processes which reduce their number.

(4) Let us consider a region near the center of a star during the contractive evolution which can give rise to extremely high temperatures. From Table I (last two columns) one can see that at temperatures $T \sim 10^{12}$ degrees, the density of the radiation energy and the density of the electron pairs are much greater than ρ_n, so that one can neglect the nuclear density. If such conditions are verified for a sufficiently extensive region [$R \gtrsim 10^{10}$ cm], a very peculiar situation arises. The mass of the radiation and of the electron pairs increases $\sim T^4$. The gravitational energy of this mass varies as $-\frac{3}{5}(4\pi/3)^{1/3}GM^{5/3}\rho^{1/3}$. At low densities the gravitational energy is negligible in comparison with the total relativistic energy of the nuclei, radiation, and electrons. But if $\rho_{rad}+\rho_{pair}$ is $>10^7$ in a region of linear dimensions $\sim 10^{10}$ cm, the gravitational energy becomes $\sim Mc^2$. The gravitational pressure varies as $\frac{1}{3}(4\pi/3)^{1/3}GM^{2/3}\rho^{4/3}$, whereas the pressure of the relativistic electron gas and the radiation pressure vary $\sim\rho$. Thus at sufficiently high values of T and $(\rho_{rad}+\rho_{pair})$ the gravitational pressure becomes and remains greater than the radiation pressure (in the outer layers of the high density region) and determines a contraction of the gas. These conditions are verified when the negative gravitational energy

$$-\tfrac{3}{5}GM^2/R = -\tfrac{3}{5}(4\pi/3)^{1/3}GM^{5/3}\rho^{1/3}$$

becomes comparable to the total energy of the star Mc^2. The increase of the gravitational mass of the star at expense of the potential gravitational energy implies a change of the gravitational field due to the star, and thus the variation of the mass must be accompanied by a gravitational wave which produces this change of the field. A similar variation but of opposite sign is produced when energy is carried away by neutrinos in β-disintegration processes. Obviously the contraction considered above cannot continue indefinitely and must be counterbalanced by losses of energy (and mass) by radiation, electrons, and neutrinos.

There exists also the effect of the gravitational red-shift, which produces an apparent decrease of the energy of the electrons and photons and which becomes appreciable in the considered case:

$$\Delta V/r \sim (GM/R)/c^2 \sim (GM^2/R)/Mc^2 \sim 1.$$

The paradoxical aspect of the phenomenon in which gravitational mass of electron pairs is created by a gravitational field induces us to admit that on the condition of such strong interaction between the gravitational field and other fields some new physical process counteracts the transformation and makes it impossible. The most plausible assumption seems to be the one that the neutrino emission prevents the increase of the mass and of the gravitational contraction by means of induced β-ray processes.

In this connection it seems noteworthy to us that accepting Friedman's idea of the expanding universe, one can calculate the increase of the gravitational energy of the receding nebulae by means of the Newtonian potential. Assuming that some 10^9 years ago the whole mass of the observed galaxies was concentrated in a reduced volume of linear dimensions ~ 1 parsec, one can make a very rough calculation of how much

gravitational energy the observed galaxies have acquired, and one finds that the average energy per proton is $\sim 10^{17}$ ev. Thus, if we accept the idea of Weizsäcker, Chandrasekhar, and Henrich[4] on the prestellar stage of the universe and assume that the gravitational energy of expansion was produced at expense of the particle-energy, we must say that no equilibrium could possibly exist at an earlier epoch with such an amount of energy per particle.[5]

But the analysis of the abundance and distribution of the isotopes of the chemical elements in the universe strongly suggests the idea that nuclei were formed in the whole universe in similar conditions. We assume that such uniformity of distribution could be attained only in conditions which approximate a statistical equilibrium. In order to study this possibility, we can apply the formulae (5) to the equilibrium among nuclei, electrons, and photons. The calculations are similar to those used in the construction of Table I. Here we want to mention only some general results.

At temperatures $T > 10^{10}$, the constant γ is determined essentially by the concentration of neutrons and protons. The concentration of heavier nuclei is entirely negligible and only the concentration of $^4He_2$ is appreciable. The concentration of the heavier nuclei increases gradually in the temperature region between 3×10^9 and 10^9 degrees ($x_0 \sim 2$ or 5). The analysis of the nuclear structure (mass defect as function of Z and $A-Z$) shows that the stability of the nuclei is closely related to the probability of the β-disintegration processes, and the formation of stable nuclei follows closely the evolution of the concentration of electron pairs, photons, and neutrons. The formation of heavier nuclei by the decrease of the temperature from 6×10^9 to 10^9 degrees follows in the order of increasing atomic weights from lightest to heaviest nuclei. An easy calculation shows that at temperatures of a few billion degrees the nuclear photo-effect becomes of great importance and gives rise to the emission of many neutrons, so that equilibrium is possible with a high concentration of neutrons. At temperatures below 10^9 degrees the neutron concentration vanishes and the usual cyclical thermonuclear reactions take place. All these conclusions derive from the formulae (5) corrected by the introduction of the cut-off factors $G(p_s)$.

The limits of applicability of these formulae depend on the induced β-ray processes. In accordance with a fundamental idea of G. Gamow and M. Schoenberg related to the so-called "urca-processes," at temperatures $\gtrsim 10^{10}$ degrees, we can expect the β-ray processes to acquire such an intensity that the energy losses due to the neutrino emission must invalidate the possibility of equilibrium, and thus the law of conservation of energy (2) becomes out of our control. We think that this fast loss of energy by neutrinos was at a certain epoch in competition with the expansion of stellar matter in the non-equilibrium process which increased the gravitational energy of the universe.

Leaving the highly speculative consideration on the prestellar stage of the universe, we want to call attention to the fact that β-ray processes introduce a new limitation to the concept of temperature in an assemblage of nuclei and light particles because the non-applicability of the conservation law (2) implies the impossibility of equilibrium and of identification of the constant β with $(kT)^{-1}$. Of course, one can introduce the notion of temperature also for a nucleus as is done usually in order to measure the average energy per nucleon. But even in nuclear matter the equilibrium becomes impossible when the average energy per particle is greater than the rest energy of the meson $\mu c^2 \sim 10^8$ ev because at higher temperatures irreversible collision processes take place with production of unstable mesons. Thus the temperature $T_u \sim 10^{12}$ degrees must be an upper limit also for heavy particles.

In this paper we shall not discuss the problems of compatibility of the supplementary indeterminacy with the relativistic invariance. Also the production of mesotron showers by collision of high energy nuclei and correlated phenomena were not considered. An account of these problems will be published elsewhere in a short time.

---

[4] Weizsäcker, Chandrasekhar, and Henrich, Astrophys. J. **95**, 288 (1942); Physik. Zeits. **39**, 633 (1938).

[5] G. Wataghin, Phys. Rev. **63**, 137 (1943).

Letters to the Editor

PROMPT publication of brief reports of important discoveries in physics may be secured by addressing them to this department. The closing date for this department is the third of the month. Because of the late closing date for the section no proof can be shown to authors. The Board of Editors does not hold itself responsible for the opinions expressed by the correspondents. Communications should not in general exceed 600 words in length.

An Attempt at Finding the Relationship Between the Nuclear Force and the Gravitational Force

K. C. WANG AND H. L. TSAO
Department of Physics, National University of Chekiang, Meitan, Kweichow, China

June 2, 1944

THE best we know about the nuclear force is that it is of short range type. Its analytic form is still unknown. The meson theory of nuclear force is, up to the present at least, inconclusive.[1] On the other hand, the gravitational force is explained by the theory of general relativity. If we temporarily disregard the theory of general relativity and pay attention to the important fact that both the nuclear force and the gravitational force are attractive, we may assume that these two forces are of the same origin. Let us tentatively take the function

$$V=-Ae^{K/r} \tag{1}$$

as the mutual potential between any two nuclear particles, i.e., between two protons, two neutrons, or one proton and one neutron, with A and K as constants. Then, as the distance r between the particles becomes much larger than K, Eq. (1) turns out to be

$$V=-A-(AK/r)-\cdots. \tag{2}$$

In this expression, the first term on the right-hand side is a constant, and therefore is of no consequence. Thus

$$V(r)=-AK/r. \tag{3}$$

On the other hand, the gravitational potential between the two nuclear particles of masses M and M' should be given by

$$V=-G(MM'/r). \tag{4}$$

If the nuclear force and gravitational force are really of the same origin, we must have, from (3) and (4),

$$AK=GMM'=1.83\times10^{-45}\text{ erg cm}, \tag{5}$$

since $G=6.66\times10^{-8}$ and $M=M'=1.66\times10^{-24}$. Recently, Ragan, Kanne, and Taschek,[2] from the proton-proton scattering experiment, found that the potential between two protons can be represented by a rectangular well of width $2e^2/mc^2$ and depth 10.5 Mev. Now if from our equation (5), we put K as the Compton wave-length of electron, i.e., $K=\hbar/mc=3.83\times10^{-11}$ cm, we get $A=4.80\times10^{-45}$, and if we substitute these values of K and A into (1), we find the potential $V=10.5$ Mev at $r=1.51e^2/mc^2$ which is only a little smaller than the experimental value of $2e^2/mc^2$. In fact, if the potential is not a straight rectangular well but a slightly curved one, for the same depth of potential, a smaller value of r is expected. If, instead of Eq. (1), we take

$$V=-(B/r)e^{K/r}=-(AK/r)e^{K/r} \tag{6}$$

as the nuclear potential function, we get the result $V=10.5$ Mev at $r=1.62\ e^2/mc^2$ which checks even better with the experimental value. Thus we may tentatively state that:

$$\begin{aligned} V&=-(B/r)e^{K/r} \quad \text{for } r>a \\ V&=-(B/a)e^{K/a} \quad \text{for } r\leqq a \end{aligned} \tag{7}$$

for a certain value of a, the exact value of which is of no great importance at present. Since the value of K is *not* purely arbitrary, but is chosen as the Compton wave-length of electron, the agreement between the experimental and the calculated value is perhaps not accidental, and may indicate that the electron, as has long been suggested, plays an important role in nuclear interactions. If it is required to avoid the rather artificial way of "cutting off" of the expression (7) at $r=a$, we give an alternative expression

$$V=-A\exp\left[\frac{K}{r}-\left(\frac{K'}{r}\right)^n\right], \tag{8}$$

with n lying between 1 and 2, and K' a new constant which may tentatively be put as the Compton wave-length of meson, i.e., $K'=\hbar/m'c\approx\hbar/180mc$, but this makes the width of the potential well smaller than $1.51\ e^2/mc^2$. It will be seen in a paper by M. S. Wang[3] that good results for the binding energy of deutron and the scattering cross section of protons by fast neutrons can actually be obtained by calculations in employing either the potential function (1) or (6). In conclusion, we express our gratitude to discussions with our colleague, Professor H. P. Soh.

[1] H. A. Bethe, Phys. Rev. **57**, 260, 390 (1940).
[2] G. L. Ragan, W. R. Kanne, and R. F. Taschek, Phys. Rev. **60**, 628 (1941). See also T. H. Osgood, J. App. Phys. **14**, 53 (1943).
[3] M. S. Wang, Phys. Rev. **66**, 103 (1944).

Proton Primaries of Atom-Annihilation Cosmic Rays

DANA T. WARREN
Department of Science, The Municipal University of Omaha, Omaha, Nebraska
August 7, 1944

MILLIKAN, Neher, and Pickering have presented the atom-annihilation hypothesis of cosmic-ray origin in two recent papers.[1] In I, footnote 4, they point out that the magnetic effects depend only on the energy of the primary particle, and consequently their hypothesis would not distinguish one kind from another. In II, page 245, they insist that their results would be valid only for electron primaries, not for mesotrons or protons. Their reasoning in this case depends on a determination of the kinetic energy available when a helium atom decomposes into two electrons or into two protons, respectively. The latter, of course, gives about half as much kinetic energy, from which they conclude that the latitude of appearance would be appreciably higher.

In view of the recent experimental indications[2] and theoretical calculations[3] concerning the protonic nature of the primaries, it seems important to point out that I is correct, and not II. This is because the magnetic effects depend, not on kinetic energy, but on total energy, which is of course the same for both kinds of disintegrations. This can readily be seen, for instance, from the table of values that relates the magnetic deflection variable (called r_e in I, Fig. 2) in stoermers with the energy in electron volts.[4,5] A given value of the kinetic energy corresponds to a larger value of r_e for protons than for electrons, and this effect very closely neutralizes the decrease in mass annihilated. A detailed calculation can be made on the basis of Eq. (12) of reference 4. For the case of electrons, this reduces to Eq. (66) of reference 5. On the basis of this relation are drawn the values scaled in I, Fig. 2 (copied from Fig. 14 of reference 5), specifically labeled electron energies. For protons, however, the equation takes the form

$$r_e = 0.130\mathcal{E}^{\frac{1}{2}}(1+1.86/\mathcal{E})^{\frac{1}{2}},$$

when r_e is in stoermers and $\mathcal{E}$ is the kinetic energy in Bev.

When these equations are applied to the values given in II, page 245, for electrons (1.88 Bev) and protons (0.94 Bev), we obtain $r_e = 0.178$ stoermer for electrons and 0.165 stoermer for protons. This difference of 7 percent in the value of r_e would correspond to a latitude difference of about 1°, instead of the 6° stated in II. Similar calculations for the other atom-annihilation bands give differences of 1 percent or less, which would be quite unobservable.

We conclude, therefore, that the atom-annihilation hypothesis is quite independent of the nature of the primary cosmic radiation involved. This does not apply, however, to alpha-particles, with their double charge.

[1] R. A. Millikan, H. V. Neher, and W. H. Pickering, Phys. Rev. **61**, 397 (1942) (hereafter called I); Phys. Rev. **63**, 234 (1943) (called II).
[2] E.g., T. H. Johnson, Rev. Mod. Phys. **11**, 208 (1938).
[3] J. Hamilton, W. Heitler, and H. W. Peng, Phys. Rev. **64**, 78 (1943).
[4] G. Lemaitre and M. S. Vallarta, Phys. Rev. **43**, 87 (1933).
[5] T. H. Johnson, Rev. Mod. Phys. **10**, 193 (1938).

Efficiency of Production of Continuous *X* Radiation

PAUL KIRKPATRICK
Stanford University, Stanford University, California
August 2, 1944

FOR over ten years we have had in the work of Sommerfeld and others the basic structure of a proper theory of continuous x-ray production, but little has been done to put the predictions of theory into numerical forms which could be compared with experiment. We have now completed computation of the elementary electric dipole moments for radiation between the quantum limit and 1.431A resulting from collisions of electrons in the energy range from 15 to 90 kev with atoms in the range from $Z=13$ to $Z=92$. The results of these computations, together with a description of the computational procedure, will shortly be submitted for publication.

From these computations one readily obtains W, the theoretical total energy of continuous spectrum x radiation in unit frequency interval per bombarding electron per atom per cm² of target material. This is a numerical result known for a variety of bombarding potentials V, radiation frequencies, and target atomic numbers Z. By graphical integration of W over all frequencies from zero to the quantum limit, the total continuous x-ray energy per electron per atom per cm² is obtained. This quantity is, of course, a function of Z and V and it has been evaluated for a variety of values of these parameters.

To deduce the efficiency of such x-ray production one needs to know the total energy lost per atom per cm² by an electron of velocity ratio β while penetrating the target material. The formula of Williams[1] as modified by Webster may readily be put in the form:

Energy loss per electron per atom per cm²
$$= 5.62\times10^{-30}Z\beta^{-1.4}.$$

By simple division we get the efficiencies reported at the Berkeley meeting of the American Physical Society.[2]

TABLE I. Theoretical efficiencies expressed in percent.

β_0	V (kilovolts)	$Z=13$	$Z=47$	$Z=70$	$Z=92$
		Efficiencies			
0.20	10.53	0.042	0.137	0.346	0.555
0.30	24.66	0.077	0.270	0.474	0.685
0.40	46.52	0.132	0.438	0.675	0.895
0.50	79.00	0.179	0.645	0.971	1.25
0.526	90.00	0.182	0.693	1.06	1.34

The total continuous spectrum energy R emitted during the complete stoppage of an electron may be evaluated by a further graphical integration of the form

$$R=\int_0^{\beta_0}\frac{dR}{dE}\frac{dE}{d\beta}d\beta,$$

where E is the electron kinetic energy and β_0 is the maximum or initial value of β. The first derivative in the integrand is, in absolute value, the calculated efficiency aforementioned; it is, of course, a function of β. The second derivative in the integrand is a function of β obtained by differentiating the relativistic kinetic energy expression. The integration was carried out for some

twenty cases and the over-all efficiency of continuous x-ray production obtained by dividing R by the initial electron energy. These theoretical efficiencies, expressed in percent, are shown in Table I.

These values are to be compared with observed efficiencies. Compton and Allison have summarized existing work in the equation

$$\text{Efficiency} = 1.1 \times 10^{-9} Z V,$$

in which V is in volts and the efficiency is a fraction rather than a percentage. The calculated efficiencies all increase with increasing Z and V but not in all cases proportionally as the experimenters have found. The increase with Z for the three higher voltages is an accurate proportionality in each case but at lower voltages an upward concavity appears. As to the increase of calculated efficiency with V the curve is linear for the higher values of Z but misses the origin; for lower Z the curves go through the origin but are slightly concave downward. On the whole, the agreement between theory and experiment as to the functional relation between efficiency and Z and V is as good as could have been wished, in view of the difficulties of such observations and the approximations (neglect of relativity and screening) of the theory.

The theoretical efficiencies are from 50 to 100 percent greater than those given by the summarizing equation of Compton and Allison, but they lie within the spread of the results of the several observers. A discrepancy in this sense should be expected since the theoretical emission extends to zero frequency and thus includes a minor, though not negligible, contribution from a spectral region unavailable to measurement because of heavy absorption. This agreement encourages the hope that all the observable features of thick-target x radiation may be found explicable by fundamental theory.

[1] Compton and Allison, *X-Rays in Theory and Experiment* (1935), p. 76.
[2] P. Kirkpatrick, Bull. Am. Phys. Soc. **19**, 7 (July 22, 1944).

Further Remarks on the Difficulties of the Meson Theory

D. Iwanenko
The State University, Sverdlovsk, U.S.S.R.
August 7, 1944

SOME time ago Oppenheimer and his collaborators[1] arrived at the conclusion that mesons should be described by pseudoscalar equations and possess zero spin because vector equations for the mesons of the spin unity lead to unadmissibly high cross sections at various scattering effects. This point of view seems to be supported in recent publications of Pauli and Dancoff and Fröhlich.[2] We may remark that pseudoscalar mesons behave satisfactorily only for electromagnetic scattering (e forces), but in cases of scattering under the influence of specific nuclear g forces, there is no essential difference between behavior of vector and pseudoscalar particles. For instance, the cross sections for the scattering of pseudoscalar mesons on neutrons grow unlimitedly at high energies. The very reason for this behavior lies in the presence in the commutation rules for field quantities of the terms of dipole type having the form ν^2. This can be deduced on the lines of the analysis applied previously by us to the vector case.[3]

Most immediately this can be inferred from the fact that pseudoscalar mesons, if transferring nuclear interactions, lead to the forces of the dipole type, as vector mesons do, and it is just this coupling of the dipole type between nucleons and mesons which leads to the high cross sections.

In our opinion there is no essential ground for preferring the pseudoscalar description of mesons as this also needs further amendment.

As to the removing of these dipole difficulties, we remark first of all that the reaction of the mesonic field on the radiating nucleonic dipole is described in the classical picture firstly by a Heisenberg term containing the second time derivative of the nucleonic dipole and secondly by a term with the third time derivative, just as in the case of the radiation damping force acting on a vibrating charge. This latter term was introduced by Bhabha and the present writer.[4] It is important to emphasize that Heisenberg's term will be absent for the point source models of the nucleonic dipole, so that the whole reaction of damping is expressed then by the term with third derivative. In the quantum theory the damping was introduced simultaneously by Heitler, Wilson, and Sokolow,[5] and these authors have shown that upon taking the damping into account the cross sections for the scattering of vector mesons on nucleons and of the scattering of light on mesons remain limited at high energies. Further calculations of Sokolow and myself show that the introduction of the damping for pseudoscalar equations also removes the difficulty of the growing cross sections for the scattering under the influence of specifically nuclear forces. Preliminary calculations show also that the unpleasant divergent part of the **polarization** of vacuum due to virtual mesons remains finite.[6]

[1] R. F. Christy and S. Kusaka, Phys. Rev. **59**, 405 (1941).
[2] W. Pauli and S. M. Dancoff, Phys. Rev. **62**, 85 (1942); Fröhlich, Phys. Rev. **62**, 180 (1942).
[3] D. Iwanenko and A. Sokolow, Phys. Rev. **60**, 277 (1941); J. Phys. Moscow **5** (1941).
[4] D. Iwanenko and A. Sokolow, J. Phys. Moscow **3**, 12 (1940).
[5] A. Sokolow, J. Phys. Moscow **6** (1941); W. Heitler, Proc. Camb. Phil. Soc. **37**, 291 (1941); Wilson, Proc. Camb. Phil. Soc. **37**, 301 (1941).
[6] As reported in Phys. Rev. **60**, 277 (1941), the polarization of vacuum via mesons was calculated in collaboration with M. Rosman, now in active service.

Errata: On the Perturbation of Boundary Conditions

[Phys. Rev. **65**, 307 (1944)]

Herman Feshbach
Department of Physics, Massachusetts Institute of Technology, Cambridge, Massachusetts

THE abbreviated derivation of Eq. (3.7) and the corresponding equations (4.1) and (5.6) in the paper "On the perturbation of boundary conditions" has permitted some misinterpretation.

Formula (3.7) applies only when ψ_n has the eigenvalue k^2. If the eigenvalue of ψ_n is K_n^2, then the term $(k^2-K_n^2)\int\psi_n G_k dv$ should be added to right-hand side of (3.7). The same term should be added to (4.1). The corresponding term of Eq. (5.6) is $(K_n^2-k^2)\int \mathbf{A}_n \cdot \mathbf{G}_k dv$.

Proceedings of the American Physical Society

MEETING AT BERKELEY, CALIFORNIA, JULY 22, 1944

THE 262nd meeting of the American Physical Society was held in Berkeley, at the University of California, on Saturday, July 22, 1944. In spite of the continually decreasing number of graduate students, and the continued preoccupation of most physicists in war work, the attendance, which varied from 65 to over 100, was the largest at any Pacific Coast meeting since the start of the war. About 35 members of the Society and guests had luncheon together at the Faculty Club. Brief remarks were made at the luncheon by Dr. K. K. Darrow, Dr. E. U. Condon, Dr. Otto Stern, and Dr. Paul Kirkpatrick.

As in the case of the preceding Pacific Coast meeting, very few contributed papers were anticipated, and accordingly arrangements were made for four invited papers. These papers undoubtedly added greatly to the interest of the meeting and to the size of the attendance. But the unexpected receipt of 18 contributed papers, none of which was read by title, resulted in a program definitely too long for a single day. The morning session opened at 9:30 A.M. and adjourned at noon. The afternoon session opened at 1:30 P.M. and adjourned at 5:20 P.M. During the morning session two invited papers were presented, *viz.*,

Specific Ionization and Energy Loss of Cosmic Rays. WAYNE E. HAZEN, *University of California.*

Microwave Oscillation Generators Using Velocity Modulated Electron Beams. EDWARD U. CONDON, *Westinghouse Research Laboratories.*

During the afternoon session the following two invited papers were presented:

Applications of Radioactive Tracers to the Physiology of Plants. ROY OVERSTREET, *Experiment Station, College of Agriculture, and Radiation Laboratory, University of California.*

Some Aspects of Our Present Understanding of Elementary Particles. JOSEPH W. WEINBERG, *University of California.*

Abstracts of the eighteen contributed papers follow.

R. T. BIRGE
Local Secretary for the Pacific Coast

Abstracts of Contributed Papers

1. Cascade Showers in Lead. WAYNE E. HAZEN, *University of California.*—The calculations for number of electrons and positrons in a shower as a function of depth have been carried out lately to an accuracy of a few percent.[1] These latest calculations give curves for number of particles *versus* depth that are practically identical in shape with previous curves.[2] The important difference is that the corresponding curves are for initiating particles differing in energy by a factor of ~ 1.4. In photographs of a cloud chamber that contained eight lead plates, 50 complete cascade showers have been observed. The observed showers can best be compared with theory by plotting number of particles at the shower maximum *versus* total number of particles in the shower. Theory predicts essentially a straight line with slope 0.2. All but one of the experimental points lie above this straight line. The observed showers contain only one-half the predicted total number of particles for a given size of shower maximum. Since a large number of the electrons have energies as low as three Mev, it is possible that scattering and increase in ionization for $E<1.5$ Mev would account for the discrepancy.

[1] H. J. Bhabha and S. K. Chakrabarty, Proc. Ind. Acad. Sci. **A15**, 464 (1942).
[2] B. Rossi and K. Greisen, Rev. Mod. Phys. **13**, 240 (1941).

2. Growth of Water Drops in a Wilson Cloud Chamber. E. O. BARRETT, *University of California.*—Water drops formed in a Wilson cloud chamber were photographed with periodic illumination and their velocity was measured. The drop size was determined by means of Stokes' law and the square of the radius of the drop was found to vary linearly with time as soon as the drop was large enough to register photographically. A 60-cycle neon light that moved with constant velocity during the exposure was turned on by the expansion valve. This light was photographed on the same frame and its flashes were used to establish the zero of the time scale for the drop images. It was observed that the straight line obtained from the experimental points intersected the time axis about 0.1 sec. after the zero. This fact seems to indicate that the rate of growth of the drops is smaller during the first 0.1–0.2 sec. and then reaches a constant value. The slope of the straight part of the curve was found to be 7.8×10^{-6} cm²/sec.

3. The Average Specific Ionization of Cosmic-Ray Mesotrons in Hydrogen. LESTER L. SKOLIL, *University of California.*—Counter-controlled cloud-chamber photographs of cosmic-ray mesotron tracks in hydrogen have been taken. The chamber was operated in such a way that

the average specific ionization could be obtained from the number of drops that condensed on positive ions. A triple-coincidence counter telescope was employed, with two counters below the cloud chamber and one above. Sufficient lead was placed above and below the top counter so that electron tracks could be distinguished from mesotron tracks. The average specific ionization, excluding energy transfers greater than 800 ev (clusters of more than thirty-two drops), is essentially 10.5 ion pairs per cm of hydrogen at N.T.P.

4. Radiofrequency Dielectric Properties of a Cellulosic System at Low Moisture Contents. W. C. DUNLAP, JR., AND B. MAKOWER, *Western Regional Research Laboratory.*—As background for a study of electrical moisture testing by radiofrequency methods, measurements were made of the radiofrequency dielectric properties of dehydrated carrots, a material typical of those on which such methods are used. Measurements were made of the dielectric constant ϵ and specific conductivity σ (a.c. and d.c.) as functions of moisture content (1.5–21.6 percent), temperature (1.5°C–39.8°C), frequency (18 kilocycles–5 megacycles), density (0.792–1.45 g/cm³) and particle size (small and medium). ϵ increases little with moisture content up to 6–8 percent; above this region ϵ increases rapidly. Increase of temperature increases both the value of ϵ and the rate of change of ϵ with moisture. At 1.5°C there is no detectable change of total σ with increase in moisture until 6–8 percent is reached; above this region the variation becomes exponential. At higher temperatures this apparent discontinuity disappears. Particle size has little effect upon ϵ or σ, for a given bulk density. Increase of bulk density increases ϵ and total σ uniformly on a logarithmic scale for all frequencies. A brief discussion will be given of the theory of the properties observed.

5. Control of Glycol Vapor Concentration in Room Air. C. E. NIELSEN, *Department of Physics,* AND K. B. DEOME, *Division of Veterinary Science, University of California.*—The vapors of certain glycols, non-toxic to man, are effective in killing air-borne bacteria. The effectiveness depends critically both upon the amount of water vapor and upon the amount of glycol vapor present. In consequence, satisfactory clinical experiments cannot be made without stabilizing both humidity and glycol vapor pressure. Although humidity is controllable, no method of controlling glycol vapor pressure under room conditions has been devised. The Wilson cloud chamber offers an approach to this problem. When room air is cooled by adiabatic expansion, droplets will grow upon nuclei normally present if the temperature falls below the dew point. The addition of glycol vapor should permit condensation with a lesser expansion, glycol in the droplets lowering their vapor pressure and causing them to grow in an atmosphere not saturated with water vapor. Reduction in the expansion required, water vapor pressure being maintained constant, should thus indicate the vapor pressure of glycol. Experiments indicate that glycol does reduce the expansion required for condensation, and that the occurrence of condensation can serve to control the rate of addition of glycol to maintain constant glycol vapor pressure.

6. On Electron Microspectroscopy. L. MARTON, *Division of Electron Optics, Stanford University.*—The energy losses of fast electrons corresponding to K levels of light elements, and observed first by G. Ruthemann,[1,2] were used by J. Hillier[3] in an instrument designed for the investigation of the composition of small specimens. His instrument, called an "electron microanalyzer," consists of an inverted electron microscope producing a small probe on the surface of the specimen, with analysis of the transmitted beam and image formation by the shadow method. Our investigations show that the energy losses can be observed in a transmission type of electron microscope. For such a purpose an attachment is built on to the Stanford electron microscope replacing the transparent fluorescent screen used for end-on viewing the image. The attachment consists of a disk, coated with fluorescent material, and provided with a small slit through which part of the highly magnified image can be directed into a magnetic analyzer extending below the microscope. A simultaneous observation of both the highly magnified image and its velocity spectrum is therefore achieved. The area used for the velocity analysis can be made variable by changing the end magnification and keeping the slit width constant. The magnetic analyzer is of 135°, direction focusing type. Observation, temporarily at least, is on a fluorescent screen inclined toward the beam axis and approximately in the correct position for the velocity focal plane. Some of the obtained results are discussed.

[1] G. Ruthemann, Naturwiss. **29**, 648 (1941).
[2] G. Ruthemann, Naturwiss. **30**, 145 (1942).
[3] J. Hillier, Phys. Rev. **64**, 318 (1943).

7. X-Ray Monochromatization by Four Balanced Filters. PAUL KIRKPATRICK AND C. K. CHANG, *Stanford University.*—A limitation of Ross' balanced filter method is the physical impossibility of entirely suppressing $a-b$ outside the pass band, $a(\lambda)$ and $b(\lambda)$ being the fractions transmitted by filters A and B, respectively. This limitation may be surmounted by using two similar filters of element A and two of element B. From an x-ray source adjacent beams, defined by similar diaphragms, are allowed to pass to a common ion chamber. An ion current observation is made with the superposed A filters in one beam and the superposed B filters in the other. One A and one B filter are then transposed and a second current reading is taken. The difference between these currents is then a summation to which each wave-length contributes an amount proportional to $(a-b)^2$. In Ross' method the corresponding magnitude is $(a-b)$. Thus the contrast between the pass band contribution (where a/b may be of the order of 3) and the contribution from other spectral regions (where $a/b \cong 1$) is greatly accentuated by the four-filter method and a monochromatic effect may be achieved with filters which have been only very roughly balanced.

8. Linearity of d.c. Vacuum-Tube Voltmeters. SEVILLE CHAPMAN, *Stanford University.*—In d.c. vacuum-tube

voltmeters having a balanced double-triode circuit, the meter is usually connected between the plates of the two tubes. If, however, the load resistors are inserted in the cathode circuits, rather than in the plate circuits, and the meter is connected between the two cathodes, the plates being connected directly to power supply, it is shown that without loss of sensitivity the departure from linearity between input voltage and meter reading is reduced by a factor of from 2 to 4 in practical cases. Thus an increase in sensitivity by a similar factor can be obtained, or a less sensitive meter may be used for performance equivalent to that of the usual circuit. When degeneration from additional cathode resistors is employed in the usual circuit, its performance is improved, but it does not equal that of the suggested circuit. Practical examples are compared with theoretical calculations. With an ordinary 250-volt unregulated power supply the suggested circuit will give a meter deflection of 1 milliampere per volt input with a single 6F8-G tube, sensitivity being independent of normal line voltage fluctuations. This high sensitivity arises from the low impedance of cathode loaded stages.

9. The Spirotron. LAURENCE E. DODD, *University of California at Los Angeles.*—As a means, theoretically possible, of stopping very high speed particles by deceleration using potential gradients applied in successive steps as in the cyclotron, but at the same time avoiding correspondingly high frequencies of field reversal, which may be impractical to obtain, the present paper proposes to whittle down such high velocity a selected component at a time. The name "spirotron" is given to such a design. The type of spiral implied by this term is that of a tapering helix rather than a plane curve as at present. A succession of several of these in series, of different pitches, with their axes at definite angles of inclination with each other, should serve to stop particles of higher velocity than could be dealt with in the reversed cyclotron because of frequency difficulties.

10. A Simple Adaptation of the Ultraviolet Photographic Spectrophotometer to Direct Visual Measurement. LOUIS A. STRAIT, W. D. KUMLER, AND FRANK M. GOYAN, *College of Pharmacy, University of California.*—The conventional u.v. photographic spectrophotometer of the rotating sector or stationary variable diaphragm type is adapted to direct visual measurement by substituting a fluorescent screen for the photographic plate. Monochromatic measurement of optical density or transmission may be made with speed comparable to conventional photoelectric photometers and there is an advantage in flexibility with regard to type and size of sample which may be measured. A quick survey of qualitative absorption may be made conveniently by using a Baly tube and observing the absorption spectrum on the screen. Where photographic photometry of an unknown is to be carried out, the desired concentration may be readily found in the same way, saving photographic plates as well as time. Potassium chromate solutions ranging in optical density at 2800A from 0.04 to 1.3 have been used, and the duplicate-measured transmission values deviate from the theoretical by a maximum of 3 percent with a mean deviation of 1.6 percent. More detailed data will be reported elsewhere. A suitable screen may be made by depositing a uniformly fine suspension of anthracene (in a base such as cellulose acetate or butvar) on a glass screen made by removing the emulsion from a photographic plate.

11. The Measurement of Absolute Efficiencies of Gamma-Ray Counters. WENDELL PEACOCK, *Massachusetts Institute of Technology.*—By measuring various radioactive isotopes, using coincidence counting methods, one may determine the absolute efficiency of gamma-counters and the absolute rate of disintegration of the radioactive isotopes. By the use of the isotopes Na^{24}, Co^{60}, Mn^{54}, I^{131}, Y^{86}, Fe^{59}, Mn^{56}, and Co^{58}, the absolute efficiency of screen wall copper, platinum, and bismuth counters was determined. With the isotopes Br^{82}, Au^{198}, I^{130}, Mn^{52}, Na^{22}, and V^{48}, the efficiency curves thus determined were confirmed. The efficiency curves thus obtained were in substantial agreement with the theory proposed by V. Droste. With several isotopes, each emitting a single monochromatic gamma-ray, it is possible to compare the efficiency of gamma-ray detecting instruments at various energies rather quickly. Isotopes with conveniently long half-lives and emitting gamma-rays of energies above 1.5 Mev are not yet available, but Be^{7}, Cu^{63}, Mn^{54}, and Zn^{65} serve at lower energies. By the use of these isotopes in connection with Y^{86} and Na^{24}, the efficiency curve can be extended from 0.4 Mev to 2.75 Mev. The absolute efficiency of the measuring device can be obtained with a source for which the absolute disintegration rate is known. For this purpose Co^{60} (5.3y) has been used.

12. Direct and Fluorescence Excitation of the L_{III} Level in Thick Targets of Thorium. BURR G. BURBANK, *Stanford University* (Introduced by Paul Kirkpatrick).—The ratio P of the probability of exciting the L_{III} shell of thorium by direct electron bombardment to the probability of exciting the same shell by photoelectric ionization in a thick target was determined by observation of normally emergent x-rays from an oil-cooled thorium-target x-ray tube. The intensities at the peak of the $L\alpha_1$ line and in the continuous background on each side were measured with a Bragg spectrometer. The target was then covered with a palladium foil thick enough to stop all bombarding electrons, and these intensities were again measured. The $L\alpha_1$ line from the covered target could be produced only by the photoelectric ionization process, while the $L\alpha_1$ line from the bare target could be produced partly by each process. By taking into consideration the relative intensities and the mean depths of production of the continuous rays from the palladium and the thorium, P was calculated for a range of voltages from 40 to 100 kv, and was found to decrease from a value of 3.1 at 40 kv to 1.98 at 100 kv.

13. A High Voltage D.C. Regulator Entirely A.C. Operated. J. F. MCGEE, *Stanford University.*—The regulator is of the fundamental degenerative type, as catalogued by Hunt and Hickman[1] for low voltage applications and

suggested for higher voltages. It is used in conjunction with a half-wave voltage-doubler power supply in the x-ray research laboratory. The present regulator circuit is distinguished from others of comparable stabilization in that: (a) it is entirely a.c. operated, the usual reference battery of several hundred volts being replaced by the highly regulated and separate plate supply voltage of the d.c. amplifier; (b) it makes use of an *RC* combination which for short duration fluctuations of voltage has the effect of increasing the fraction of the high voltage that is compared with the reference voltage.

[1] F. V. Hunt and R. W. Hickman, Rev. Sci. Inst. **10**, 6 (1939).

14. Planck's Universal Constant of Action. SAMUEL R. COOK, *Sacramento, California.*—The paper purports to find a relation between Planck's two constants, the unit electric charge and what Planck called his universal "quantum of action" h. Planck considered that the two constants were independent, and that although the two constants were essential in developing his radiant heat formula, they were entirely independent of each other. The paper purports to show, first, that Planck's first constant, which he considered as a mere formal constant, is in reality the real universal constant of action, being the unit charge of electricity e. The paper also purports to show, second, that the ratio of the values of the two constants e and h is a definite constant of proportionality k. Since the discovery by Planck of the constant h, which when multiplied by the frequency of radiation gives the value of the energy of any radiation quantum $h\nu$, the exact explanation of the nature of the constant h has been in question. The paper shows that e, the electric charge on an electron, is the real "constant of action" and that h is a constant which acts as a factor to measure the energy developed in the radiation quantum developed by e. The ratio of e and h is determined as a constant k.

15. A New Method of Determining the Fraction of Electrons in Cosmic Radiation. ROBERT R. BROWN, *University of California* (Introduced by Wayne E. Hazen).—A cloud chamber containing seven lead plates, three of 0.2-cm thickness and four of 0.7-cm thickness, was operated by a three-counter telescope above the chamber. The counters were made of thin glass and the usual copper cylinder was replaced by a layer of graphite paint. Above the counters and the chamber was a thin metal roof. The equivalent stopping power of the thin metal roof, the walls of the counters, and the wall of the cloud chamber was ~10 Mev. The electrons and mesotrons that entered the chamber were differentiated by their shower effects, penetration, and ionization. The probability that an electron would pass through the chamber without initiating a shower is extremely small. On the other hand, the probability that a mesotron would initiate a shower while passing through the absorber is extremely small. The advantage of this method over that using a cloud chamber and a magnet is that the incoming particle spectrum is not distorted by a strong magnetic field. The advantage of this direct cloud-chamber method over the indirect counter method is that the cloud-chamber results depend on the cascade theory of showers only so far as the determination of the lower energy limit is concerned.

16. Rigorous Calculation of an Electrostatic Immersion Lens. RUDOLF G. E. HUTTER, *Division of Electron Optics, Stanford University.*—Previous investigations have shown that the electrostatic immersion lens, given by the axial potential distribution, $\phi(z)=\phi_0 e^{x \arctan z/a}$, is the simplest electrostatic lens for which Newton's image equations are satisfied throughout the field. The axial potential distribution of this lens is found to approximate that of the electrostatic lens consisting of two cylinders of unequal radii which are connected to two potentials $V_1=\phi_0 e^{-x\pi/2}$ and $V_2=\phi_0 e^{+x\pi/2}$. The general solution of the paraxial ray differential equation is derived. Based on this solution and the fact that Newton's image equations are satisfied, exact expressions are derived for all important optical quantities such as the focal lengths, the location of the four cardinal points, the magnification, the object-image relation, and the spherical and chromatic aberration for any object position. The optimum positions of an object are determined so that the chromatic and spherical aberrations are reduced to a minimum. All quantities are represented graphically as functions of the ratio of the asymptotic voltages V_2/V_1. A plot of the equipotential lines in space is given for a special value of the voltage ratio.

17. Theoretical Efficiencies of Continuous X-Ray Production. PAUL KIRKPATRICK, *Stanford University.*—Computations of continuous x-ray intensities on the basis of the Sommerfeld theory, as supplemented by subsequent contributors, have been completed for potentials to 90 kv, wave-lengths from 0.181A to 1.431A, and representative atomic numbers throughout the range. By combining these results with Williams' theory of the electron stopping power of matter, values of production efficiency have been obtained. The following table gives the ratios of emitted x-ray energy (all frequencies and all directions) to total energy loss suffered by electrons *of the stated energies* when traversing matter of the given Z.

Z	25 kv	40 kv	90 kv
13	0.0013	0.0018	0.0028
47	0.0048	0.0068	0.0115
70	0.0069	0.0097	0.017
92	0.0087	0.0125	0.021

The total continuous spectrum energy emitted during complete stoppage of a 90-kv electron is almost directly proportional to the atomic number of the stopping element, rising to 1.90×10^{-9} erg at $Z=92$.

18. The Mean Depth of Production of Continuous X-Rays in Thick Targets of Thorium. BURR G. BURBANK, *Stanford University* (Introduced by Paul Kirkpatrick).—A thick target of thorium was bombarded by 40–100 kv electrons incident obliquely in a direction making a grazing angle of 30° with the target surface. The intensities of several selected wave-lengths of the continuous spectrum propagated in a direction at right angles to the direction of bombardment were observed with a Bragg spectrometer

for a variety of orientations of the target with respect to an axis of rotation coinciding with the electron beam. By Stoddard's modification of Kulenkampff's method, the mean depths of production were deduced from the slope of a plot of the logarithm of the observed continuous intensity *vs.* the secant of the angle of rotation of the target. Mean depth values were obtained as functions of wave-length and bombardment voltage. The average value of the mean depth of production within the spectral range between the high frequency limit and the L_{III} absorption limit increases from 6.0×10^{-5} cm at 40 kv to 22.2×10^{-5} cm at 100 kv. The total range along the path of the electrons in the thorium, as calculated by Williams' formula, is about 10 times the average mean depth of production.